Metamaterials for Space Applications

Chiral particles and transmission-line networks for cloaking applications

Final Report

Authors: Pekka Alitalo and Sergei Tretyakov
Affiliation: Department of Radio Science and Engineering, TKK Helsinki University of Technology

ESA Researcher(s): Jose M. Llorens and Luzi Bergamin

Date: 11.6.2008

Contacts:

Sergei Tretyakov
Tel: +358-9-451-2243
Fax: +358-9-451-2152
e-mail: sergei.tretyakov@tkk.fi

Leopold Summerer
Tel: +31(0)715655174
Fax: +31(0)715658018
e-mail: act@esa.int

Available on the ACT website
http://www.esa.int/act

Ariadna ID: 07/7001d
Study Duration: 4 months
Contract Number: 21261/07/NL/CB

Abstract

This report presents the work done at the Department of Radio Science and Engineering (DRSE), Helsinki University of Technology (TKK) and the ESA–ESTEC Advanced Concepts Team (ACT), on the project "Metamaterials for space applications." The goal of this project is to study specific examples of recently developed metamaterial-related approaches to cloaking, and especially, study the potential of these approaches for space applications. The selected approaches are compared with each other and also to other approaches found from the literature.

The project kick-off meeting was held at ESA–ESTEC in Noordwijk, the Netherlands, on 10.12.2007 and the project officially started on 14.1.2008.

The research topics that are carried out as a collaborative work between DRSE and the ACT, are mentioned below in the workplan of the project.

Project goals and workplan

The goals of the project are 1) to give an overview of various cloaking approaches, 2) concentrate on design principles of two selected techniques, and 3) give detailed description of the design, benefits, drawbacks and potential for space applications of these selected techniques.

The research items suggested in the original project and accepted by the DRSE research team together with the ACT during the kick-off meeting are:

1. Coordinate-transforming cloak based on chiral inclusions;
2. cloak based on networks of transmission lines;
3. investigation of the potentials for realization of the cloaks studied in items 1 and 2 in the optical frequency range;
4. comparison of the two approaches in items 1 and 2 with other approaches for cloak design;
5. study of fundamental physical limitations of different types of cloaks (mainly the cloak types studied in items 1 and 2);
6. the ACT will provide some examples of space applications, where the feasibility of the cloaks studied in items 1 and/or 2 will be investigated;
7. the generalized form of field transformations will be studied, but this research item is optional, and does not constitute the priority of the study.

It must be acknowledged that part of the work in item 3 has been conducted by prof. Constantin Simovski (DRSE-TKK) and part of the work in item 7 has been conducted by prof. Igor Nefedov (DRSE-TKK).

Contents

1 Introduction

This Section briefly describes the background and motivation for this project, i.e., the most relevant literature related to the project and the work done at DRSE before the start of the project.

1.1 Metamaterials

The project deals with so-called metamaterials, which is a class of artificial materials. Since the name "metamaterial" is often used for describing very different materials and structures, we want to clarify what is regarded as a "metamaterial" within this project. Firstly, a metamaterial is described by the fact that it is artificial (man-made), or, more precisely, the inclusions comprising the material are artificial, and that the material exhibits, in a certain frequency range, electromagnetic properties which are not found in nature [1]. Secondly, within this project we include also structures composed of two-dimensional or three-dimensional transmission-line networks into the category of metamaterials [2, 3]. In both cases (a material composed of either separate inclusions or transmission-line networks), the period of the microstructure of the "material" must be considerably smaller than the wavelength at the operating frequency.

1.2 Design of cloaks and invisible structures

The goal of the project is to study various cloaking techniques and approaches, mainly from the design point of view, and estimate their feasibility in general for space applications. Because the work of the ACT is concentrated on high operating frequencies, special attention for potential of high-frequency operation is given to the cloaks discussed in this report. Here, the term "high-frequency" refers to frequencies up to the visible range.

What is cloaking, or, more precisely, what do we mean by cloaking? At least within this project, we rely on the following description: cloaking of an object means the reduction of the total scattering cross section of this object. If we assume that we have a certain volume in which we can place this object, i.e., a volume inside the "cloaking device", this object can be composed of an arbitrary material and can be of any size and shape as long as it fits inside the specified volume [4, 5]. This requirement basically means that in the volume that is cloaked, there is zero field.

Also, the concept of invisibility has been closely related to cloaking in the recent literature. The difference is that invisibility means the reduction of the total scattering cross section of a *specific* object. This can be achieved for example by cancelling the induced dipole moments of the scatterer (object to be made invisible) by another object, in which dipole moments of the opposite direction are induced [6]. Thus, the combination of these objects scatters very little, whereas both objects independently scatter strongly. Moreover, the fields need not be zero inside the "invisible object." Invisibility can be also understood as cloaking, if the object to be made invisible consists of, e.g., a perfectly conducting hollow enclosure since inside this enclosure, there are no fields.

From the design point of view (and even more so from the point of view of realization possibilities), the various known cloaking/invisibility techniques are very different, thus all of them have certain benefits and drawbacks. Especially, the design of coordinate-transforming

cloaks [5] is in principle very simple in terms of finding suitable material properties, but the design of the material itself is a much more demanding problem, since exotic values of ε and μ usually require engineered materials. Relaxation of the requirements from the "ideal" cloaking situation usually makes the design and realization of the required material much easier.

1.3 Literature overview on different cloaking/invisibility techniques

Although in this project we concentrate on cloaking instead of invisibility, we list here the most important papers published in scientific journals on these both topics. The reader must note that there is also an increasing amount of literature related to cloaking, but in this Section we only give the references related to the introduction of the different approaches to cloaking. For example, the approach of [5] has been further studied and developed in many papers in the recent years.

Cloaking which is based on creating a volume with zero field in space, was first described in [4, 5], although mathematically a similar method has been previously presented [7]. The approach of [4, 5] requires the use of metamaterials with effective relative permittivity (ε_r) and/or permeability (μ_r) less than 1. The first realization of such a coordinate-transforming cloak, based on the design principle of [5], was presented in [8]. In general, the operation of these types of cloaks is limited mostly by the strongly dispersive ε_r and/or μ_r, resulting in a very narrow bandwidth where the desired cloaking effect is observable. The structure presented in [8] operates as a cloak for TE-polarization only, for which the electric field is orthogonal to the 2-D plane where cloaking is possible. The approach of [8] has been extended for the TM-polarization in [9].

It must be noted that the cloaking methods discussed in [4] and [5], resp., differ in the way how the so-called coordinate transformation is conducted, although the main idea is the same. The approach of [5] is somewhat limited as compared to the approach of [4], but in its basic form it is more easily applied to real cloaks since it includes impedance matching with the medium surrounding the cloak. Furthermore, the approach of [4] has been proposed to have a possibility to include transformation of also time [10]. This extension broadens the possibilities in the design of cloaking devices but due to the fact that such transformations are even more complicated than the ones relying just on the transformation of spatial coordinates, they are not considered in this report. To the best of our knowledge, no concrete proposal of a cloak of this type has been presented.

Invisibility, the meaning of which was explained in Section 1.2, has been considered in the literature by many authors during the past few decades, see, e.g., [11, 12, 14]. Recently, this subject has been broadened such as to include cloaking as well [6, 15, 16]. This extension can be done simply by creating a scatterer with zero field inside. Then, a material cover is created around this scatterer in such a way that the induced dipole moments of the scatterer and the cover are canceled. For example, the scatterer can be a hollow sphere, composed of metal, since inside this object there is zero field in the ideal case. The problems of utilizing such cloaks relate to the realization of materials with exotic material parameters, which inherently leads to strongly dispersive materials.

Also various other materials, devices, or structures that are used to reduce the total scattering cross section of different types of objects, have been studied in the recent literature. In [17]

hard surfaces[1] are effectively used to reduce the scattering from an antenna strut, but the inherent drawback of this approach is that the operation of the "device" is limited to basically one incidence angle. For other angles of incoming radiation, the structure is actually expected to increase the scattering. In [18] the concept of using a so-called superlens, i.e., a slab with ε_r and μ_r being both negative is introduced in order to cancel the scattering from line or dipole sources located in the near-field of this superlens. Since the methods introduced in [17, 18] are clearly very different from actual cloaks (again, by cloaking we mean the reduction of an arbitrary object's total scattering cross section), these approaches are not considered in this report as "cloaks".

Based on the above discussion, at this point we can identify two different approaches to obtain cloaking: coordinate transformation and invisibility. These two approaches can be considered as the main cloaking techniques, based on which many other variations of cloaking devices are designed. In addition, this report deals with another, more recently proposed method of cloaking. This method is based on the use of so-called transmission-line networks that can be designed for cloaking of specifically shaped objects [19].

1.4 Rationale of the report

This work mainly focuses on two specific cloaking techniques: the chiral cloak and the transmission-line approach mentioned above. The chiral cloak, which is based on the use of chiral particles for creating the needed ε_r and μ_r, is an example of the general coordinate-transformation approach. These two cloaking techniques are studied in detail in Sections 2 and 3, respectively, with emphasis on design aspects. These two techniques were chosen because of the experience the DRSE team has of these subjects, and because they both have important benefits with regards to other cloak designs found in the literature.

The fundamental limitations of various cloaking approaches present important insight on the applicability of these devices and techniques, especially from the space application point of view. The fundamental limitations of the chiral and transmission-line cloaks are studied in Section 4. The three main cloaking methods (coordinate transformation, invisibility, transmission lines) are compared with each other in Section 5, where also the benefits and drawbacks of these methods are listed.

Section 6 is focused on a few specific example applications, where the transmission-line approach to cloaking has been seen to have potential. The development of the coordinate transformation to more general approaches to transform fields are presented in Section 7. These studies are related to cloaking, but actually they have a much more general meaning and can find applications for various purposes. Two different generalizations are presented, one derived by the DRSE research team and one derived by the ACT.

[1] A hard surface can be defined by the following boundary conditions: $\mathbf{H}_l = 0$, $\mathbf{E}_l = 0$, where l denotes the propagation direction along the surface. See more references in [17].

2 Chiral cloak

2.1 Operation principle and design guidelines

The operation principle of any coordinate-transforming cloak is based on the transformation of the spatial coordinates of the electromagnetic (EM) space in such a way that a volume in the physical space ("lab space") is left with zero field [4, 5]. The transformation of coordinates can be done in many ways, see Fig. 1 [5]. For cloaking applications, it is preferred to make the transformation in such a way that the rays of impinging electromagnetic radiation go around a volume in the lab space. The relation between the two coordinate systems can be thought of as stretching of the EM space. It is easy to imagine that when the coordinates of the EM space are "stretched", there is created a volume which does not contain "space" at all. If a cylinder in the lab space corresponds to a line in the EM space, we have a cylindrical cloak and if a sphere in the lab space corresponds to a point in the EM space, we have a spherical cloak, see Fig. 2 [5].

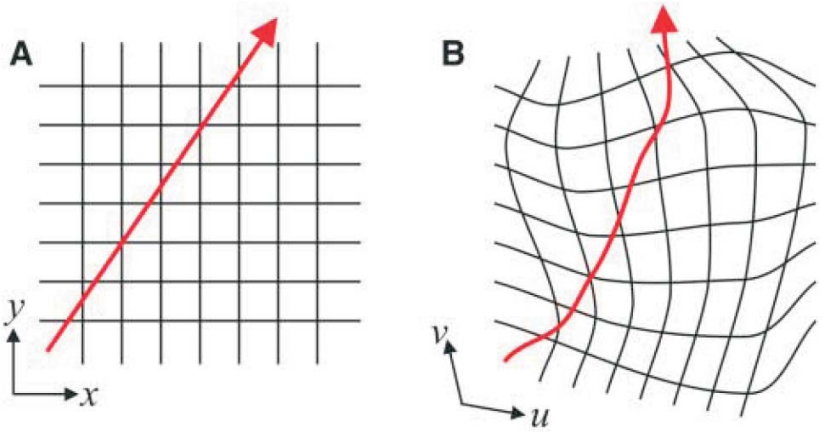

Figure 1: (a) A field line in free space with the background Cartesian coordinate grid shown. (b) The distorted field line with the background coordinates distorted in the same fashion. The field in question may be the electric displacement or magnetic induction fields **D** or **B**, or the Poynting vector **S**, which is equivalent to a ray of light [5].

The recently proposed electromagnetic cloaks based on coordinate-transformation approach demand very exotic and difficult-to-realize material parameters of cloaking media. In particular, for dual-polarization operation the relative effective permittivity and permeability must be equal. The known designs of the radial EM properties utilize either only magnetically-polarizable particles (split rings)[2] [8] or electrically polarizable particles (needles) [9]. This means that these devices can work only of one of the two orthogonal polarizations. Conceptually one can try to mix the two types of the particles together, but this is not a simple—if at all possible—solution, because the particles will strongly interact with each other, creating double-resonance response.

We have recently proposed to use particles of only one kind, which, however, give both electric and magnetic responses [20]. The main advantage of this design is that both electric and magnetic responses are produced by the same particles, so that the frequency dispersion

[2]Split rings possess also electric response but only in the plane of the particles.

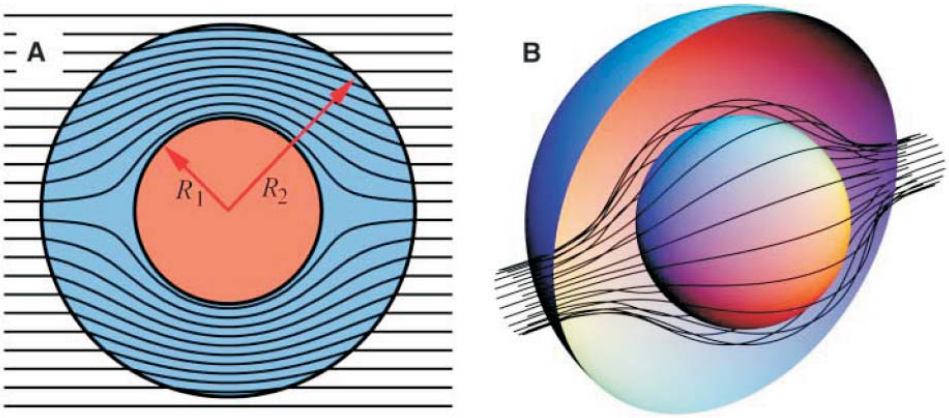

Figure 2: A ray-tracing program has been used to calculate ray trajectories in the cloak, assuming that $R_2 \gg \lambda$. The rays essentially following the Poynting vector. (a) A two-dimensional (2D) cross section of rays striking our system, diverted within the annulus of cloaking material contained within $R_1 < r < R_2$ to emerge on the far side undeviated from their original course. (b) A 3D view of the same process [5].

of both effective material parameters can be tuned to be very similar. The idea of using chiral particles [3] to realize artificial magneto-dielectrics with equal effective parameters was, to the best of our knowledge, first proposed in [22] and also described in [1]. Here we discuss how this approach can be used for cloaking applications.

The "ideal" distributions of relative permittivity and permeability for a cylindrical cloak read [5, 8]

$$\varepsilon_\rho = \mu_\rho = \frac{\rho - a}{\rho}, \quad \varepsilon_\varphi = \mu_\varphi = \frac{\rho}{\rho - a}, \quad \varepsilon_z = \mu_z = \left(\frac{b}{b-a}\right)^2 \frac{\rho - a}{\rho}, \tag{1}$$

where a is the cloak internal radius and b is the external radius.

For special cases, depending on the cloak that is needed (polarization of the electromagnetic wave from which an object needs to be cloaked is limited, etc), these equations can be simplified, since the dispersion relation inside the cloak remains unaffected if the values of the products $\varepsilon_\rho\mu_z$, $\varepsilon_\varphi\mu_z$, $\mu_\rho\varepsilon_z$, and $\mu_\varphi\varepsilon_z$ do not change [9].

Equations (1) were simplified for a cloak operating only for TE-polarization (to reduce complexity) to [8]

$$\varepsilon_z = \left(\frac{b}{b-a}\right)^2, \quad \mu_\rho = \left(\frac{\rho - a}{\rho}\right)^2, \quad \mu_\varphi = 1, \tag{2}$$

while for TM-polarization they can be simplified to [9]

$$\mu_z = 1, \quad \varepsilon_\varphi = \left(\frac{b}{b-a}\right)^2, \quad \varepsilon_\rho = \left(\frac{b}{b-a}\right)^2 \left(\frac{\rho - a}{\rho}\right)^2. \tag{3}$$

[3] *chirality* means handedness: an object or a system is called chiral if it differs from its mirror image, and its mirror image cannot be superposed on the original object.

For the chiral cloak operating simultaneously for both polarizations, the simplification of (1) was chosen to be [20]

$$\varepsilon_\rho = \mu_\rho = \left(\frac{b}{b-a}\right)\left(\frac{\rho-a}{\rho}\right)^2, \quad \varepsilon_\varphi = \mu_\varphi = \varepsilon_z = \mu_z = \left(\frac{b}{b-a}\right). \tag{4}$$

The distribution (4) is chosen this way in order to obtain simplification of the material parameters in terms of manufacturing: by choosing the transformation to have radial (i.e., ρ-) dependence only for the radial part of ε and μ, this material is possible to create with spirals as, e.g., shown in Fig. 4. The simplification (4) naturally produces material relations that do not satisfy the ideal boundary conditions for cloaking, i.e., there will be some reflections from the cloak surface, as will be evident also for materials satisfying (2) or (3). The confirmation of the cloaking effect using the simplified material parameters (4) was presented in [20] by full-wave simulations, see Fig. 3.

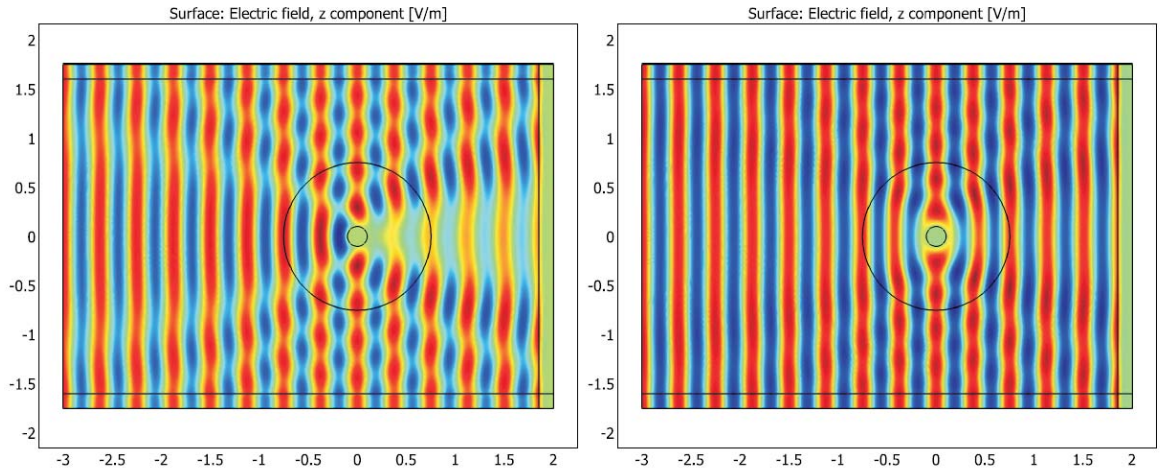

Figure 3: Full-wave simulated electric field for a plane wave incident on a copper cylinder (left) and on a cloaked copper cylinder (right) [20]. The outer and inner radii are $b = 7.5$ cm and $a = 1$ cm, respectively. The operational frequency is $f = 8$ GHz. In this case the diameter of the cloak is $4\,\lambda$.

To design the cloak the necessary characteristics as well as the density of the inclusions of chiral particles has to be determined. Thereto we can make use of the Clausius-Mossotti formula valid for sparse mixtures [13]

$$\varepsilon_r = 1 + \frac{n\alpha_e}{\varepsilon_0 - \frac{1}{3}n\alpha_e}, \quad \mu_r = 1 + \frac{n\alpha_m}{\mu_0 - \frac{1}{3}n\alpha_m} \tag{5}$$

where α_e is the electric and α_m is the magnetic polarizability of a single inclusion and n is the inclusion density. Here we assume that the chirality of the mixture is compensated by using an equal number of right- and left-handed particles, i.e. the chiral constant becomes zero.

By demanding $\varepsilon_r = \mu_r$ we find that the polarizabilities must satisfy

$$\frac{\alpha_e}{\varepsilon_0} = \frac{\alpha_m}{\mu_0} \tag{6}$$

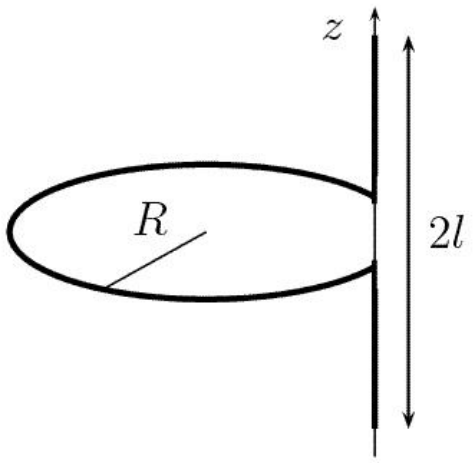

Figure 4: Geometry of the spiral. The loop with radius R lies in the plane that is orthogonal to the z-axis of the figure (note that in the described cloak the orientation of the spiral is not the same as in this figure, the spirals are placed radially in the cloak [20].)

We call such inclusions “optimal spirals". The particular inclusion shape can vary. It can be the so-called “canonical spiral" which consists of a loop (radius R) connected to the wire of length l (Fig. 4). Or it can be a usual spiral of one or more turns. Using the known analytical models of chiral particles [24], the particle shape can be optimized to meet the requirement (6). For the canonical spiral the condition reads

$$l = k\pi R^2. \tag{7}$$

Next, we can provide the desired profile of the permittivity and permeability along ρ by varying the density of inclusions n. This can be solved from (5):

$$n = 3\varepsilon_0 \Re\left\{\frac{1}{\alpha_e}\right\}\frac{\varepsilon_\rho - 1}{\varepsilon_\rho + 2} \tag{8}$$

where ε_ρ is the target value of the permittivity.

Finally, let us discuss the potential advantages and disadvantages of the chiral cloak.

- It works for both polarizations using particles of only one kind.
- The frequency dispersion of both permittivity and permeability is nearly the same (close to the resonant frequency).
- The optimization of spiral to balance electric and magnetic response also optimizes the effectiveness of field-particle interactions [25].
- The complicated particle shapes make fabrication more difficult, especially for optical applications.
- The effect of losses in the inclusions is expected to be similar to that in the known design based on split rings.

2.2 Potential for high-frequency operation

Manufacturing chiral cloaks for high-frequency (up to the visible light) is a challenge mainly due to the complicated and three-dimensional shapes of the inclusions. Two relatively novel nano-manufacturing techniques can be potentially used to realize such structures: development of 3D chiral nanoshells from strained films and physical vapour deposition technique (reactive sputtering).

Physical vapour deposition technique employs oblique angle deposition and controlled substrate motion to form a structure composed of three-dimensional nanometre scaled columns of designed shape. It allows the fabrication of films with a carefully engineered structure at the sub-micron scale. The coatings can be deposited by reactive sputtering involving a metallic target and oxygen + nitrogen as reactive gases. Very recent improvements involve gas pulsing to cope with the instabilities of the reactive sputtering process. The Reactive Gas Pulsing Process (RGPP) [23] can be implemented to get various shapes of gradients and compositions through the thickness (close to 500 nm) of the film. With RGPP technique, gradients through the film can be adjusted from the substrate/coating interface to the top surface of the coating, i.e. from oxide to nitride or inversely, and with different profiles.

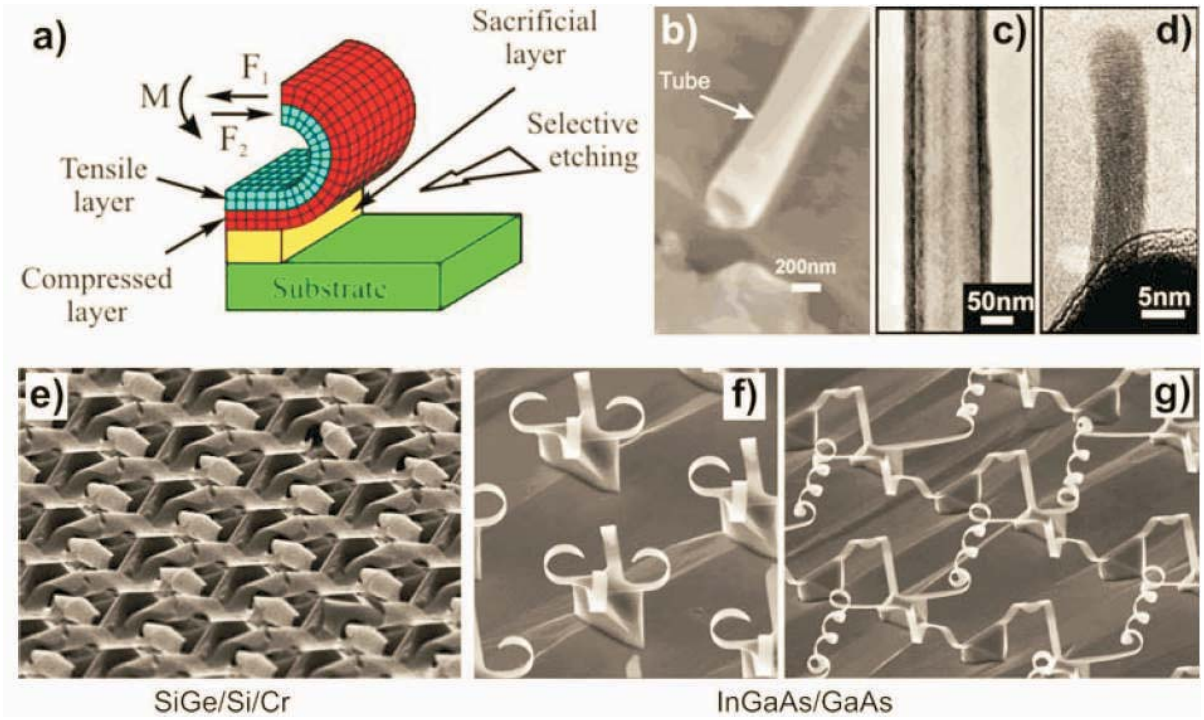

Figure 5: a) Schematic illustration of the detaching from the substrate and bending of the strained film; b) Example of Au/Ti nanotube with the length of 10 cm; c) InGaAs/GaAs multiturn (chiral) nanotube; d) InGaAs/GaAs one-turn nanotube; e), f), g) - examples of regular chiral arrays of metal-semiconductor and semiconductor shell structures.

Alternatively, 3D spiral particles of nano-dimensions can be manufactured using nanoshell formation from strained films [26–28]. A multilayered thin film containing layers of different strains is grown on the substrate and lithographically patterned; being detached from the

substrate (for instance, by etching of underlying sacrificial layer) the planar thin-film structures transform into 3D shells under action of internal strains. This method allows fabrication of a great variety of architectures in the form of precise 3D bent, corrugated, and rolled-up nanoshells from different materials (dielectrics, metals, semiconductors, and hybrid ones). It is suitable for mass production of precise elements with local curvature radii from 100 micrometers to one nanometer and fully compatible with the IC technology. Variety of possible architectures, precision and scalability to nanosizes, reproducibility make this approach very promising for mass fabrication of metamaterials. Individual metal and semiconductor nanotubes are shown on Fig. 5, individual helices with diameters down to 7 nm were demonstrated [26]. To the best of our knowledge, optical characterization of electromagnetic properties for such nanostructures has not been reported yet. Therefore, we cannot discuss their potentials for designing invisibility devices in more detail.

3 Transmission-line cloak

This section deals with an approach to cloaking based on so-called transmission-line (TL) networks as "material" blocks of different shapes, so that inside these networks there are volumes of space where there is effectively zero field. The difference to the field-transformation cloaks discussed in Section 2 is that there is no "stretching" of space or time coordinates. The cloaking effect is simply produced by allowing field propagation only in certain parts of the volume that is occupied by the TL network, while the wave propagation properties in the TL network are kept similar to the surrounding medium, which is free space in all of our examples.

The transmission-line network can be formed by a mesh of simple unloaded transmission lines, connected at each intersection, or the transmission-line network can be loaded by some bulk reactive elements (capacitors or inductors) at each cell. In the first case of an unloaded mesh, the structure is dispersion-free, if the filling dielectric does not change its permittivity in the operation frequency band. This gives a good potential for broad-band operation and for cloaking from pulses. However, its phase-delay factor is different from that of free space (at least $\sqrt{2}$ larger for a two-dimensional mesh). This means that there is inevitably some "shadow" behind the cloak due to a phase mismatch between the wave coming through the cloak and the wave in free space. In case of the loaded mesh, it is possible to chose the loads so that the phase constant of the mesh is the same as of free space, eliminating the shadow. This, however, comes at a cost of frequency dispersion of the effective parameters of the mesh, which means limited operation bandwidth. In this report we consider the unloaded mesh cloak.

3.1 Operation principle and design guidelines

The operation principles, basic design guidelines, and some specific examples of TL cloaks are presented in detail in [19, 21, 29–31]. In short, the design concerns two issues: dispersion and impedance. *Dispersion* means dependence of the propagation factor of waves along the mesh of connected transmission lines on the frequency. For the ideal operation of the cloak (simulating free space), dispersion should be the same as for plane waves in free space, that is, the propagation constant k and the frequency ω are proportional ($k = \omega/c_0$, where c_0 is the speed of light). *Impedance* refers to the ratio between the averaged transverse (to the propagation direction) electric and magnetic fields in free space and in the transmission-line network. Again, for the ideal operation of the cloak the impedance inside the cloak should not change, providing reflection-free operation. In free space, the wave impedance is $\eta_0 = \sqrt{\mu_0/\epsilon_0} \approx 377$ Ohm.

With unloaded transmission lines it is not possible to design a mesh with the ideal dispersion (ideal phase velocity). For this reason, for electrically large cloaks there is an additional design requirement of making sure that the electrical diameter of the cylindrical or spherical cloak is such that the phase difference between the wave passing through the cloak and the wave travelling the same distance in free space approximately equals $2\pi n$ ($n = 1, 2, 3, \dots$) for the specified frequency range [30, 31].

In the case of an unloaded 2-D network, the phase velocity in the network is [19]

$$v_{\text{phase}} = \frac{c_0}{\sqrt{2}}, \tag{9}$$

and in the case of an unloaded 3-D network it is

$$v_{\text{phase}} = \frac{c_0}{\sqrt{3}}, \tag{10}$$

where c_0 is the speed of light in vacuum. In both cases the material filling of the transmission lines is assumed to be vacuum, since filling by some other material will decrease the phase velocity even more and therefore will increase scattering.

The importance of studying the dispersion is to find out the region of isotropic wave propagation inside the network [19]. Note that in some cases the isotropy of the network is not required (i.e., when the wave needs to go only along one direction), but for cloaks in the general sense (cylindrical and spherical cloaks), the propagation inside the network needs to be isotropic in order to have the cloak operating the same way for all angles of incidence. What restricts the isotropy, is simply the period of the network [19]. For example, with the period of 8 mm, the isotropic propagation is obtained for all frequencies below ~ 4 GHz, where 8 mm$\approx \lambda_0/10$, see Fig. 6.

The importance of studying and designing the impedance of the network comes from the necessity to have the network properly matched with free space, or some other medium surrounding the cloak. As can be seen e.g. from the impedance plots of Fig. 7, the impedance of the network varies very slowly as a function of the frequency. The optimal impedance of the network (e.g., $120\pi\ \Omega$ for free space matching) can be obtained only at a single frequency point. Nevertheless, due to the slow variation of the impedance, we can expect to obtain almost perfect matching with the surrounding medium in a large frequency band [19]. Therefore, for designing a cloak for a certain frequency region, one must 1) make sure that the network is isotropic in the whole frequency band (if isotropy is needed), i.e., make sure that the period of the network is small enough, and, 2) design the TLs of the network so that the optimal impedance matching is obtained around the center frequency of the needed frequency band.

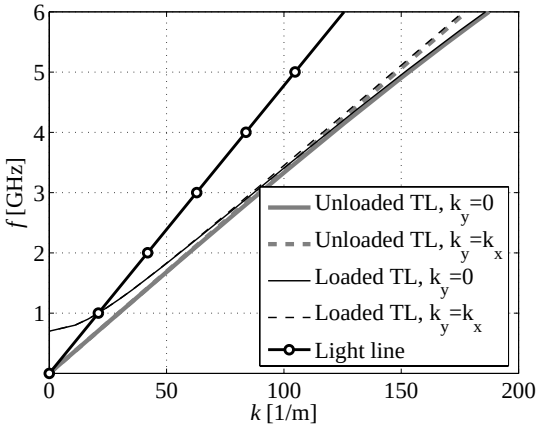

Figure 6: Analytically calculated dispersion curves of unloaded and loaded TL networks for axial and diagonal propagation [19]. The period of the networks is 8 mm.

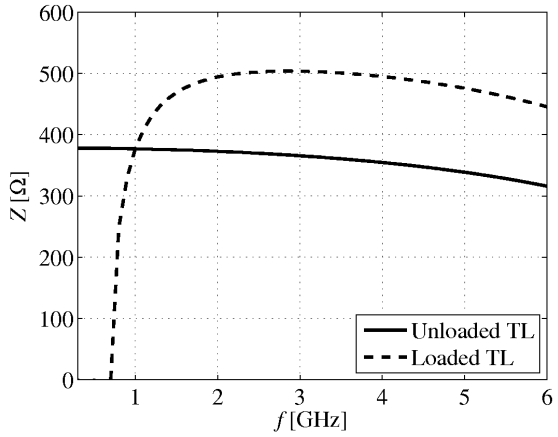

Figure 7: Impedance of unloaded and loaded TL networks [19]. Both networks are designed for the optimal impedance matching with free space ($120\pi\ \Omega \approx 377\ \Omega$) at the frequency of 1 GHz. Only axial propagation in the networks is considered. For other directions of propagation, the impedance is different in the frequencies where the propagation is anisotropic.

3.2 Example cloaks

3.2.1 Electrically small cylindrical cloak

An electrically small cylindrical cloak (with the diameter smaller than the wavelength of the electromagnetic radiation) was designed and simulated in [29]. The optimal impedance matching with free space was designed to be around 2 GHz, and at that frequency the diameter of the cylindrically shaped array of metal rods, that is supposed to be cloaked with the TL network approach, was approximately one third of the wavelength. Significant reduction of the total scattering cross section of this object in a relatively large frequency band was demonstrated, see Fig. 8 [29].

Experimental demonstration of this type of cylindrical TL cloak is still do be done, but the measurement setup at DRSE unfortunately is not capable to conduct measurements at such low frequencies, as will be discussed in the following subsections. In order to enable the experimental demonstration of this cloak, it was decided that a new cloak should be designed for operation above 3 GHz, since already at 3 GHz the available measurement setup is useable.

Following the design principles of [29] and the references therein, we designed a cloak for operation around the frequency 3 GHz, as shown in Fig. 9. It is possible to distinguish in the center region of the structure the concealed metallic wires. A square TL network spans within the gaps left between the wires. The triangular blades surrounding the network and connected to it are responsible of emitting and capturing the electromagnetic waves. It is possible to change the length of those blades by increasing its width. As compared to the cloak in [29], we have basically just scaled the dimensions down to increase the operation frequency, see Table 1 in [31] for details. The designed cloak was modelled with Ansoft HFSS full-wave commercial electromagnetic simulation software. Since the problem at hand is inherently a 2-D-problem, we can simplify the simulation model by taking only one period of the cylindrical cloak and assigning PEC (perfect electric conductor) boundaries in the xy-planes for modelling of the infinite periodic structure. Note that the electric field is always parallel to the z-axis in this case.

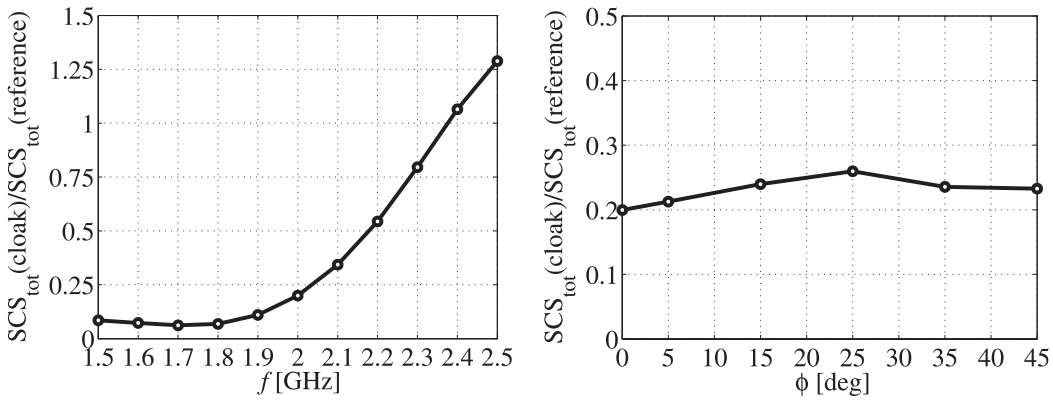

Figure 8: (a) Ratio of the HFSS-simulated total SCS of cloaked and uncloaked reference objects as a function of the frequency. (b) Ratio of the HFSS-simulated total SCS of cloaked and uncloaked reference objects at the frequency 2 GHz, as a function of the incidence angle of the illuminating plane wave [29].

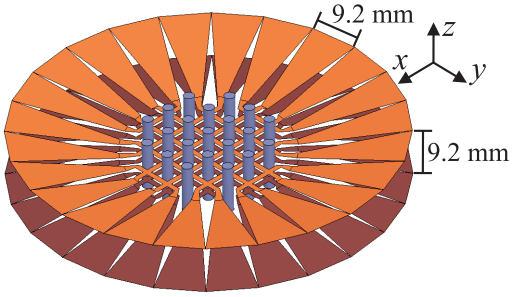

Figure 9: HFSS-model of the simulated TL-cloak (with an array of metallic rods, that we want to cloak, inside) having diameter about one third of the wavelength at the center frequency of operation.

The reference object, i.e., the object that we want to cloak or reduce scattering from, is in this case a cylindrical array of PEC rods parallel to the z-axis (see Fig. 9). We simulate the model and calculate the scattering to all angles ϕ from the solution and compare this scattering data to another simulation model which encompasses only the reference object. To see how good the obtained "cloaking" is, we calculate the total scattering cross sections from both simulation models and look at their ratio as a function of the frequency. See Fig. 10 for the result, demonstrating the large bandwidth where the cloaked scatterer scatters less than the uncloaked scatterer (i.e., the ratio of the total SCS is below 1) [31]. In fact, the bandwidth is so large that the band where the SCS-ratio is below 1, is not visible due to the finite number of frequency points that were simulated. See [31] for a more detailed discussion of the results.

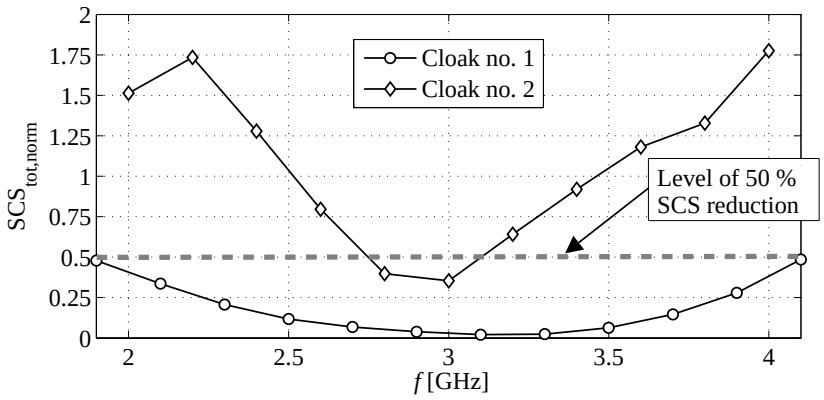

Figure 10: Ratios of the HFSS-simulated total SCS of cloaked and uncloaked reference objects as a function of the frequency [31]. Cloak no. 1: electrically small cloak. Cloak no. 2: electrically large cloak.

3.2.2 Electrically large cylindrical cloak

An electrically large cylindrical cloak, with the diameter larger than the wavelength of the electromagnetic radiation, was designed and simulated in [30]. Based on those full-wave simulations, the most significant reduction of the reference object's total scattering cross section was obtained around 3 GHz, and at that frequency, the diameter of the cylindrically shaped array of metal rods (that is supposed to be cloaked with the periodic array of TL networks) was approximately four wavelengths. Improved reduction of the total scattering cross section of this object, at the design frequency of 3 GHz, is now demonstrated, see Fig. 10. This improvement is obtained simply by tuning the network impedance of the previous design [30]. See [30, 31] for a more detailed discussion of the design and the results.

3.2.3 Experimental demonstration

An experimental demonstration of "cloaking" with the proposed transmission-line approach has been developed within the project. In this case the studied 2-D cloak has a square shape for simplicity and the measurements are conducted in a measurement cell (waveguide) that allows us to effectively measure the situation of an infinitely periodic structure with just one period of the structure inside the waveguide (basically the same idea as in [8]).

The results presented in [32] demonstrate that the network impedance can be matched with free space in a real-life scenario with real transmission lines and manufacturing non-idealities, etc. The field emitted by a line source is coupled into the network and the field travels through the TL-network, that encompasses an array of metallic rods, coming out on the other side of the network. When the same measurement is conducted without the network in place (i.e., only the array of metallic objects is illuminated), the fields are seen to strongly scatter from the front edge of the array. This is obvious since the period of the array of rods is about one sixth of the wavelength (an electrically dense array of metallic objects is basically impenetrable to the impinging electromagnetic field, see, e.g., Fig. 12 in [19]). See Fig. 11 for the measured electric field snapshots [32]. The description of the measurement setup along with the other obtained results are presented in more detail in [32].

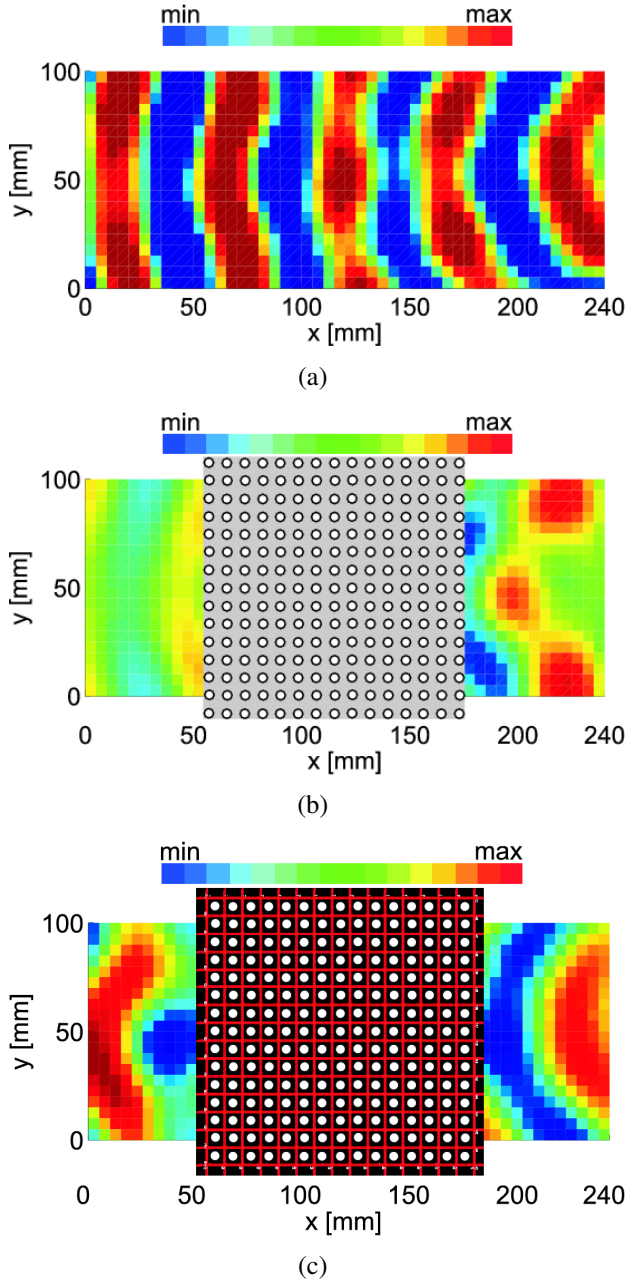

Figure 11: Color online. Snapshots of the measured time-harmonic electric field distributions at 5.85 GHz. The source is placed at $x = 250$ mm, $y = 50$ mm. (a) empty waveguide, (b) reference object inside the waveguide, (c) reference object and the transmission-line network inside the waveguide. The "transition layer" connected to the network is not shown in (c) for clarity [32].

3.3 Potential for high-frequency operation

For the frequency range $f < 100 \ldots 300$ GHz subwavelength (cross section smaller than quarter-wavelength) waveguides with low losses and comparatively small dispersion represents nothing exotic. This can be for example a microstrip or even a two-wire line.

For higher frequencies subwavelength waveguides are exotic. The following reasons can be identified:

- Since the wavelength is short, the transmission line becomes optically long (that leads to more strong attenuation and signal distortion than for an optically short line with a given loss per unit length and given dispersion).
- The metal wires or strips become lossy due to plasmon oscillations excited in them.
- Known dielectric waveguides (e.g. integrated waveguides, coated and non-coated rods, structured or non-structured fibers) are not subwavelength at THz frequencies (0.5-3 THz) and moreover at optical (from far infrared to visible) frequencies. This is so because low-loss dielectrics have moderate permittivity that does not shorten the wavelength enough to concentrate the guided mode field in a subwavelength cross section.

The study of the huge literature devoted to THz, far IR, mid-IR, near IR waveguides and waveguides for visible light shows that before the spurt of metamaterials in the XXI century no researcher considered the subwavelength concentration of the field in a waveguide as an objective [33–36]. The problem of the miniaturization of optical waveguides up to the subwavelength level has been recently considered of importance since new optical applications (nanochips, nanofilters, nanoimaging devices) were indicated in papers [40–42].

At microwaves only hollow metal waveguides and dielectric rod waveguides operate with wave beams. In the THz and optical ranges majority of known transmission lines guide wave beams. A subwavelength THz microstrip (Goubau) lines (effective transversal size $0.2 \ldots 0.3\lambda$) even with expensive sapphire or hollowed quartz substrates have strong ohmic losses and the propagation in them is practically possible only to the distance of the order of a few mm [39]. The same concerns coplanar THz lines [38]. In [37] low-loss flexible and subwavelength (due to high permittivity of the plastic core) THz fibers were reported but their frequency band is essentially restricted by $300 - 500$ GHz where the dielectric losses start to grow fast versus frequency from the 0.5 THz threshold.

At optical frequencies the situation is even worse, because in addition to high losses two other main issues take place : stronger dispersion and narrower frequency band. In the visible range the best known result for subwavelength waveguides is the signal transmission to the distance of the order of 100 λ obtained using nanochains of silver colloids. The mechanism of the subwavelength propagation of light is the electrostatic coupling between localized plasmons [43]. In fact, after publication of seminal works [40–42] subwavelength optical waveguides have been created only for the visible range at the price of rather high losses, strong dispersion and narrow frequency band of guided waves [43]. The worst situation corresponds to the far IR (3-10 THz) where the halcogenide glass becomes opaque (at 10 THz from higher frequencies) and quartz becomes lossy (at 3 THz from lower frequencies). Only diamond, berillium and sapphire can serve as the substrate of a microstrip or a coplanar line. Simultaneously ohmic losses in metals strongly grow as compared to the THz range. The literature data on subwavelength waveguides is not available for this range. Theoretically such waveguides as microstrip or coplanar lines are still possible here, but they will be expensive and their maximal length hardly will exceed 50-100 λ. For mid- and near-infrared ranges subwavelength waveguides can be probably obtained with the same attenuation as their analogues in the visible

range if one uses special halcogenide glass, diamond, sapphire or quartz as the matrix. For these frequency ranges one should use surface plasmons instead of localized plasmons, and, respectively, a structure with several parallel metal nanowires [44] instead of a chain of metal nanoparticles [42].

For instance, a low-loss and weakly dispersive THz or optical transmission line guiding the light to the distance exceeding $1 \ldots 2$ cm should present a cross section not smaller than $\lambda/2$ (λ is the wavelength in the surrounding medium). Otherwise, the length of the waveguide should be restricted by a few mm for the THz range, by one-two hundreds μm for the IR range and by several tens μm for the visible. In principle, one can find exotic ways to overcome these limits (the use of active elements, etc.) but we do not consider here these prospectives. In this section we have mainly focussed on the commonly recognized and broadly cited literature data.

4 Fundamental limitations of selected cloaking techniques

In this section we list the most important fundamental limitations of two different cloaking techniques: the coordinate transformation approach and the transmission-line approach.

It must be noted that the following limitations apply as such for *passive* cloaks, i.e., we assume that the cloak structures or materials are composed of only passive inclusions. If we allowed sources to be placed inside these materials, the fundamental limitations regarding, e.g., dispersion, would not apply anymore [45]. Although the introduction of sources would allow more efficient cloaks, e.g., in terms of bandwidth, the realization of such active metamaterials is not considered to be feasible with the current technology. Introduction of sources would also bring completely new problems in the design of cloaks, e.g., the inherent problem of stability related to metamaterials with active circuits [46].

4.1 Coordinate-transforming cloaks

4.1.1 Energy propagation

The goal of the coordinate-transforming cloaks as proposed e.g. in [4, 5, 20], is that the electromagnetic fields surrounding the cylindrical or spherical cloak are guided around the cloaked region in such a way that the phase front in front and behind the cloak are not disturbed by the cloak. When cloaking from waves in free space, this type of cloaking naturally requires that the phase velocity inside the cloak exceeds the velocity of the same wave in free space. This requirement can be achieved with, e.g., certain types of (meta)materials composed of resonant inclusions [8].

The main problem is that in any real-life situation, where we can never expect to work at a single frequency point, the waves that need to be guided inside the cloak carry some energy [47]. The energy velocity (group velocity) cannot exceed the speed of light in any passive material. If the cloak is meant to operate in a very narrow frequency band (as, e.g., in [8]), this non-ideality of group velocity will probably not deteriorate the cloak operation dramatically. When a larger operation bandwidth is required, the scattering is not solely defined anymore by the scattering of a time-harmonic wave. Instead, the energy pulse that hits the cloak will be distorted. Additionally, it is well known that not only the energy velocity is smaller than the speed of light, but it decreases as the phase velocity increases. This means that close to the inner boundary of the cylindrical or spherical cloak, the group velocity will approach zero as the phase velocity approaches infinity [48, 49]. See Fig. 12 for a snapshot of ray propagation inside a field-transformation cloak when rays going through the outer region of the cloak have already passed the cloak, while the rays going through the inner part are delayed [49].

The problem of energy propagation in any passive coordinate-transformation cloak is critical for real-life application. In practice this means that verification of scattering from designed cloaks cannot be understood only based on, e.g., simulations conducted in the frequency domain and that the operation of the cloak will much depend on the shape of the energy pulse that hits the cloak.

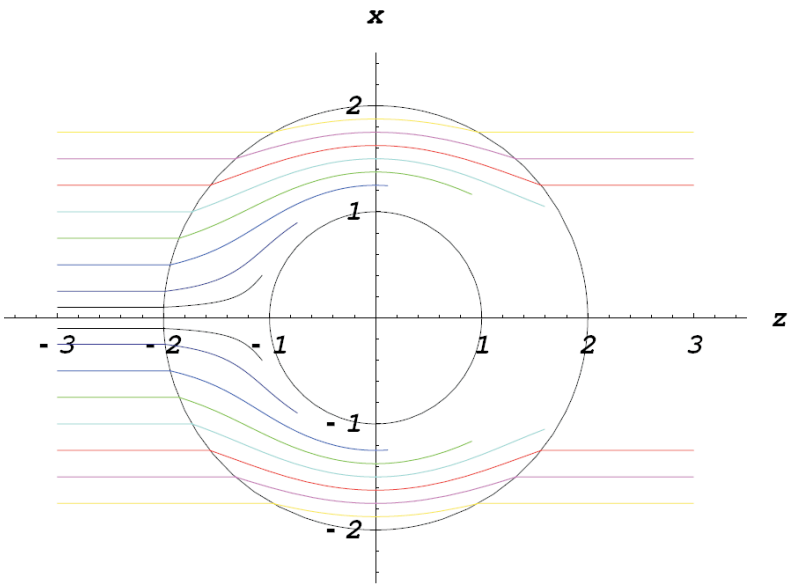

Figure 12: Ray tracing for beams entering the cloak at different points along the x-axis [49].

4.1.2 Dispersion and bandwidth

It is obvious that any field-transformation cloak will require (meta)materials having exotic material parameters, such as $\varepsilon_r < 1$ and/or $\mu_r < 1$. The realization of this kind of material parameters with passive materials is possible only while allowing strong dispersion [1]. Thus, the bandwidth of operation for any field-transformation cloak (bandwidth where the total scattering cross section can be significantly reduced) will be mostly limited by the dispersion of the material parameters. In [48] the bandwidths of two different cloaks were compared. One cloak was designed for single-frequency operation and the other for a finite bandwidth. Results indicate a relative bandwidth of operation, where the total scattering cross section of a PEC cylinder was reduced with the cloak, of a few percents in the best case. Furthermore, this result does not take into account the effect of the non-ideal energy propagation velocity, as discussed in the previous subsection. See Fig. 13 for the simulated total scattering cross sections, normalized to the scattering of a bare PEC cylinder [48].

4.1.3 Losses

Losses will be present in any concrete cloak, especially if resonant inclusions are needed. This fact arouses a fundamental limitation since an ideal cloak would need a lossless material. Also, losses impose another problem, related to the design of the metamaterial cloak: in order to obtain impedance matching, with free space for example, the material parameters at the outer surface of the cloak, i.e., at the interface with free space, must satisfy for a cylindrical cloak

$$\varepsilon_\rho = \frac{1}{\varepsilon_\varphi}, \tag{11}$$

$$\mu_\rho = \frac{1}{\mu_\varphi}, \tag{12}$$

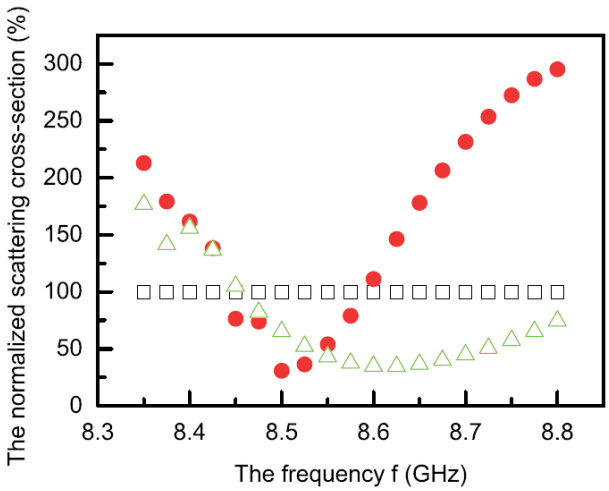

Figure 13: Total scattering cross sections of a PEC cylinder (squares), and two coordinate-transforming cloaks (circles and triangles), all normalized to the total scattering cross section of the PEC cylinder [48].

while a spherical cloak requires

$$\varepsilon_\rho = \frac{1}{\varepsilon_\varphi} = \frac{1}{\varepsilon_\theta}, \tag{13}$$

$$\mu_\rho = \frac{1}{\mu_\varphi} = \frac{1}{\mu_\theta}, \tag{14}$$

where the subscripts ρ, φ, and θ mark the radial and angular components of the relative material parameters.

Looking at the previous equations, one can easily notice that the existence of losses makes perfect impedance matching impossible with passive materials (if, e.g., ε_ρ is lossy, ε_φ must be "active").

4.1.4 Cloaking of electrically large bulky objects

This limitation does not apply to this cloaking approach, since the cloak can hide a complete volume such as a cylinder or a sphere.

4.1.5 Operation at very high frequencies

This limitation does not apply to this cloaking approach. There is no *fundamental* limitation on the operation frequency.

4.2 Transmission-line cloak

As the main operation principle of the transmission-line cloak is to transport waves inside a network of transmission lines, leaving the space between adjacent TLs "undetected" (see Section 3

for more details), the fundamental limitations are not so severe as e.g. with the field transforming cloaks. This is simply because there is no need to create "materials" with wave propagation velocities exceeding the speed of light in vacuum.

4.2.1 Energy propagation

This limitation does not apply to this cloaking approach, since a cloak can be made using networks of unloaded transmission lines. In this case the group (energy) velocity is equal to the phase velocity [19]. If the ideal phase velocity is required, the energy propagation velocity will be different than the phase velocity and the cloak will be more dispersive [19]. As discussed in Section 3, this ideal phase velocity can be achieved by capacitive and inductive loading.

4.2.2 Dispersion and bandwidth

As discussed in [19] and in Section 3, the use of unloaded transmission-line networks has an inherent drawback when cloaking objects placed in free space: the phase velocity of the wave inside the network is slightly slower than the speed of light in vacuum. This problem can be overcome by periodically loading the network by, e.g., capacitors and inductors, but this solution strongly restricts the bandwidth of operation in terms of both dispersion and impedance and makes the energy propagation velocity different from the phase velocity [19]. That is why the most significant benefits from using the transmission-line approach (i.e., simple structure, large bandwidths) are obtained only by employing the unloaded TL networks. As has been observed in Section 3, the limitations regarding the phase velocity are actually not a severe problem since very efficient cloaking can be obtained even with unloaded TL-network cloaks.

4.2.3 Losses

Losses will be present in any concrete cloak. This fact arouses a fundamental limitation since an ideal cloak should be lossless. In the case of the TL-cloak, the losses are due to ohmic losses in metal, which are known to be very moderate at low frequencies (approximately up to 300 GHz, see Section 3.3).

4.2.4 Cloaking of electrically large bulky objects

The first limitation of a TL cloak concerns the impossibility of wrapping a continuous object, as it was pointed out in previous sections. However, it is possible to consider the object as if it were composed of discrete parts, while keeping the same effective cross-section. The size of the discrete parts can not be freely chosen. It should be smaller than the period of the TL network in order to guarantee isotropic wave propagation [19].

The limitation set to the cloaked object's inclusions is somewhat misleading, since the adjacent inclusions can be connected (physically, electrically, etc.), which means that the cloaked object can actually be a two- or three-dimensional mesh, see Fig. 14.

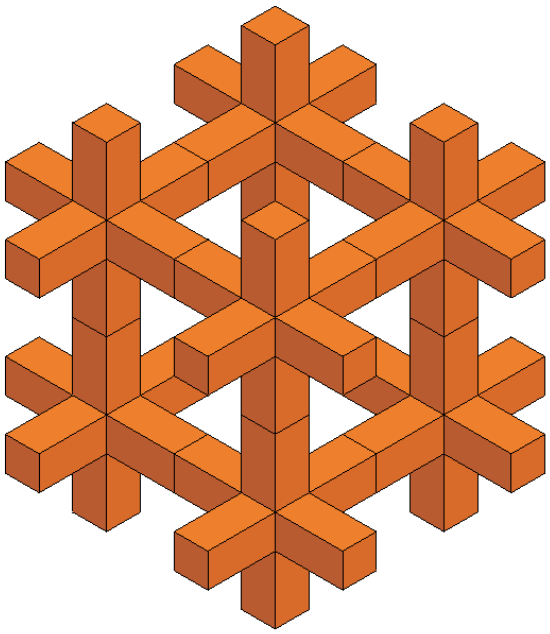

Figure 14: An example of a three-dimensional mesh ($2 \times 2 \times 2$ unit cells) that can be cloaked with a 2-D or a 3-D TL-network.

4.2.5 Operation at very high frequencies

The principle of operation of any transmission-line cloak is the coupling of waves from a homogeneous medium surrounding the cloak inside a TL network. It is well known that trasmnission lines operating at very high frequencies and satisfying all the aforementioned conditions do not exist. The limitations of the high-frequency operation were thoroughly discussed in Section 3.3. There we conclude that approximately below 300 GHz there are no fundamental problems in realization of transmission lines. In contrast, above that frequency the transmission lines are either too large (not subwavelength) or too lossy and dispersive.

5 Comparison of different cloaking techniques and approaches

In this Section we go through the most important cloaking techniques and try to summarize their benefits and drawbacks. Here we restrict ourselves to consider only passive structures and materials. Some cloaking techniques are left out from this comparison because of their limitations as compared to the techniques studied here (for example, the structure proposed in [18] can cloak only dipole scatterers and the structure proposed in [17] works only for a fixed angle of incidence).

In Table 1 we have summarized some main properties of the following cloaking techniques: 1) coordinate transformations, 2) transmission-line networks, and 3) invisibility. Invisibility is here considered as making a perfectly conducting (hollow) cylinder or a sphere invisible by covering it with a material that cancels the dipole moments induced in this conducting "shell". Also, it must be noted that here we do not consider the chiral cloak (see Section 2) separately from other coordinate-transforming cloaks, since its benefits and drawbacks are naturally similar to other cloaks based on the same principle. Basically, the only difference of the chiral cloak as compared to other coordinate-transforming cloaks presented in the literature is that it works for both polarizations simultaneously.

Table 1: C
omparison of different 2-D cloaking methods

Cloaking method	Coordinate transf.	TL networks	Invisibility
Cloak geometry (2D)	annular (arbitrary in theory)	arbitrary	annular (in known designs)
Principle of operation	anisotropy	fields inside TLs	cancellation of dipole moments
Theoretical (TE)	YES	YES	YES
Theoretical (TM)	YES	YES	YES
Theoretical (TE&TM)	YES (chiral cloak)	YES	YES
Realization (TE)	YES	YES	NO
Realization (TM)	NO	NO	NO
Realization (TE&TM)	NO	NO	NO
Material req. (TE)	$\mu_r < 1$ (anisotropic)	metal	$\varepsilon_r < 1$ and/or $\mu_r < 1$
Material req. (TM)	$\varepsilon_r < 1$ (anisotropic)	metal	$\varepsilon_r < 1$ and/or $\mu_r < 1$
Bandwidth	very small	very wide	average
Energy velocity	$v_{\mathrm{group}} \neq v_{\mathrm{phase}}$	$v_{\mathrm{group}} = v_{\mathrm{phase}}$	$v_{\mathrm{group}} \neq v_{\mathrm{phase}}$
Structure	inhomogeneous	homogeneous	homogeneous
Manufacturing	difficult	easy	difficult
Cloaked volume	continuous	2-D/3-D-mesh	continuous
extension to 3-D	possible but difficult	possible but increases scattering	inherent

It is rather factitious to fully compare the different cloaking techniques, since they are so different that all of them are superior as compared to the others at least in some aspects. As a very obvious example, the TL-method cannot cloak homogeneous, bulky objects, but the other two methods can. Therefore, in order to have an objective comparison between different cloaking methods, the comparison should start by defining the problem. After knowing the problem, it will be quite simple to choose the "best" cloak for the specific problem at hand, for example using the data in Table 1.

Nevertheless, we will next give a more detailed description of the benefits and drawbacks of each cloaking technique, in more detail than in Table 1.

5.1 Coordinate transformation cloaks

Benefits

- Offers a very logical and "intuitive" form of cloaking: a volume in space is defined in such a way that inside this volume, there are no fields.
- Literature gives rather detailed design guidelines for obtaining the material parameters required for specific dimensions of cloaks.
- Works for both polarizations separately or simultaneously (depends on the realization of the metamaterial).
- There are no fundamental limitations on the frequency of operation.

Drawbacks

- Inherently requires an anisotropic material which is also strongly inhomogeneous. This automatically makes the manufacturing of this type of cloaks somewhat difficult.
- Due to the required resonant-type materials ($\varepsilon_r < 1$ and/or $\mu_r < 1$), the bandwidth of operation is very limited and the design and manufacturing of separate resonant inclusions are difficult.
- The energy velocity (group velocity) is inherently different from the phase velocity. This difference is responsible of an increase of the scattering, mostly determined by the shape of the exciting pulse.
- Ideal cloaking requires that the material parameters (or at least one of them) go to zero at the inner surface of the cloak. This will introduce a singularity, which may be problematic.

5.2 Transmission-line cloaks

Benefits

- Simple operation principle and simple structure.
- Literature gives detailed design guidelines for obtaining wanted cloaking behavior.
- Unloaded cloaks have very wide operation bandwidths with efficient cloaking.
- The energy velocity is equal to the phase velocity.

Drawbacks

- Severe limitations on the size and shape of the volume that can be cloaked (see Section 4).
- Current technology allows operation for TE-polarization only, but there is no fundamental restriction even for operation for dual-polarization.
- Operation of any type of transmission-line cloak is limited to (approximately) below 300 GHz (see Section 3.3).

5.3 Invisibility

Benefits

- Offers a very logical and "intuitive" form of cloaking: a volume in space is "created" in such a way that inside this volume, there are no fields (and, thus any object or objects can be put inside this volume).
- Literature gives rather detailed design guidelines for obtaining the material parameters required for specific dimensions of cloaks.
- Works for both polarizations separately or simultaneously (depends on the realization of the metamaterial).
- The metamaterial making the cloak can be isotropic and homogeneous.
- There are no fundamental limitations on the frequency of operation.

Drawbacks

- Requires a metamaterial with exotic material parameters. This makes the manufacturing of this type of cloaks somewhat difficult.
- Due to the required resonant-type materials ($\varepsilon_r < 1$, $\mu_r < 1$), the bandwidth of operation of any realizable cloak is limited.
- The energy velocity (group velocity) is inherently different from the phase velocity. This will cause increased scattering but the amount of this increase strongly depends on the shape of the exciting pulse.

6 Possible applications of the transmission-line cloak

This section discusses some possible applications that can benefit from the reduction of the total SCS, offered by cloaks based on the transmission-line approach. Here we want to concentrate on applications suitable for the TL-approach specifically, because it is more limited in terms of type of objects that can be cloaked. With cloaks that can "hide" a complete volume such as a sphere or a cylinder, it is quite obvious that such cloaks can server a number of applications. What is interesting in view of space applications, is the question if the "simplified" cloaking, offered by the transmission-line approach, can find important applications where the benefits offered by this approach can be utilized.

6.1 Invisibility shutter

An important problem existing in current technology was identified by the ACT. It concerns the shielding of electromagnetic radiation (EMR) sensible devices from the high energy interplanetary radiation (HER). In general, any electronic device shipped in a spacecraft is tagged with a radiation dose. This number establishes the amount of radiation the device can absorb while being reliable.

The problem in the design of a payload carrying an EMR sensor is that the metallic shield protecting it from the radiation must present an aperture in order to allow the sensor to be illuminated. In Fig. 15 we illustrate this concept schematically. The idea is to study whether a specific TL-cloak can be designed in such a way that the cloak would cover the opening in the camera shield, while letting through the wavelengths imaged with the camera and stopping (absorbing) the high-energy particles.

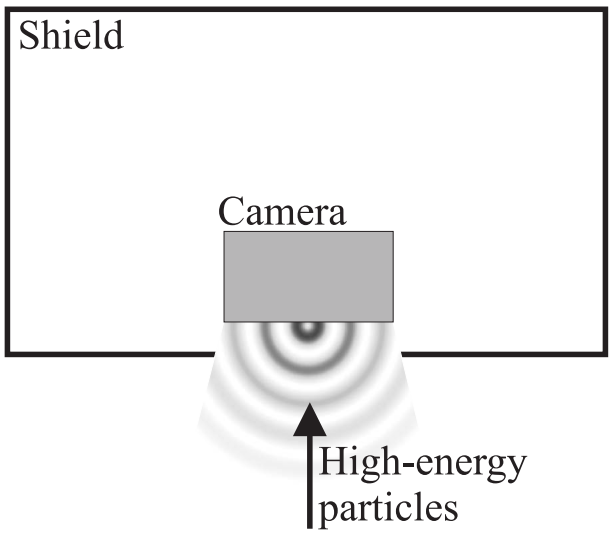

Figure 15: Illustration of the problem: a necessary opening in a shield protecting a camera lets through harmful high-energy particles.

The sensors working under such conditions (CCD, APS, etc.) used to operate at wavelength shorter than typically 14 μm. In order to absorb the HER, the "cloaked" volume (i.e., the volume inside the cloak surrounding the TLs) can be filled, e.g. with aluminium rods.

Based on the study on the high-frequency operation of the TL-cloak (see Section 3.3), it is clear that the biggest problem for this specific cloaking application is the lack of good conductors at such high frequencies.

It must be noted though that the "invisibility shutter" is a very good example of an application that would benefit of the TL-approach to cloaking, since it uses the most important benefits of this approach: the possibility to "squeeze" the incoming field through an array or mesh of some highly absorbing material. It is clear (based on the discussion in Section 3.3) that approximately below the frequency 300 GHz, this application idea has great potential, if suitable frequency ranges, where this type of protection from high-energy particles, could be found.

6.2 Reduction of scattering from support structures blocking antenna apertures

In some cases, especially in satellites and spacecrafts that usually have very limited surface area for mounting antennas, it may be problematic to mount all the antennas in such a way that their apertures are left unblocked by support structures of other antennas or, e.g. by metallic pillars used to reinforce the spacecraft. In this case the proposed transmission-line cloak (or some modification of the types of cloaks presented here) can be used to strongly mitigate the blockage of these structures, thus simplifying the task of designing the spacecraft. See Fig. 16 for an illustration of the problem. The types of struts/blocking objects that can be cloaked with this method are naturally limited by the fact that the object must fit inside the TL cloak, as discussed before. Also, with the known method of coupling waves from free space to the cloak (TL network) [19] the cloaking can be achieved only for one polarization. This means that the antenna that is blocked must emit only linearly polarized radiation. Example of such an antenna is, e.g. a horn antenna as shown in Fig. 16.

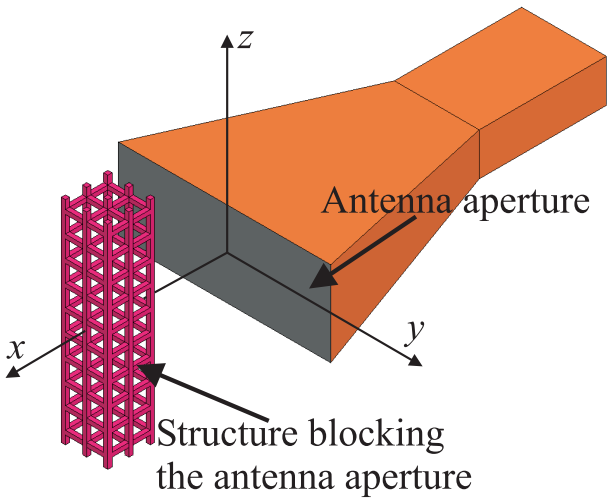

Figure 16: Antenna and a support structure blocking its aperture.

6.2.1 Cloaking a structure which blocks a Gaussian beam

To demonstrate the operation of a transmission-line cloak for reducing the blockage of antennas, we simulate the electrically small TL-cloak having the period of 5 mm and corresponding reference object. The geometry and dimensions of the cloak and the cloaked object are the same as in Section 3: The period of the cloak $d = 5$ mm, the diameter of the cloak (the network without the transition layer) $6d = 30$ mm, the other dimensions are as in Fig. 9. The cloaked object is as shown in Fig. 9 with the period 5 mm and the diameter of the PEC rods 2 mm.

Again, we use the possibility of simulating a vertically infinite periodic structure, thus reducing the complexity of the simulation model. Instead of illuminating the model with a plane wave, as was done in Section 3, we define a Gaussian beam that is directed at the reference object/cloak. A Gaussian beam is radiated, e.g., by a corrugated horn antenna. The Gaussian beam's focal point is at $x = -100$ mm (the origin is at the center of the reference object/cloak) and the beam width at the focal point is 60 mm. The electric field of the incident field is parallel to the z-axis. See Fig. 17 for the simulation results of the electric field distributions with and without the reference object/cloak, conducted with Ansoft HFSS.

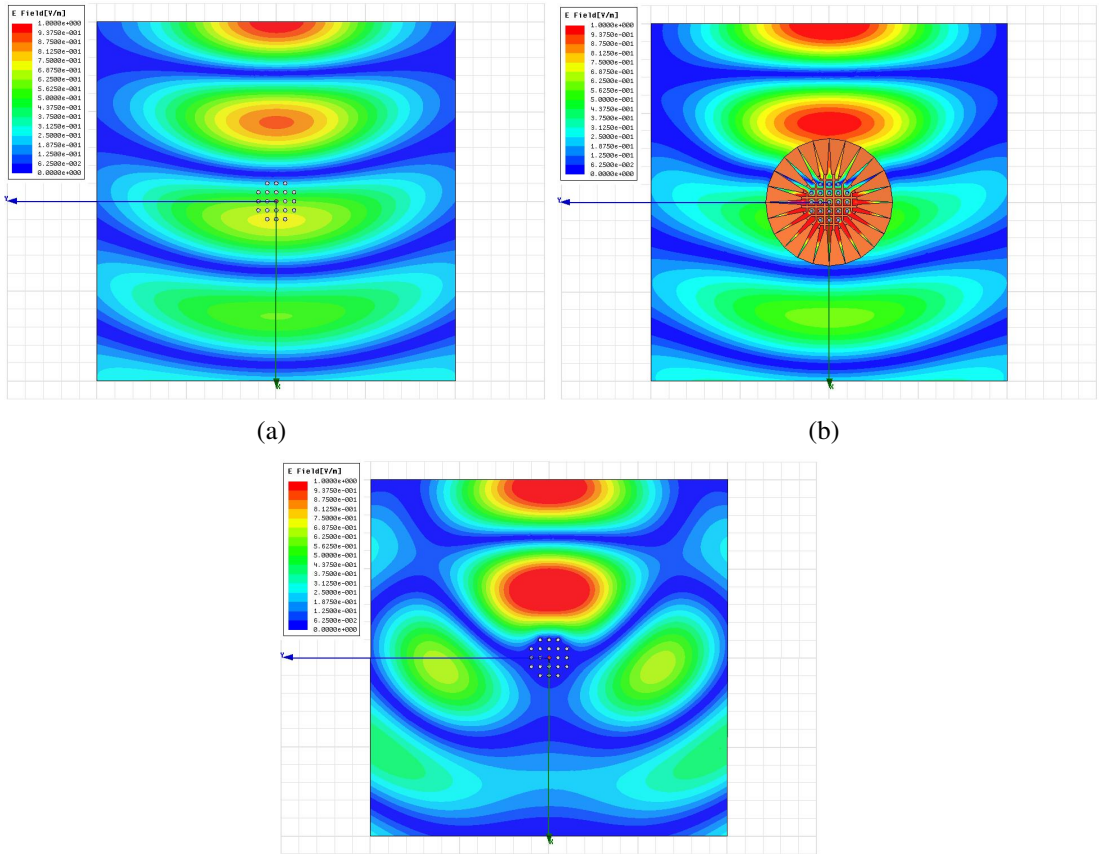

(a) (b)

(c)

Figure 17: HFSS-simulated electric field distributions at $f = 3$ GHz. (a) incident field. (b) reference object with the cloak. (c) bare reference object.

Fig. 17 demonstrates that the beam is nicely preserved when the cloak is used, but without the cloak, the beam is strongly split by the metallic object blocking the beam. To further

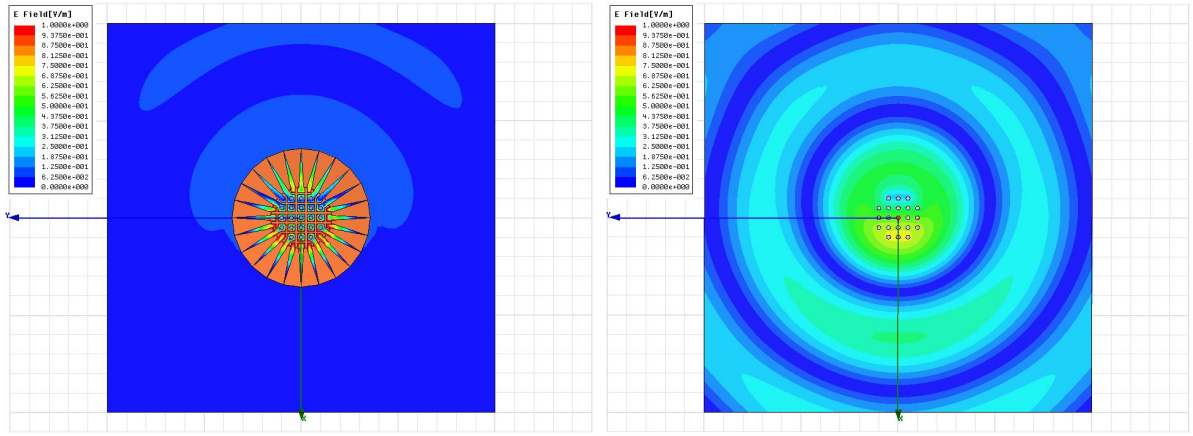

(a) (b)

Figure 18: HFSS-simulated electric field distributions of the *scattered field* at $f = 3$ GHz. (a) reference object with the cloak. (b) bare reference object.

illustrate the operation of the cloak, we can plot the scattered fields in this same situation. See Fig. 18 for the simulated distributions of the scattered electric field, in the case with the cloak and without the cloak.

6.2.2 Cloaking a structure which blocks a dipole antenna

To gain more insight into the effect of blockage and cloaking on the directivity pattern of a real antenna, we have (by suggestion of the ACT) simulated a $\lambda/2$-dipole with a metallic structure blocking it. The Ansoft HFSS simulation model is shown in Fig. 19, without the cloak. The used cloak is exactly the same as in the previous subsection, i.e., the electrically small TL-cloak with period of 5 mm, presented in Section 3. The blocking object is designed to fit inside the cloak which is now simulated with a finite height of 6×9.2 mm$= 55.2$ mm. One period of the cloak structure in the vertical direction is equal to 9.2 mm. Since in the simulation model the problem is cut in half by the used PEC boundary, the actual cloak height is 27.6 mm (the same as that of the blocking structure, see Fig. 19). The resulting directivity patterns at 3 GHz, 3.1 GHz, and 3.2 GHz are shown in Fig. 20, demonstrating that the optimal cloaking performance is obtained around 3.1 GHz, as can be expected based on the results of Fig. 10. We see that with the cloak almost ideal dipole pattern is achieved.

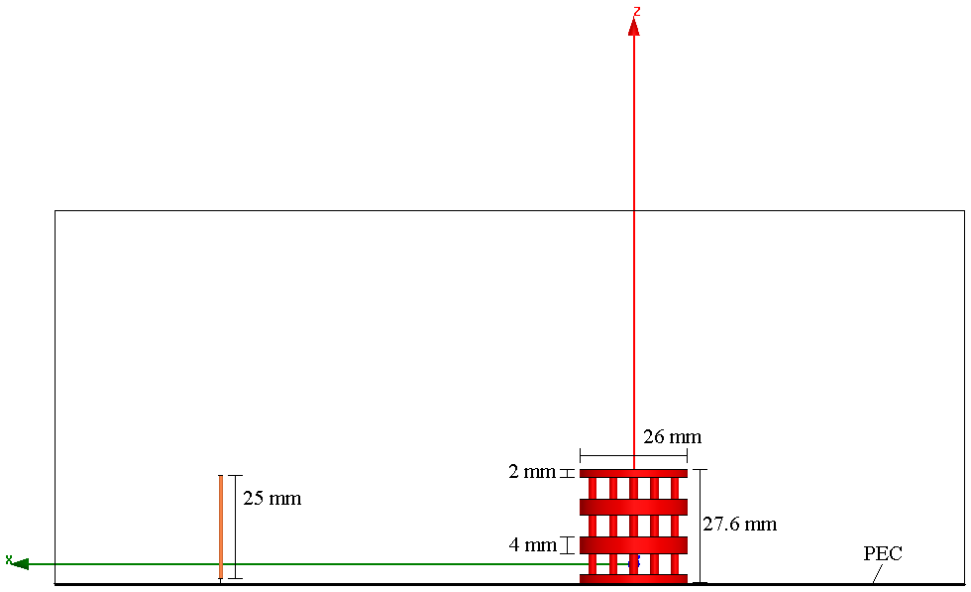

(a)

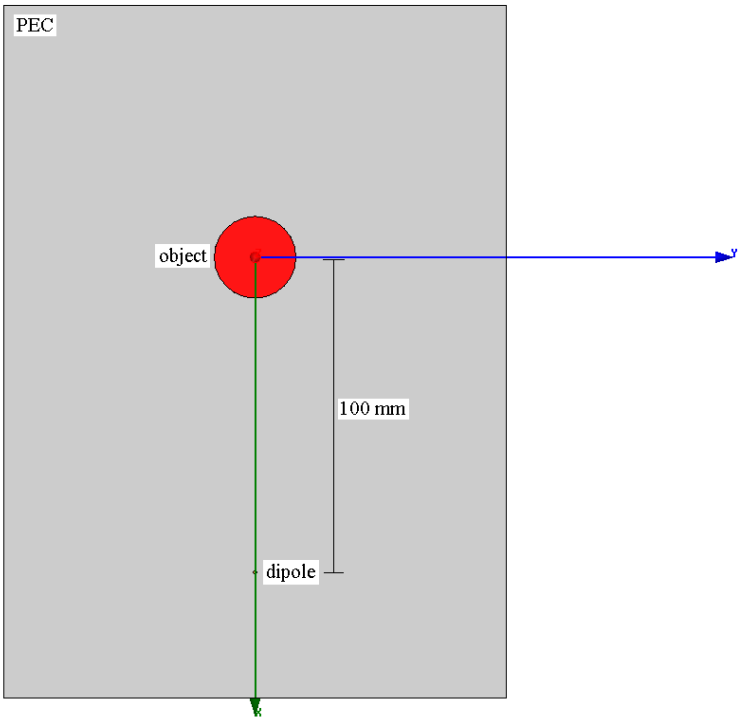

(b)

Figure 19: HFSS model of the dipole antenna with a metallic cylindrical object blocking its radiation (blocking object shown in red). (a) sideview. (b) topview. The cylindrical object is the same as in the previous Subsection (two-dimensional array of cylinders), but now also horizontal, cylindrical "discs" are embedded in it to demonstrate the volume that can be cloaked. The simulation model is simplified by introducing a PEC boundary as shown in the figure, i.e., only half of the dipole and the blocking object (and cloak) need to be simulated.

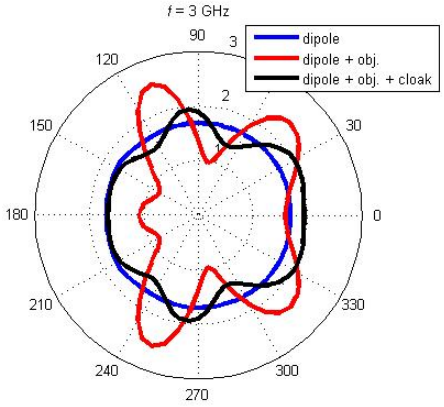

(a)

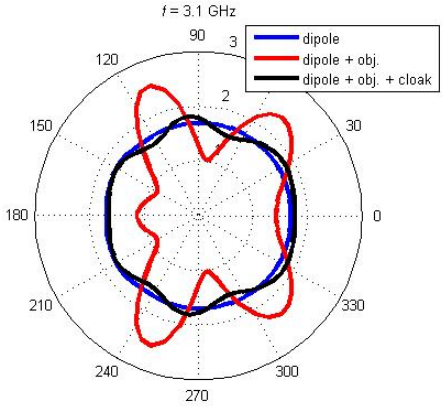

(b)

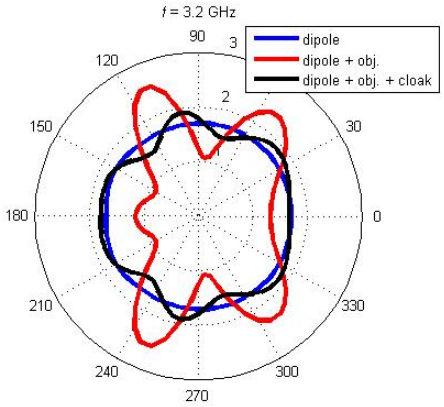

(c)

Figure 20: Simulated directivity patterns (linear scale) at 3 GHz, 3.1 GHz, and 3.2 GHz. The object blocking the antenna is in the direction 180^0.

6.3 Impedance-matched lenses

In a conventional microwave or optical lens, there exists a problem of impedance mismatch, meaning that the impedance of the lens material is different from that of the surrounding space (usually free space). This introduces undesired reflections, which reduce the power transmitted through the lens. In optics, this problem can be overcome (at lest in a certain frequency range) using multi-coated lenses. However, in the design of microwave lenses the required thickness of layered covering becomes prohibitively large. The only known theoretical possibility to match the lens material with free space is to use magnetic materials, such that $\mu_r = \epsilon_r$, but there are no materials with such properties in the microwave range.

Thus, it is highly desirable to find a way to create impedance-matched waveguiding structures with the propagation constant different from that of free space. The use of such artificial materials would allow to realize reflection-free microwave lenses. Analyzing our results on the transmission-line cloak (Section 3) one can note that the artificial material developed there is actually of the type needed for a better design of microwave lenses. Indeed, unloaded meshes of transmission lines can be designed so that their impedance is the same as that of free space, while the propagation constant is different, providing necessary means for refraction while eliminating reflections.

Although this application is nothing like a cloak (in this case we actually want to enhance the difference in the wavenumbers inside the TL network and the surrounding space), it is based on the idea of cloaking. The principle is that with the TL cloak approach, we can in an easy way control the wavenumber *and* the impedance of the TL structure. In the cloaking application, we would like to have exactly the same wavenumber in the TL cloak as in the surrounding medium while tuning the impedance of the cloak to match the surrounding medium's wave impedance in a certain frequency band.

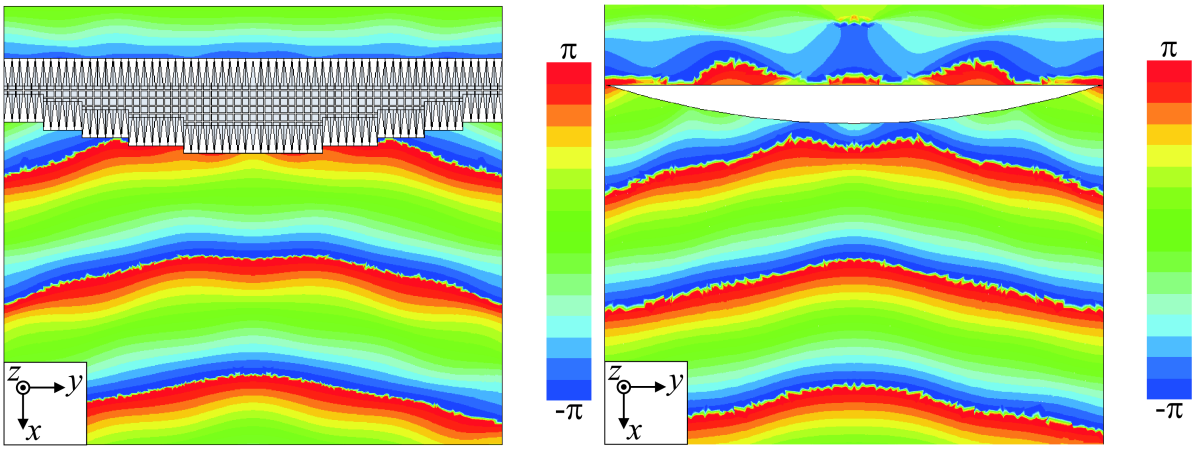

(a) (b)

Figure 21: HFSS-simulated electric field phase distributions at 2.4 GHz for (a) a transmission-line lens, and (b) a reference dielectric lens with $\varepsilon_r = 4.66$. In both cases a plane wave travelling to the $+x$-direction, with electric field parallel to the z-axis, illuminates the lenses [51].

For the *lens* applications, the requirement is that the wavenumber must be different than in the medium surrounding the lens, in order to have a refraction effect. This is easily implemented

in our case just by filling the transmission lines with a dielectric. By filling the transmission lines with a dielectric, we naturally change also the impedance, but as explained earlier, it can always be tuned to match a certain impedance by changing the physical dimensions of the TLs. In general, this approach enables us to mitigate an important drawback of traditional dielectric lenses: the inherent mismatch with free space (or some other medium surrounding the lens) [51]. See Fig. 21 for a plot of the simulated electric field phase in the cases of two different lenses (one lens is based on the TL-cloak approach and the other is a dielectric lens), demonstrating that the impedance matching can be strongly improved using the proposed method (the phase front on the side of incoming wave is preserved in the case of the TL-lens). The conducted full-wave simulations [51] confirm that the reflectance (as compared to the dielectric lens) is lowered in the best case (for this specific example) by more than 10 dB, and the relative bandwidth where more than 4 dB reduction is obtained, is about 17 percent [51].

7 Generalized field-transformations

Besides the concrete applications of transformation media for cloaking, fundamental aspects of the idea of transformation optics were investigated during this study, which led to the formulation of alternative approaches to transformation media. It should be noted that both methods do not just apply to cloaking, but to much wider classes of transformations.

7.1 DRSE approach

The principle of the proposed approach for the analytical study of general type of field transformations was first presented in [52]. Within this project we have extended this principle to obtain expressions allowing more general field transformations [53, 54].

As basic idea of this approach the coordinate transformations are replaced by field transformations. In Refs. [53, 54] transformations of the type

$$\mathbf{E}(\mathbf{r}) = F(\mathbf{r},\omega)\mathbf{E_0}(\mathbf{r}) + \sqrt{\frac{\mu_0}{\varepsilon_0}}A(\mathbf{r},\omega)\mathbf{H_0}(\mathbf{r}), \tag{15}$$

$$\mathbf{H}(\mathbf{r}) = G(\mathbf{r},\omega)\mathbf{H_0}(\mathbf{r}) + \sqrt{\frac{\varepsilon_0}{\mu_0}}C(\mathbf{r},\omega)\mathbf{E_0}(\mathbf{r}), \tag{16}$$

are considered, with $F(\mathbf{r},\omega)$, $G(\mathbf{r},\omega)$ $A(\mathbf{r},\omega)$ and $C(\mathbf{r},\omega)$ being arbitrary differentiable functions. Substituting Eqs. (15) and (16) into the Maxwell equations and demanding that the original fields $\mathbf{E}_0$ and $\mathbf{H}_0$ satisfy the free-space Maxwell equations, one finds in a straightforward way the necessary media properties and eventual sources (charges and currents) needed to establish the required transformation. In its most general form field transforming metamaterials allow to design materials with arbitrary constitutive relation. The detailed derivations that relate the set field transform to the required material parameters are presented in [53, 54].

7.2 ACT approach

This approach is a generalization of the idea of [10]. As the main observation it is found that the Maxwell equations divide into two sets of equations with mutually excluding field content, one set depending on $\mathbf{E}$ and $\mathbf{B}$, the other one on $\mathbf{D}$ and $\mathbf{H}$. Therefore, it is possible to assign two different transformed spaces to these two sets, in other words the distortion in Figure 1 can be different for the two sets $\mathbf{E}$, $\mathbf{B}$ and $\mathbf{D}$, $\mathbf{H}$, respectively. In this way a wider class of materials can be described than with [10]. In particular, it is possible to provide a geometric interpretation of non-reciprocal and indefinite media. On the other hand, the basic characteristics of the coordinate transformation approach are retained: the medium mimics a transformed space and the transformation "do not generate sources", i.e. if the original space was source free the transformation medium will not include net charges or currents neither. The explanation of this generalized approach is presented in [55, 56].

It should be noted that the two approaches, the coordinate transformation approach [10, 55, 56] and the field transformation approach [53, 54] should be seen as complementary. In the former case the transformations are essentially non-local (the fields at a point (x, y, z) in the transformed space relate to the original fields at a different point (x', y', z') in the original

space) but the fields cannot be rescaled freely. In the latter approach the different fields can be rescaled and mixed arbitrarily, but the transformation remains strictly local. Therefore it should even be possible to combine the two ideas.

8 Conclusions

The principles and basic design guidelines of two cloaking approaches, namely, the chiral cloak and the transmission-line cloak, have been explained. The potential of these approaches for high-frequency operation (up to the visible) have been studied and the reasons for their limitations have been explained. Other fundamental limitations of the previous two cloaking approaches (chiral cloak is a specific example of a more general approach, namely, the coordinate transformation), have been also studied. These two cloaking approaches have been compared with each other and a third approach, namely, invisibility. The benefits and drawbacks of all the three approaches have been identified.

A few specific examples of possible applications (with emphasis on space applications) of the transmission-line cloak have been identified and studied. The results show that the proposed cloaks can improve the antenna performance in the presence of strong scatterers. This may find numerous applications in space technology.

Two generalized analytical techniques for obtaining arbitrary field transformations have been developed. One is based on a direct transformation of electromagnetic fields in a volume filled by a material, and the other one is a generalization of the approach based on coordinate transformations.

Acknowledgements

The authors want to thank prof. Constantin Simovski (Department of Radio Science and Engineering, TKK Helsinki University of Technology) for valuable help in writing Section 3.3 and for useful discussions regarding Section 7.1. The authors also want to thank prof. Igor Nefedov (Department of Radio Science and Engineering, TKK Helsinki University of Technology) for collaboration in the work regarding Section 7.1.

References

[1] S. Tretyakov, *Analytical modeling in applied electromagnetics*, Norwood, MA: Artech House, 2003.

[2] G.V. Eleftheriades and K.G. Balmain, *Negative-Refraction Metamaterials: Fundamental Principles and Applications*, Hoboken, NJ: John Wiley & Sons, 2005.

[3] C. Caloz and T. Itoh, *Electromagnetic Metamaterials: Transmission Line Theory and Microwave Applications*, Hoboken, NJ: John Wiley & Sons, 2006.

[4] U. Leonhardt, "Optical conformal mapping," *Science*, Vol. 312, pp. 1777–1780, 2006.

[5] J.B. Pendry, D. Schurig, and D.R. Smith, "Controlling electromagnetic fields," *Science*, Vol. 312, pp. 1780–1782, 2006.

[6] A. Alù and N. Engheta, "Achieving transparency with plasmonic and metamaterial coatings," *Phys. Rev E*, Vol. 72, 016623, 2005.

[7] A. Greenleaf, M. Lassas, G. Uhlmann, "On nonuniqueness for Calderon's inverse problem," *Math. Res. Lett.*, Vol. 10, No. 5-6, pp. 685–693, 2003.

[8] D. Schurig, J.J. Mock, B.J. Justice, S.A. Cummer, J.B. Pendry, A.F. Starr, and D.R. Smith, "Metamaterial electromagnetic cloak at microwave frequencies," *Science*, vol. 314, pp. 977–980, 2006.

[9] W. Cai, U. K. Chettiar, A. V. Kildishev, and V. M. Shalaev, "Optical cloaking with metamaterials," *Nature Photonics*, Vol. 1, pp. 224–227, 2007.

[10] U. Leonhardt and T.G. Philbin, "General relativity in electrical engineering," New Journal of Physics, Vol. 8, p. 247, 2006.

[11] M. Kerker, "Invisible bodies," *J. Opt. Soc. Am.*, Vol. 65, No. 4, pp. 376–379, 1975.

[12] H. Chew and M. Kerker, "Abnormally low electromagnetic scattering cross sections," *J. Opt. Soc. Am.*, Vol. 66, No. 5, pp. 445–449, 1976.

[13] A. Sihvola, *Electromagnetic Mixing Formulas and Applications*, IET, 2000.

[14] A. Sihvola, "Properties of dielectric mixtures with layered spherical inclusions," *Microwave Radiomet. Remote Sens. Appl.*, pp. 115–123, 1989.

[15] A. Alù and N. Engheta, Plasmonic materials in transparency and cloaking problems: mechanism, robustness, and physical insights, *Optics Express*, Vol. 15, No. 6, pp. 3318–3332, 2007.

[16] M. G. Silveirinha, A. Alù, and N. Engheta, "Parallel-plate metamaterials for cloaking structures," *Phys. Rev E*, Vol. 75, 036603, 2007.

[17] P.-S. Kildal, A. A. Kishk, and A. Tengs, "Reduction of forward scattering from cylindrical objects using hard surfaces," *IEEE Trans. Antennas Propag.*, Vol. 44, No. 11, pp. 1509–1520, 1996.

[18] G. W. Milton and N. A. Nicorovici, On the cloaking effects associated with anomalous localized resonance, Proc. R. Soc. Lond. A: Math. Phys. Sci., Vol. 462, pp. 3027–3059, 2006.

[19] P. Alitalo, O. Luukkonen, L. Jylhä, J. Venermo, and S. A. Tretyakov, "Transmission-line networks cloaking objects form electromagnetic fields," *IEEE Trans. Antennas Propagat.*, Vol. 56, No. 2, pp. 416-424, 2008.

[20] M. Asghar et al., "Electromagnetic cloaking with a mixture of spiral inclusions," *Metamaterials'2007 Proceedings*, Rome, Italy, 22-24 Oct. 2007, pp. 957–960.

[21] P. Alitalo et al., "Realization of an electromagnetic invisibility cloak by transmission-line networks," *Metamaterials'2007 Proceedings*, Rome, Italy, 22-24 Oct. 2007, pp. 953-956.

[22] A.A. Sochava, C.R. Simovski, S.A. Tretyakov, Chiral effects and eigenwaves in bi-anisotropic omega structures, *Advances in Complex Electromagnetic Materials* (Ed. by A. Priou, A. Sihvola, S. Tretyakov, and A. Vinogradov), NATO ASI Series High Technology, vol. 28, Dordrecht/Boston/London: Kluwer Academic Publishers, pp. 85–102, 1997.

[23] N. Martin, O. Banakh, A.M.E. Santo, S. Springer, R. Sanjinès, J. Takadoum and F. Lévy, Titanium oxynitride thin films sputter deposited by the reactive gas pulsing technique, *App. Surface Science*, Vol. 185, pp. 123–133, 2001.

[24] S.A. Tretyakov, F. Mariotte, C.R. Simovski, T.G. Kharina, J.-P. Heliot, Analytical antenna model for chiral scatterers: Comparison with numerical and experimental data, *IEEE Transactions on Antennas and Propagation*, Vol. 44, No. 7, pp. 1006–1014, 1996.

[25] I. V. Semchenko, S. A. Khakhomov and A. L. Samofalov, Optimal Shape of Spiral: Equality of Dielectric, Magnetic and Chiral Properties, *Proc. NATO ARW & META'08*, Marrakesh, Morocco, 7-10 May 2008, pp. 71–80.

[26] S.V. Golod, V.Ya. Prinz, V.I. Mashanov, A.K. Gutakovsky, Fabrication of conducting GeSi/Si micro-and nanotubes and helical microcoils, *Sem. Sci. Techn.,* Vol. 16, pp. 181-185, 2001.

[27] V.Ya. Prinz, V.A. Seleznev et al., Molecularly and atomically thin semiconductor and carbon nanoshells, *Phys. Stat. Sol.* (b) Vol. 244, pp. 4193-4198, 2007.

[28] Yu.V. Nastaushev, V.Ya. Prinz, and S.N. Svitasheva, A technique for fabricating Au/Ti micro- and nanotubes, *Nanotechnology*, Vol. 16, pp. 908–912, 2005.

[29] P. Alitalo and S. Tretyakov, "Cylindrical transmission-line cloak for microwave frequencies," *Proc. 2008 IEEE International Workshop on Antenna Technology*, Chiba, Japan, 4-6 March 2008, pp. 147-150.

[30] P. Alitalo and S. Tretyakov, "On electromagnetic cloaking – general principles, problems and recent advances using the transmission-line approach," *Proc. 2008 URSI General Assembly*, Chicago, USA, 7-16 August 2008, in press (see Appendix A for the submitted version of this paper).

[31] P. Alitalo and S. Tretyakov, "Broadband microwave cloaking with periodic networks of transmission lines ," submitted to *Metamaterials'2008* (see Appendix B for the submitted version of this paper).

[32] P. Alitalo, S. Ranvier, J. Vehmas, and S. Tretyakov, "A microwave transmission-line network guiding electromagnetic fields through a dense array of metallic objects," submitted to *Metamaterials* (see Appendix C for the submitted version of this paper).

[33] K. Okamoto, *Fundamentals of Optical Waveguides*, Burligton, MA: Academic Press, 2000.

[34] K. Igo and Ya. Kokubun, *Encyclopedic Handbook of Integrated Optics*, Boca Rayton, FL: Taylor and Francis, 2006.

[35] G. Mahlke and K. G ossing, *Fiber Optic Cables*, Munich, Germany: Corning Cable System, 2001.

[36] K. Wang and D. M. Mittleman, "Metal wires for terahertz wave guiding," *Nature*, Vol. 432, p. 376, 2004.

[37] L.-J. Chen, H.-W. Chen, T.-F. Kao, J.-Y. Lu, and C.-K. Sun, "Low-loss subwavelength plastic fiber for terahertz waveguiding," *Optics Letters*, Vol. 31, p. 308, 2006.

[38] M.Y. Frankel, S. Gupta, J.A. Valdmanis and G.A. Mourou, "Terahertz Attenuation and Dispersion Characteristics of Coplanar Transmission Lines," *IEEE Trans. Microw. Theory Techn.*, Vol. 39, p. 6, 1991.

[39] Y. Xu, R. G. Bosisio, "A study of planar Goubau lines for millimeter- and submillimeter-wave integrated circuits," *Microw. Opt. Techn. Lett.*, Vol. 43, p. 290, 2004.

[40] J.-J. Greffet, "Nanoantennas for Light Emission," *Science*, Vol. 308, p. 1561, 2005.

[41] S.A. Maier, M.L. Brongersma, P.G. Kik, S. Meltzer, A.A.G. Requicha, and H.A. Atwater, "Plasmonics: A Route to Nanoscale Optical Devices," *Advanced Materials*, Vol. 13, p. 1501, 2001.

[42] L.A. Sweatlock, S.A. Maier, H. A. Atwater, J.J. Penninkhof, and A. Pollman, "Highly confined electromagnetic fields in arrays of strongly coupled Ag nanoparticles,'" *Phys. Rev. B*, Vol. 71, p. 235408, 2005.

[43] N. Engheta, "Circuits with Light at Nanoscales: Optical Nanocircuits Inspired by Metamaterials," *Science*, Vol. 317, p. 1698, 2007.

[44] G. Shvets, A. Trendafilov, J.B. Pendry and A. Sarychev, "Guiding, Focusing, and Sensing on the Subwavelength Scale Using Metallic Wire Arrays," *Phys. Rev. Lett.*, Vol. 99, p. 053903, 2007.

[45] S.A. Tretyakov, "Meta-materials with wideband negative permittivity and permeability," *Microwave and Optical Technology Letters*, Vol. 31, No. 3, pp. 163–165, 2001.

[46] S.A. Tretyakov and S.I. Maslovski, "Veselago materials: what is possible and impossible about the dispersion of the constitutive parameters," *IEEE Antennas and propagation magazine*, Vol. 49, No. 1, pp. 37–43, 2007.

[47] U. Leonhardt, "Optical metamaterials: Invisibility cup," *Nature Photonics*, Vol. 1, pp. 207–208, 2007.

[48] H. Chen, Z. Liang, P. Yao, X. Jiang, H. Ma, and C.T. Chan, "Extending the bandwidth of electromagnetic cloaks," *Phys. Rev. B*, Vol. 76, p. 241104, 2007.

[49] H. Chen and C.T. Chan, "Time delays and energy transport velocities in three dimensional ideal cloaking," arXiv:0712.3985 (online).

[50] I. Walter, H. Hirsch, H. Jahn, J. Knollenberg, H. Venus, "MERTIS – a highly integrated IR imaging spectrometer," *Proc. SPIE*, Vol. 6297, pp. 62970X-1 – 62970X-11, 2006.

[51] P. Alitalo, O. Luukkonen, J. Vehmas, and S.A. Tretyakov, "Impedance-matched microwave lens," *IEEE Antennas and Wireless Propagation Letters*, in press (published online in IEEExplore).

[52] S.A. Tretyakov and I.S. Nefedov, "Field-transforming metamaterials," *Metamaterials'2007 Proceedings*, Rome, Italy, 22-24 Oct. 2007, pp. 474-477.

[53] S.A. Tretyakov, I.S. Nefedov, and P. Alitalo "Generalized field transformations using metamaterials," submitted to *Metamaterials'2008* (see Appendix D for the submitted version of this paper).

[54] S.A. Tretyakov, I.S. Nefedov, and P. Alitalo "Generalized field-transforming metamaterials," submitted to *New Journal of Physics*, arXiv:0806.0489 [physics.optics] (see Appendix E for the submitted version of this paper).

[55] L. Bergamin "Triple-spacetime metamaterials," submitted to *Metamaterials'2008* (see Appendix F for the submitted version of this paper).

[56] L. Bergamin "Generalized transformation optics from triple spacetime metamaterials," submitted to *Physical Review A*, arXiv:0807.0186[physics.optics] (see Appendix G for the submitted version of this paper).

Appendix A

The following paper has been accepted for publication in the Proceedings of the 2008 URSI General Assembly, to be held 7-16 August 2008, in Chicago, USA.

On electromagnetic cloaking – general principles, problems and recent advances using the transmission-line approach

Pekka Alitalo* and *Sergei Tretyakov
TKK Helsinki University of Technology, Department of Radio Science and Engineering,
SMARAD Center of Excellence, P.O. Box 3000, FI-02015 TKK, Finland
pekka.alitalo@tkk.fi, sergei.tretyakov@tkk.fi

Abstract

Principles, historical background and recent developments on the subject of electromagnetic cloaking are discussed. The problems related to the propagation of energy inside some previously proposed cloak structures are explained. One recently proposed approach to achieve cloaking, namely, the use of transmission-line networks, is presented in more detail and the principles of this approach are compared to other cloaking methods.

1. Introduction

The subject of cloaking objects from arbitrary electromagnetic fields propagating e.g. in free space, has aroused a lot of interest after the publication of the recent work by Greenleaf et al. [1], Leonhardt [2], Pendry et al. [3] and the research groups of Engheta [4–6] and Smith [3,7]. In [1–7] two different methods aimed for the reduction of an object's total scattering cross section were discussed. In [4–6] a way of making objects invisible using a specific material cover to cancel the dipolar scattered fields of the object to be made invisible, is presented. In [1–3,7] the cloak material cover is designed in such a way that the electromagnetic fields are zero in the cloaked region, i.e., the fields are guided around the cloaked object. Although the method introduced in [4–6] in principle differs significantly from cloaking (by cloaking we mean reduction of the scattering from an arbitrary object), this method can also be used for similar cloaking purposes as in e.g. [2,3,7], if the object to be made invisible is placed inside an enclosure made of a perfectly conducting material. The approach proposed in [2,3] and designed for TE polarization in [7] has been developed also for TM polarization [8] and for operation for both polarizations simultaneously [9]. In addition, there has been recently a lot of work done to estimate feasibility and scattering properties of such cloaks, see, e.g., [10]. An alternative approach, as compared to [2,3], aimed to obtain arbitrary field transforms by starting directly from the required field distributions, has been recently presented [11].

Although the subject of cloaking (or invisibility) has aroused huge amount of interest after the publication of e.g. [1–4], it was, in fact, studied already a few decades ago [12,13], when a similar method as suggested in [4] was used to cancel the scattering from spherical and ellipsoidal objects. Also in [14] the scattering properties of multilayered spheres were studied. The use of hard surfaces for reducing the scattering from antenna struts was thoroughly studied already some time ago, see, e.g., [15]. Although the design proposed in [15] is somewhat limited in view of the generality of the cloaking phenomenon (this approach is strongly anisotropic since scattering of an object can be significantly reduced only for waves with a fixed direction of arrival), it is still to this date the only approach to cloaking which has been shown to work in practice for a specific application. Recently, also other alternative approaches to cloaking have been suggested. In [16] it is shown that line or dipole sources positioned near to a so called superlens (a material slab with effectively negative permittivity and permeability) are cloaked due to localized resonance effects. Although this approach is very interesting in the scientific sense, it seems to be even more difficult in view of realization, as compared to e.g. [2–4].

Recently, the use of transmission-line networks matched with the surrounding medium (e.g., free space), has been suggested for cloaking objects made of 2D or 3D meshes composed of an arbitrary material [17–19]. This cloaking method differs significantly from the previously discussed methods since it is based on enabling the incoming electromagnetic wave to go through the object instead of going around it (or cancelling the induced dipole moments) in a very simple way just by coupling the incoming wave to a network of transmission lines. This approach has the clear drawback of limiting the object to be cloaked to a mesh or an array of small objects, but the advantage obtained is a very simple structure and the ease of manufacturing. Also, as shown and discussed in [18,19], in certain cases the operational relative bandwidth (where cloaking is achieved) can be up to 40 percent or more, which is considerably more than what can be obtained by using materials composed of resonant inclusions [7].

2. Energy velocity in cloaks composed of passive inclusions

One significant problem with the cloaking approach introduced in [2,3] is the fact that the electromagnetic wave must go around the object (or the region which is supposed to be cloaked) in a way that the wave on both

sides of the cloak is left undisturbed by the cloak/cloaked object. This requires that the wave propagation velocity inside the cloak is faster than outside the cloak. For the phase velocity at a single frequency point this is not a problem, as it was demonstrated e.g. in [7], but for the energy propagation velocity (group velocity) this requirement is impossible to achieve when using cloaks composed of passive components and materials. The negative effect of the inevitable phase and group velocity mismatch on the cloaking phenomenon strongly depends on the type of the pulse (signal) that impinges on the cloak. If the pulse is very narrow in the frequency, it is clear that the mismatch effect is not very strong and cloaking can be achieved, at least to some extent. On the other hand, cloaking with realizations as suggested e.g. in [7,8] is inherently restricted to a very narrow frequency band since the cloak materials are composed of strongly resonant inclusions. The cloaking methods based on the cancellation of the dipole scattering [4–6,12–14] are also expected to have similar problems when the object to be cloaked is placed inside a perfectly conducting enclosure, which in turn is made invisible by the cloak material cover, since also in this case energy cannot go along a straight line but it must go around the cloaked object.

As discussed in [17,18], the transmission-line approach to cloaking has the benefit of fairly simple design and manufacturing, and in certain cloak designs (unloaded networks), the group velocity is actually equal to the phase velocity. On the other hand, when the group velocity equals the phase velocity, the problem is that they obviously cannot be ideal when cloaking objects situated in free space [18]. It must also be noted that since inside a transmission-line cloak only waves of voltages and currents propagate, the so called matching layer between the network and the surrounding medium dictates for which polarization cloaking can be achieved. At the moment, no feasible realization for a transmission-line cloak operating for two orthogonal polarizations has been suggested.

3. Operation of the transmission-line cloak

The principle of operation of the transmission-line cloak is thoroughly explained in [18]. The main idea is that a network of transmission lines is designed in such a way that at the operating frequency the wave propagation (voltages and currents) is isotropic or at least very close to isotropic. This means that the period of the network must be much smaller than the wavelength at the operational frequency. If a wave in free space could be coupled into this network, the space between the transmission lines of the network would be ideally cloaked from this wave since in the network the wave travels only inside the sections of transmission line. In order to have perfect cloaking effect, the wave propagation inside the network must be identical to the wave propagation in the surrounding medium. As shown in [18], this is impossible to achieve with a simple (unloaded) transmission-line network when the surrounding medium is free space. This is due to the fact that inside the network, the waves propagate slightly slower than in the material which is filling the individual sections of transmission line. One way to get past this problem is to use a loaded transmission-line network [17,18]. This choice has the drawback of resulting in a difference between the phase (v_p) and the group (v_g) velocities ($v_p = c_0$, $v_g < c_0$, where c_0 is the speed of light). Thus, with the loaded transmission-line cloak we end up with a similar problem regarding the energy propagation, as e.g. with the cloaks discussed in [2,3]. See Fig. 1 for the dispersion and impedance in two example networks, a loaded and an unloaded one. The unloaded network has the same parameters as in [18], but the loaded network is periodically loaded by series capacitors ($C = 0.67$ pF) and also by shunt inductors ($L = 101.3$ nH), as opposed to the capacitively loaded network in [18]. The impedance of the lines in the loaded network is $550\ \Omega$. From Fig. 1a we see that the loaded network has the ideal phase velocity at two frequencies (1.25 GHz and 3 GHz in the studied example case). Also, the impedance of both networks can be tuned to be very close to the ideal value of $120\pi\ \Omega$ on a relatively large bandwidth, as can be seen from Fig. 1b.

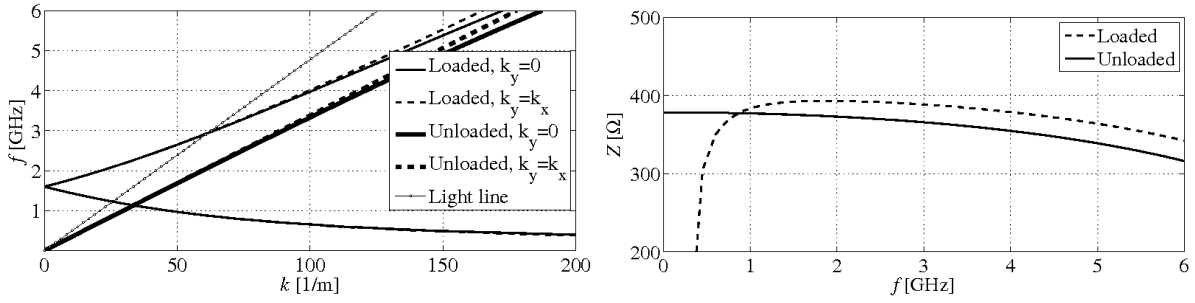

(a) (b)

Figure 1: (a) Dispersion and (b) impedance for the studied networks. The period d of both networks is equal to 8 mm [18]. The total wavenumber in the networks is $k = \sqrt{k_x^2 + k_y^2}$.

4. Cloaking metal meshes with cylindrically shaped transmission-line networks

The most practical transmission-line cloak is clearly the simplest unloaded one, since in that case the phase and group velocities are equal, and the obtainable operation bands are the largest [18]. The drawback in this structure is that when cloaking objects in free space, the phase and group velocities differ slightly from c_0. As was discovered in [18,19], a cylindrical cloak like this still scatters very little (as compared to a metallic, uncloaked object), when its diameter is small compared to the wavelength (e.g., smaller than a half wavelengths). Also, it was found that for a cloak with a fixed diameter, there are other, higher frequency ranges, where the cloak scattering is greatly reduced. These points occur at the frequencies where the cloak's diameter is simultaneously close to a multiple of the wavelength inside and outside the cloak [18].

Here we reproduce the results for a small cylindrical cloak presented in [19] (diameter equal to $0.32\lambda_0$ at the design frequency of 2 GHz) and use the same network design for creating a cloak which is large compared to the wavelength. To obtain an electrically large cloak, we simply increase the diameter of the small cylindrical cloak, while keeping the period and other dimensions of the transmission lines similar to those used in [19]. With the help of the scattering simulations done for a homogenized cloak in [18], we have estimated a suitable diameter of the electrically large cloak to be $52d$ (d is the network period and here $d = 8$ mm) for a cloak operating around 2...3 GHz. For the simulation of the large cylindrical cloak, we cut the model in half with a PMC boundary inserted in the middle of the cylinder. The transition layer, as in [19], is designed in such a way that basically the whole surface around the cloak is covered by the "antennas" that are composed of gradually enlarging parallel strip transmission lines (with equal width and separation). For the large cylindrical cloak, the separation between the "antenna" strips and their width are both equal to 7.73 mm (at the interface with free space). The length of the "antennas" is equal to 40 mm [19]. See Fig. 2 for the ratios of the simulated total scattering cross sections of the both cloaks and the corresponding reference cases, and Fig. 3 for snapshots of the simulated electric field distributions in the large cylindrical cloak ($52d \approx 4\lambda_0$ at 3 GHz) and its reference case. For both cloaks the reference cases are cylindrically shaped arrays of PEC rods that fit inside the cloaks [17–19].

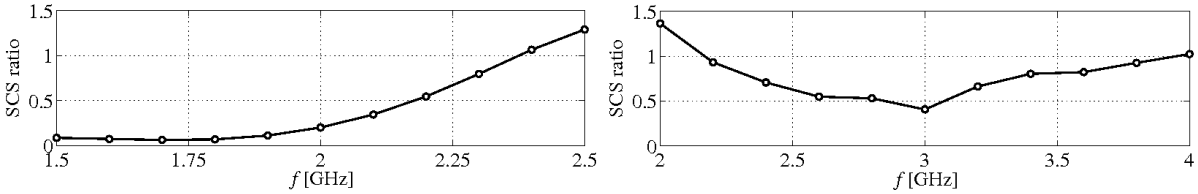

(a) (b)

Figure 2: Ratios of the HFSS-simulated total scattering cross sections. (a) Electrically small cylindrical cloak as presented in [19]. (b) Electrically large cylindrical cloak. When the ratio is less than 1, the cloak's (with reference object inside) total scattering cross section is less than that of the uncloaked reference object's.

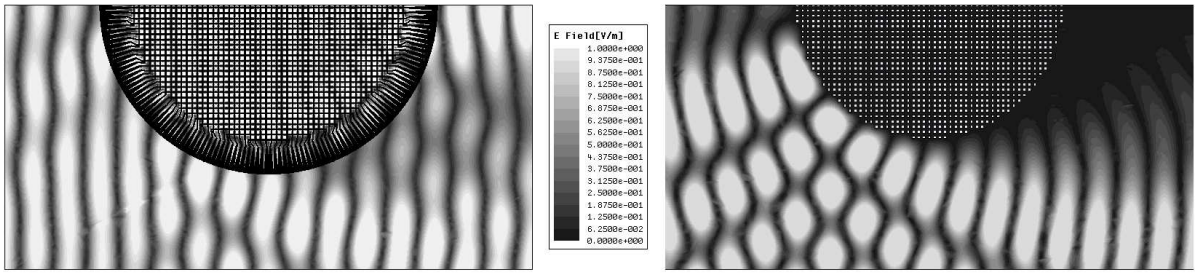

(a) (b)

Figure 3: Snapshots of the HFSS-simulated total electric field distributions at 3 GHz for (a) cloak (metal strips illustrated as black) with the reference object inside and (b) bare reference object (the PEC rods illustrated as white squares). A plane wave with electric field normal to the figure plane travels from left to right.

5. Conclusion

We have discussed the basic principles and problems of cloaking related to the various cloaking methods presented in the literature. It is clear that regarding cloaking of pulses (waves carrying energy and information), there are some problems that are bound to limit the applicability of some suggested cloak structures. The mismatch of the phase and group velocities, inherent to certain types of (passive) cloaks, clearly needs more study before the reduction of the cloaking effect can be fully understood. We have also discussed a recent alternative approach to cloaking, namely, the use of transmission-line networks. This approach has some severe limitations regarding the size and shape of the objects that can be cloaked, but on the other hand, it offers a very simple structure and ease of manufacturing, as well as relatively large operation bandwidth.

6. Acknowledgments

This work has been partially funded by the Academy of Finland and TEKES through the Center-of-Excellence program and by the European Space Agency / ESTEC contract no. 21261/07/NL/CB. P. Alitalo acknowledges financial support by GETA, Tekniikan Edistämissäätiö, and the Nokia Foundation.

7. References

1. A. Greenleaf, M. Lassas, G. Uhlmann, "On nonuniqueness for Calderon's inverse problem," *Math. Res. Lett.*, Vol. 10, No. 5-6, 2003, pp. 685–693.

2. U. Leonhardt, "Optical conformal mapping," *Science*, Vol. 312, 2006, pp. 1777–1780.

3. J.B. Pendry, D. Schurig, and D.R. Smith, "Controlling electromagnetic fields," *Science*, Vol. 312, 2006, pp. 1780–1782.

4. A. Alù and N. Engheta, "Achieving transparency with plasmonic and metamaterial coatings," *Phys. Rev E*, Vol. 72, 016623, 2005.

5. A. Alù and N. Engheta, "Plasmonic materials in transparency and cloaking problems: Mechanism, robustness, and physical insights," *Optics Express*, Vol. 15, No. 6, 2007, pp. 3318–3332.

6. A. Alù and N. Engheta,"Cloaking and transparency for collections of particles with metamaterial and plasmonic covers," *Optics Express*, Vol. 15, No. 12, 2007, pp. 7578–7590.

7. D. Schurig, J.J. Mock, B. J. Justice, S.A. Cummer, J.B. Pendry, A.F. Starr, and D.R. Smith, "Metamaterial electromagnetic cloak at microwave frequencies," *Science*, Vol. 314, 2006, pp. 977–980.

8. W. Cai, U. K. Chettiar, A. V. Kildishev, and V. M. Shalaev, "Optical cloaking with non-magnetic metamaterials," *Nature Photonics*, Vol. 1, 2007, pp. 224–227.

9. M. Asghar et al., "Electromagnetic cloaking with a mixture of spiral inclusions," *Metamaterials '2007 Proceedings*, Rome, Italy, 22-24 Oct. 2007, pp. 957–960.

10. M. Yan, Z. Ruan, and M. Qiu, "Cylindrical invisibility cloak with simplified material parameters is inherently visible," *Phys. Rev. Lett.*, Vol. 99, No. 23, 233901, 2007.

11. S.A. Tretyakov and I.S. Nefedov, "Field-transforming metamaterials," *Metamaterials '2007 Proceedings*, Rome, Italy, 22-24 Oct. 2007, pp. 474–477.

12. M. Kerker, "Invisible bodies," *J. Opt. Soc. Am.*, Vol. 65, No. 4, 1975, pp. 376–379.

13. H. Chew and M. Kerker, "Abnormally low electromagnetic scattering cross sections," *J. Opt. Soc. Am.*, Vol. 66, No. 5, 1976, pp. 445–449.

14. A. Sihvola, "Properties of dielectric mixtures with layered spherical inclusions," *Microwave Radiomet. Remote Sens. Appl.*, 1989, pp. 115–123.

15. P.-S. Kildal, A. A. Kishk, and A. Tengs, "Reduction of forward scattering from cylindrical objects using hard surfaces," *IEEE Trans. Antennas Propag.*, Vol. 44, No. 11, 1996, pp. 1509–1520.

16. G. W. Milton and N. A. Nicorovici, "On the cloaking effects associated with anomalous localized resonance," *Proc. R. Soc. Lond. A: Math. Phys. Sci.*, Vol. 462, 2006, pp. 3027–3059.

17. P. Alitalo et al., "Realization of an electromagnetic invisibility cloak by transmission-line networks," *Metamaterials '2007 Proceedings*, Rome, Italy, 22-24 Oct. 2007, pp. 953–956.

18. P. Alitalo, O. Luukkonen, L. Jylhä, J. Venermo, and S. Tretyakov, "Transmission-line networks cloaking objects from electromagnetic fields," *IEEE Trans. Antennas Propag.*, in press.

19. P. Alitalo and S. Tretyakov, "Cylindrical transmission-line cloak for microwave frequencies," *2008 IEEE International Workshop on Antenna Technology Proceedings*, Chiba, Japan, 2008, in press.

Appendix B

The following paper is under review for publication in the Proceedings of Metamaterials'2008, to be held 21-26 September 2008, in Pamplona, Spain.

Broadband microwave cloaking with periodic networks of transmission lines

P. Alitalo and S. A. Tretyakov

Department of Radio Science and Engineering/SMARAD Center of Excellence
TKK Helsinki University of Technology, P.O. Box 3000, 02150 TKK, Finland
Fax: + 358–9-4512152; email: pekka.alitalo@tkk.fi, sergei.tretyakov@tkk.fi

Abstract

In this paper we present the design and full-wave simulations of two cylindrical cloaks based on the use of free-space-matched transmission-line networks. Because of the simple structure (no resonant inclusions, no strong dispersion), these types of cloaks offer very wide bandwidths as compared to other available cloaking techniques.

1. Introduction

Recent interest in electromagnetic cloaking has resulted in a variety of different techniques to reduce the (total) scattering cross section (SCS) of different types of objects [1–8]. In this paper we concentrate on a recently suggested cloaking technique, based on the use of transmission-line (TL) networks that can be matched with electromagnetic fields travelling in, e.g., free space. If the cloaks are composed of simple two- or three-dimensional unloaded TL networks (periodic in the 2-D case), the achievable operation bandwidths are expected to be much wider than in any cloak composed of passive resonant inclusions [8]. The clear drawback of this approach to cloak design is that there are severe limitations on the size and shape of the objects that can be cloaked, since the cloaked object must fit inside the volume that is surrounded by the TL networks. In the case of cloaks composed of 3-D or 2-D TL networks, the cloaked object can occupy a volume restricted by a three-dimensional mesh as shown in Fig. 1a.

Recently, we have studied two different cylindrical cloaks capable of cloaking of 2-D TE-polarized electromagnetic waves (as, e.g., the cloak in [7]). One such cloak was designed to be electrically small (diameter of the cloaked object was about one third of the wavelength) [9] and the other one was electrically large (diameter of the cloaked object was about four wavelengths) [10]. In this paper we continue the development of both of these cloaks in order to get more insight on the obtainable frequency bandwidths where effective cloaking is achieved.

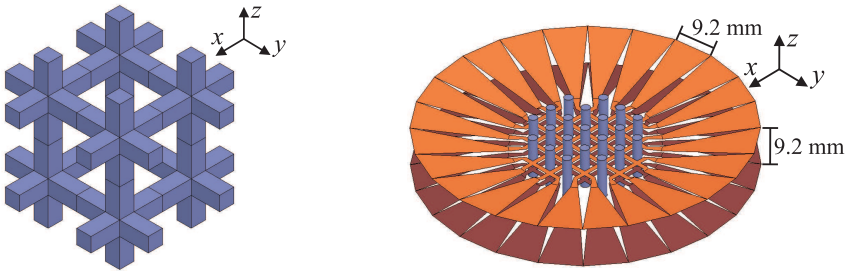

(a) (b)

Fig. 1: (a) 3-D mesh composed of 8 unit cells, demonstrating the type of volume that can be cloaked with the proposed approach. (b) HFSS-model of cloak no. 1 with the reference object inside.

2. Cloak designs

Two cloaks are studied: an electrically small cloak (cloak no. 1) with the diameter of the cloaked object being in the order of $0.3\lambda_0$ at the design frequency, and an electrically large cloak (cloak no. 2) with the diameter of the cloaked object being in the order of $4\lambda_0$ at the design frequency. In both cases the design frequency (the frequency at which the optimal impedance matching with free space is obtained) is chosen to be approximately 3 GHz.

Cloak no. 1 is based on the cloak presented in [9], which was designed to operate around 2 GHz. In order to increase the operational frequency, we have decreased the period of the network from 8 mm to 5 mm, and tuned the impedance of the TLs so that the optimal network impedance (377 Ω) is obtained around 3 GHz. Using full-wave simulations conducted with the Ansoft HFSS software (see Fig. 1b), we have obtained the design parameters shown in Table 1, where d is the network period, k_{TL} is the wavenumber of the TLs, k_0 is the free space wavenumber, w_{TL} is the width of the TLs, h_{TL} is the separation of the parallel strips composing the TLs, and D is the diameter of the cylindrical cloak (without the "transition layer" [8–10]). The diameter of the PEC rods that are cloaked, is 2 mm. The parallel strips of the "transition layer" are shortened from 40 mm to 20 mm because of the increased frequency (note that these strips are non-resonant) [9].

Cloak no. 2 is based on the electrically large cloak presented in [10], which was designed to operate around 2 GHz, but for which the best cloaking performance was shown to be around 3 GHz. This is clearly due to the mismatch between the optimal impedance matching frequency (2 GHz in [10]) and the frequency where the optimal cloak electrical thickness is achieved (approximately 3 GHz in [10]). In order to improve the impedance matching at the operation frequency of 3 GHz, we have tuned the impedance of the TLs so that the optimal network impedance (377 Ω) is obtained around 3 GHz. Otherwise the cloak and reference object structures are the same as in [10]. Using full-wave simulations conducted with the Ansoft HFSS software, we have obtained the design parameters shown in Table 1.

Table 1: Design parameters for the studied cloaks.

	d	k_{TL}	w_{TL}	h_{TL}	D
Cloak no. 1	5 mm	k_0	1.04 mm	1.5 mm	$6d = 30$ mm
Cloak no. 2	8 mm	k_0	1.34 mm	2 mm	$52d = 416$ mm

3. Simulation results

We have carried out full-wave simulations (Ansoft HFSS) for both the cloaks described above, together with the bare reference objects as in [9,10], i.e., we illuminate the structures with plane waves having the electric field parallel to the z-axis. Both cloaks are modelled as being infinitely periodic along the z-axis. In order to study the performance of the cloaks we plot the total SCS of the cloaked objects, normalized to the total SCS of the uncloaked objects ($\mathrm{SCS}_{\mathrm{tot,norm}}$), see Fig. 2. The bandwidths where cloaking is obtained ($\mathrm{SCS}_{\mathrm{tot,norm}} < 1$) are clearly very wide and for cloak no. 1 this bandwidth is actually wider than the whole simulated frequency region. Therefore it is more informative to look at a specific limit where certain reduction of the SCS is obtained. Here we choose this limit to be $\mathrm{SCS}_{\mathrm{tot,norm}} < 0.5$, which corresponds to the reduction of the total SCS by 50 % or more. From Fig. 2 we can conclude that the relative bandwidths corresponding to at least this amount of reduction of the SCS are approximately 73 % for cloak no. 1 and 11 % for cloak no. 2, with the center frequencies being 3.0 GHz and 2.925 GHz, respectively.

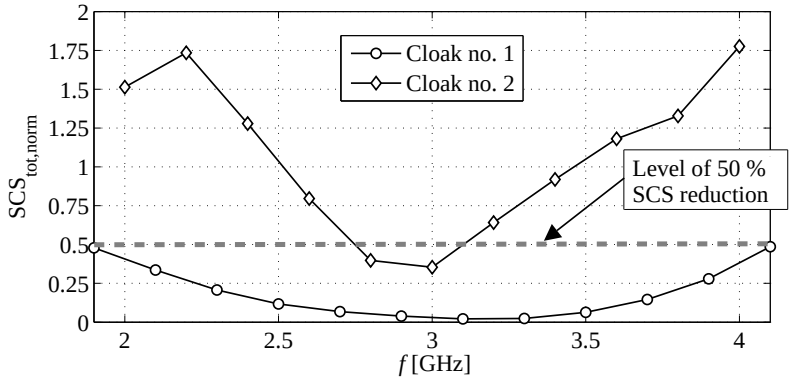

Fig. 2: HFSS-simulated total scattering cross sections of cloaked reference objects, normalized to the total scattering cross sections of uncloaked reference objects. The dashed line illustrates the level of total SCS reduction equal to 50 %.

4. Conclusion

By full-wave simulations of two electromagnetic cloaks, based on the recently proposed transmission-line approach, we have demonstrated the large frequency bandwidths in which these cloaks significantly reduce the total scattering cross sections of specific objects placed inside the cloaks. In this case the cloaked objects are arrays of infinitely long perfectly conducting rods. The total SCS is reduced by 50 % or more in relative bandwidths of about 73 % and 11 % for an electrically small cloak (diameter approximately $0.3\lambda_0$ at the center frequency) and for an electrically large cloak (diameter approximately $4\lambda_0$ at the center frequency), respectively.

Acknowledgements

This work has been partially funded by the Academy of Finland and TEKES through the Center-of-Excellence program and by the European Space Agency (ESA-ESTEC) under contract 21261/07/NL/CB (Ariadna program). P. Alitalo acknowledges financial support by GETA, Tekniikan Edistämissäätiö, and the Nokia Foundation.

References

[1] M. Kerker, Invisible bodies, *J. Opt. Soc. Am.*, vol. 65, no. 4, pp. 376–379, 1975.

[2] P.-S. Kildal, A.A. Kishk, and A. Tengs, Reduction of forward scattering from cylindrical objects using hard surfaces, *IEEE Trans. Antennas Propagation*, vol. 44, no. 11, pp. 1509–1520, 1996.

[3] A. Greenleaf, M. Lassas, G. Uhlmann, On nonuniqueness for Calderon's inverse problem, *Math. Res. Lett.*, vol. 10, no. 5-6, pp. 685–693, 2003.

[4] A. Alù and N. Engheta, Achieving transparency with plasmonic and metamaterial coatings, *Physical Review E*, vol. 72, p. 016623, 2005.

[5] U. Leonhardt, Optical conformal mapping, *Science*, vol. 312, pp. 1777–1780, 2006.

[6] J.B. Pendry, D. Schurig, and D.R. Smith, Controlling electromagnetic fields, *Science*, vol. 312, pp. 1780–1782, 2006.

[7] D. Schurig, J.J. Mock, B.J. Justice, S.A. Cummer, J.B. Pendry, A.F. Starr, and D.R. Smith, Metamaterial electromagnetic cloak at microwave frequencies, *Science*, vol. 314, pp. 977–980, 2006.

[8] P. Alitalo, O. Luukkonen, L. Jylhä, J. Venermo, and S.A. Tretyakov, Transmission-line networks cloaking objects form electromagnetic fields, *IEEE Trans. Antennas Propagation*, vol. 56, no. 2, pp. 416-424, 2008.

[9] P. Alitalo and S. Tretyakov, Cylindrical transmission-line cloak for microwave frequencies, Proceedings of *2008 IEEE International Workshop on Antenna Technology*, pp. 147-150, Chiba, Japan, 4-6 March 2008.

[10] P. Alitalo and S. Tretyakov, On electromagnetic cloaking – general principles, problems and recent advances using the transmission-line approach, Proceedings *2008 URSI General Assembly*, Chicago, USA, 7-16 August 2008, in press.

Appendix C

The following paper is under review for publication in the journal *Metamaterials*.

A microwave transmission-line network guiding electromagnetic fields through a dense array of metallic objects

Pekka Alitalo, Sylvain Ranvier, Joni Vehmas, Sergei Tretyakov
Department of Radio Science and Engineering / SMARAD Center of Excellence
TKK Helsinki University of Technology
P.O. Box 3000, FI-02015 TKK, Finland

Abstract

We present measurements of a transmission-line network, designed for cloaking applications in the microwave region. The network is used for channelling microwave energy through an electrically dense array of metal objects, which is basically impenetrable to the impinging electromagnetic radiation. With the designed transmission-line network the waves emitted by a source placed in an air-filled waveguide, are coupled into the network and guided through the array of metallic objects. Our goal is to illustrate the simple manufacturing, assembly, and the general feasibility of these types of cloaking devices.

Keywords: Transmission-line network; scattering cross section; electromagnetic cloak.

I. INTRODUCTION

The interest in different types of devices and materials for dramatic reduction of the total scattering cross sections of arbitrary or specific objects, has gained a large amount of interest after the publication of recent papers [1–4]. Earlier, the subject of hiding objects or particles from the surrounding electromagnetic fields was studied over the recent decades by many others as well, e.g., [5–9].

Recently, we have proposed an alternative approach to cloaking of objects composed of electrically dense arrays of small inclusions (in principle, these inclusions can be composed of arbitrary materials) [10, 11]. Since these objects can be two-dimensional or even three-dimensional interconnected meshes of e.g. metallic rods, practical applications of these types of cloaks include hiding strongly scattering objects such as support structures situated close to antennas, creating filters (a "wall" or a slab letting through only a part of the spectrum of the incoming field), etc. Also, as it has been recently proposed, these networks offer a simple way of creating new types of matched lenses especially for microwave applications [12].

The goal of this paper is to experimentally demonstrate the simple manufacturing and assembly of the previously proposed transmission-line structure, where the transmission lines composing the network are realized as parallel metal strips. By measurements we confirm the previously predicted matching of the network with free space, as well as a possibility of transmission of fields through an electrically dense mesh of metal objects. These results demonstrate the benefits of this simple approach to cloaking and present an easy way to measure the performance of these types of periodic structures.

II. TRANSMISSION-LINE NETWORK

The transmission-line network that is used here is the same as designed in Ref. [10], with the optimal impedance matching with free space observed around the frequency of 5.5 GHz. For this design, the matching with free space and the cloaking phenomenon were verified with full-wave simulations [10]. In this paper we demonstrate the simple manufacturing and assembly of this type of structure by choosing to use a two-dimensional periodic transmission-line network with a square shape and 16×16 unit cells in the network. The edges of the network are connected to a "transition layer" (parallel metal strips gradually enlarging from the ends of the network), as proposed in Ref. [10].

By inserting the designed network inside a metallic parallel-plate waveguide (with the plates lying in the xy-plane), we effectively realize the same situation as would occur with an infinitely periodic array of networks with the periodicity along the z-axis, since here the electric field is assumed to be parallel to the z-axis (as in the example case that was studied previously [10]). See Fig. 1 for an illustration of the transmission-line network with

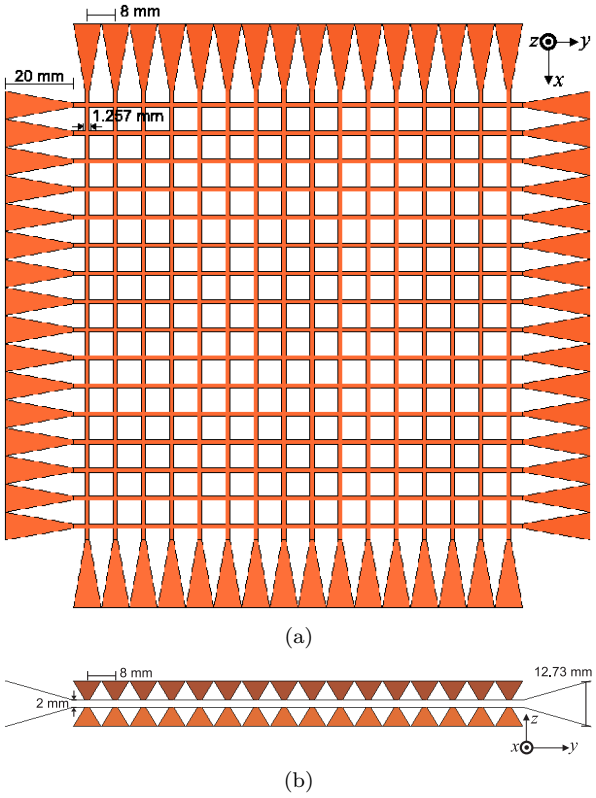

FIG. 1: Color online. Illustration of the designed transmission-line network. (a) Network in the xy-plane. (b) Network in the yz-plane.

all the necessary dimensions of the structure included.

The structure shown in Fig. 1 was manufactured by etching from a thin copper plate. The network can be simply assembled from two similar profiles (each profile as shown in Fig. 1a) just by placing them on top of each other, as shown in Fig. 1b. Ideally, the volume between these two metal objects should be free space [10]. Here, due to practical reasons, we have placed small pieces of styrofoam (with material properties very close to those of free space) between the metal strips. For assembly purposes, pieces of styrofoam are placed also on top and below the metal strips for support. These styrofoam pieces naturally do not affect the propagation properties of the transmission lines since the fields are mostly confined between the parallel strips.

In Ref. [10] the reference object, i.e., the object that we wanted to cloak (hide) from the surrounding electromagnetic fields, was an array of infinitely long perfectly conducting rods (that fit inside the neighboring transmission lines of the network). Here, we use a similar periodic structure as a reference object through which we want to guide the fields. The individual inclusions of this reference object are metal cylinders (parallel to the z-axis) with the same height as the network ($\sim$13 mm). The diameter of these cylinders is 4 mm and there are a total of $15 \times 15 = 225$ cylinders in the array.

III. MEASUREMENT SETUP

The measurement setup that is used here is similar to the one presented in Ref. [4]. With our measurements we effectively simulate an infinitely periodic structure with the periodicity in the vertical (z-) direction, by introducing a measurement cell consisting of a parallel-plate waveguide with its metallic plates lying in the xy-plane. Because of the image principle (the electric fields are assumed to be mostly parallel to the z-axis inside the waveguide), we can thus measure only one period of the structure. The difference between the measurement setup used here and the one in Ref. [4] is that here the upper plate of the waveguide is formed by a dense wire mesh, that lets through a fraction of the field inside the waveguide, instead of having a solid metallic upper plate with a hole for the probe, as was used in Ref. [4]. The mesh that we use here is the same as the one used in Ref. [13], i.e., the mesh is a thin copper plate, in which square holes of size 4 mm $\times$ 4 mm have been etched with the period of the holes being 5 mm. A small part of the field gets through this mesh and we can measure that field with a probe placed on top of the waveguide [13].

To simplify the measurement, we excite a cylindrical wave inside the waveguide with a feed probe (a coaxial probe placed inside the waveguide) and measure the transmission from this probe to the other probe ("measurement probe", placed on top of the waveguide) with a vector network analyzer (VNA, Agilent E8363A). The use of the metal mesh as a part of the top plate of the waveguide (rather than using a probe inside the waveguide) ensures that the measurement probe does not disturb the field inside the waveguide. The measurement probe on top of the waveguide is stationary, and the waveguide is moved with a PC-controlled scanner, synchronized with the VNA for precise measurements in the wanted coordinate positions. These points where the measurement of the complex S_{21}-parameter are taken with the VNA, can be arbitrarily chosen with the PC-program running the scanner. All the measurements presented in this paper were done with the steps of 5 mm. As

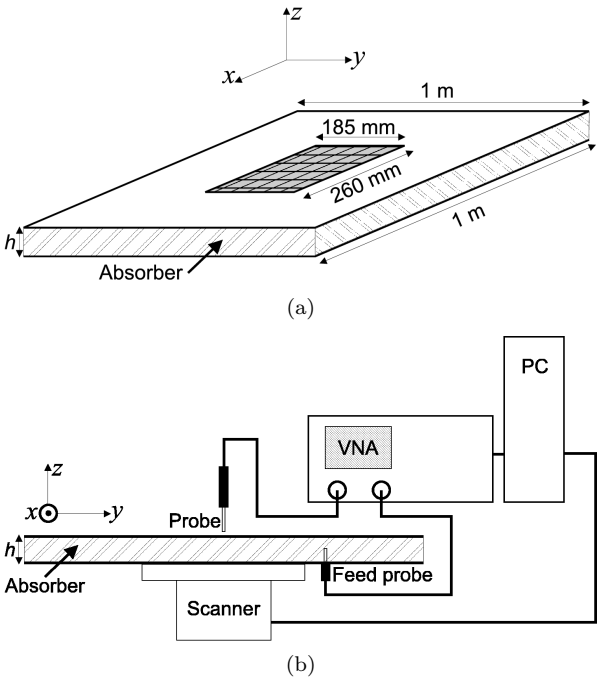

FIG. 2: Illustration of the measurement setup. (a) Waveguide with a metal mesh in the upper plate. (b) Measurement system with a VNA connected to the feed and measurement probes (the measurement probe is stationary) and a PC controlling the scanner which moves the waveguide in x- and y-directions.

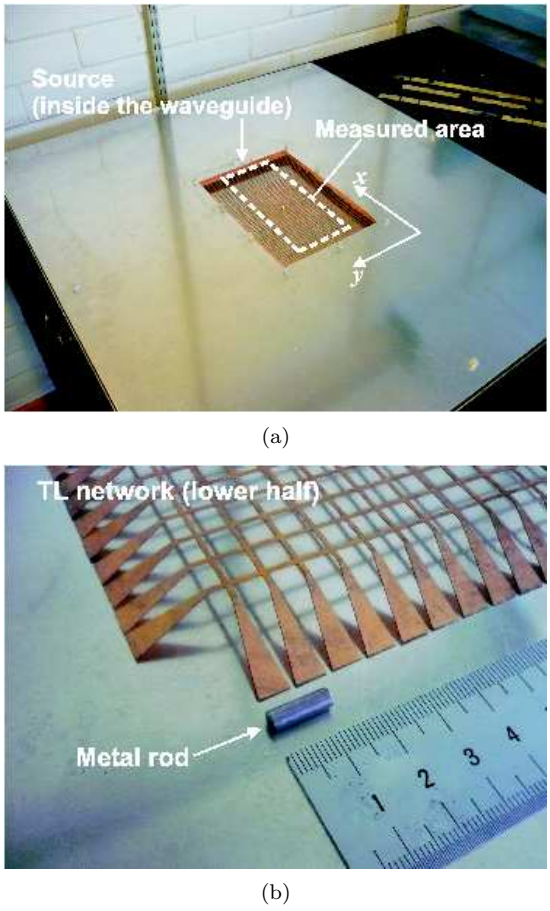

FIG. 3: Color online. (a) Photograph of the measurement setup, showing the aluminium parallel-plate waveguide and a copper mesh placed in the center of the top plate of the waveguide. (b) Photograph of the lower half of the TL network together with one metallic rod of the reference object.

the measured area is 240 mm × 100 mm, we will have the complex S_{21} measured at $49 \times 21 = 1029$ different points in the xy-plane.

The probe that we use here is a monopole oriented along the z-axis and positioned approximately at 3 mm away from the metal mesh. The probe is intentionally poorly matched at the frequencies of interest (5 GHz – 6 GHz) in order to make sure that the measurement probe does not disturb the fields inside the waveguide. The high dynamic range of the VNA makes sure that we can measure the electric field distribution inside the waveguide even with this poorly matched probe.

See Fig. 2 for an illustration of the measurement setup. The parallel-plate waveguide that we use here has the width and length of 1 m, and the height $h = 13$ mm (ideally h should be equal to 12.73 mm [10]). A part of the upper plate is removed from the center for the placing of the metal mesh (the area above which we want to measure the field distributions). The area of this mesh is 260 mm × 185 mm. The measurable area is further restricted by the used scanners. We have used two scanners, one with the movement limited to 300 mm (x-axis) and one with the movement limited to 100 mm (y-axis). The area to be measured has been decided to be 240 mm × 100 mm, centered in the mesh area. The feed probe is positioned in the center of the mesh along the y-direction and just outside the measured area in the x-direction (to have more space between the measured area and the feed), i.e., the feed probe coordinates are decided to be $x = 250$ mm, $y = 50$ mm, with the origin of this coordinate system being in one corner of the measured area. See Fig. 3 for a photograph of the measurement setup, taken from the direction of the positive z-axis, showing the empty waveguide and the metal mesh inserted as a part of the upper plate. The feed probe position and the measured area are also illustrated in the figure.

The volume between the waveguide plates, sur-

rounding the metal mesh, is filled by a microwave absorber. The large size of the waveguide ensures that the reflections from the waveguide edges are minimized (the absorber thickness in the x- and y-directions is approximately five wavelengths or more at the frequency of 5 GHz).

IV. MEASUREMENT RESULTS

Three different measurements were conducted: 1) an empty waveguide, 2) the reference object (array of 15 × 15 metal cylinders) inside the waveguide, and 3) the reference object *and* the transmission-line network inside the waveguide (with the inclusions of the reference object placed in the space between the transmission lines of the network). All the measurements were conducted in the frequency range from 1 GHz to 10 GHz, with the step of 0.025 GHz.

In the first case (empty waveguide), the results showed an expected result: at higher frequencies, i.e., at 5 GHz and up, the waveform inside the waveguide is close to the waveform produced by a line source. At lower frequencies, where the waveguide is electrically smaller, the reflections from the edges start to affect the field distributions, making them more complicated. See Fig. 4a for a snapshot of the measured time-harmonic electric field distribution at the frequency 5.85 GHz. Some reflections naturally still occur (mainly from the absorbers), but it is clear that the wave inside the waveguide resembles a cylindrical wave emanating from the point $x = 250$ mm, $y = 50$ mm.

In the second case (reference object inside the waveguide), the results were again as expected: at the higher frequencies, where it makes sense to compare the field distributions, the wavefronts emanating from the source are strongly reflected at the front boundary of the reference object. The field is seen to "split" in the center and move up or down along the reference object side. See Fig. 4b for a snapshot of the measured time-harmonic electric field distribution at the frequency 5.85 GHz.

In the third case (the reference object and the transmission-line network inside the waveguide) the field pattern on the source side is seen to be well preserved (as compared to Fig. 4a) in a certain frequency band around 5.85 GHz. Also, at the backside of the network, some field is propagating. At the position of the network (which encompasses the reference object), no field is measured, since the fields are confined inside the transmission lines. See Fig. 4c for a snapshot of the measured time-harmonic electric field distribution at the frequency 5.85 GHz.

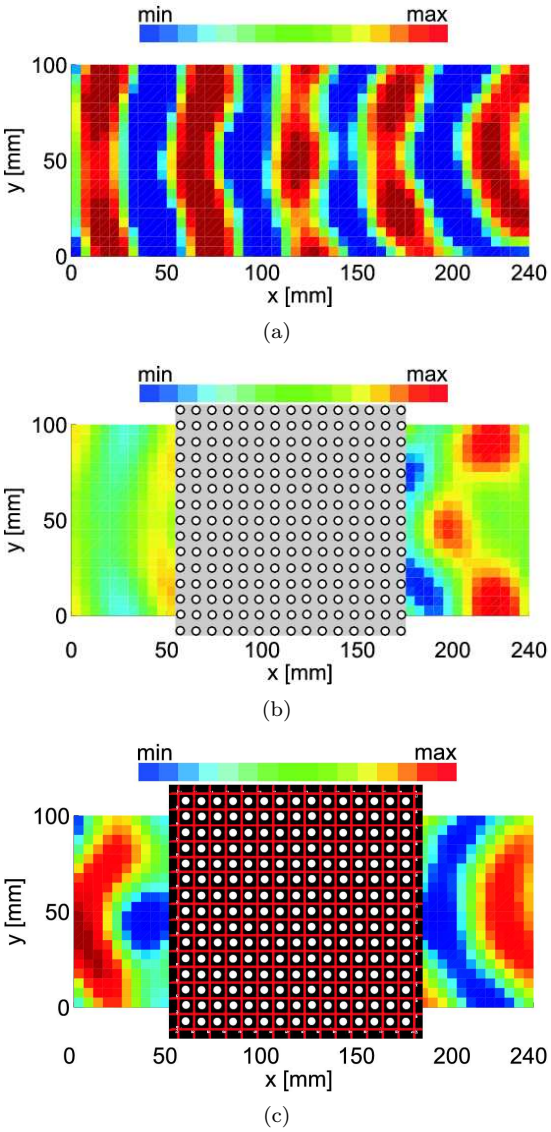

FIG. 4: Color online. Snapshots of the measured time-harmonic electric field distributions at 5.85 GHz. (a) empty waveguide, (b) reference object inside the waveguide, (c) reference object and the transmission-line network inside the waveguide. The "transition layer" connected to the network is not shown in (c) for clarity.

To further study the differences between the situations with and without the network, the phase distributions, calculated from the measured complex field data, are shown in Fig. 5, plotted only in the area between the reference object/network and the feed probe, i.e., in the area $x = 175$ mm ... $x = 240$ mm. As compared to the empty waveguide

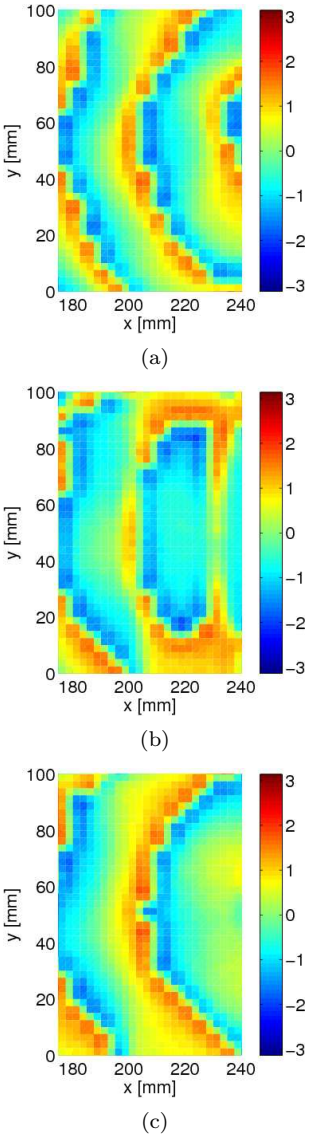

FIG. 5: Color online. Phase of the measured electric field distribution at 5.85 GHz. (a) empty waveguide, (b) reference object inside the waveguide, (c) reference object and the transmission-line network inside the waveguide. The phase distributions in each figure are interpolated from the corresponding measurement data for clarity.

(Fig. 5a), the case with the bare reference object, Fig. 5b, looks very different. This is due to the strong reflections from the front edge of the reference object. When the transmission-line network is placed inside the waveguide, together with the reference object, we see that the resulting phase distribution again is close to the one in Fig. 5a.

A more illustrative measure for the operation of the network is to compare the absolute value

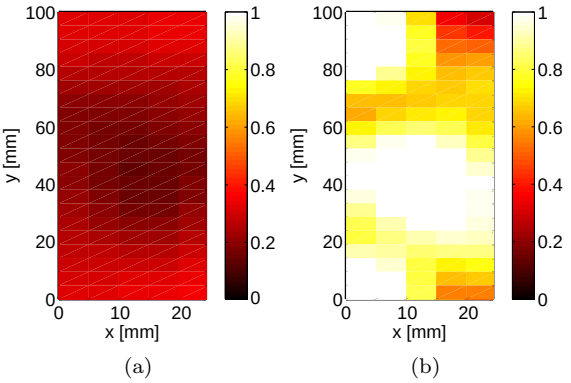

FIG. 6: Color online. Absolute value of the measured electric field distribution at 5.85 GHz, normalized to the maximum field value measured in front of the reference object/network (in the region $x = 175$ mm ... $x = 240$ mm). (a) reference object inside the waveguide, (b) reference object and the transmission-line network inside the waveguide.

of the field *behind* the reference object with and without the network in place (i.e, in the area $x = 0$ mm ... $x = 50$ mm). These results are shown in Fig. 6a and Fig. 6b, for the case without the network and with the network, respectively. As demonstrated by Fig. 6, the field amplitude behind the reference object is strongly suppressed (as compared to the field amplitude in front of this object). With the transmission-line network in place, the field amplitude behind the reference object/network is practically the same as in front.

The size of the network in this example case is comparable to the wavelength, so the inherent difference of the phase velocities between the wave propagating inside the network and the wave in free space, results in a change, or distortion of the impinging cylindrical waveform, as can be seen from Fig. 6b. The reasons for this difference in the phase velocity are discussed in Ref. [10]. Also, as the sharp edges of the square-shaped network are close to the measured area, scattering from these edges distorts the waveform. Note that the previously simulated "cloak slab" [10] was much wider than the network measured here.

To obtain efficient cloaking, i.e., to preserve the waveform of the incident wave both in front and behind the object (to reduce the total scattering cross section), one clearly needs to use a cloak which is electrically small enough and which does not have strong irregularities in its shape, not to cause significant forward scattering. It is also possible to use an electrically large cloak, dimensions of which are properly designed for a specific fre-

quency range so that the desired reduction of the forward scattering is achieved [10]. When the incidence angle of the impinging radiation is not known, the cloak naturally needs to be symmetric, i.e., cylindrical in the two-dimensional case or spherical in the three-dimensional case [10, 11]. Also, what is important in the case when the angle of the incident radiation is not known, the transmission-line network needs to be isotropic in the frequency range where most efficient cloaking is needed, i.e., the network period must be small enough as compared to the wavelength, as e.g. in the cylindrical cloak studied in Ref. [11].

V. CONCLUSIONS

We have presented a prototype of a previously proposed and designed transmission-line network for cloaking purposes. In this paper we have demonstrated the benefits of this approach, such as the simple manufacturing, and confirm by measurements the predicted impedance matching with free space and the resulting field propagation through such a network (with a periodic array of metallic rods placed between the transmission lines of the network). The results are compared with a measurement of an empty measurement cell and with a measurement of the periodic array of metallic rods, effectively behaving as an impenetrable wall at the frequencies of interest.

Acknowledgements

This work has been partially funded by the Academy of Finland and TEKES through the Center-of-Excellence program and partially by the European Space Agency (ESA–ESTEC) contract no. 21261/07/NL/CB (Ariadna program). The authors wish to thank Mr. E. Kahra and Mr. L. Laakso for valuable help with manufacturing of the prototype and with building of the measurement setup. P. Alitalo acknowledges financial support by the Finnish Graduate School in Electronics, Telecommunications, and Automation (GETA), Tekniikan Edistämissäätiö (TES), and the Nokia Foundation.

[1] A. Alù and N. Engheta, Achieving transparency with plasmonic and metamaterial coatings, Phys. Rev E 72 (2005) 016623.

[2] U. Leonhardt, Optical conformal mapping, Science 312 (2006) 1777–1780.

[3] J.B. Pendry, D. Schurig, and D.R. Smith, Controlling electromagnetic fields, Science 312 (2006) 1780–1782.

[4] D. Schurig, J.J. Mock, B. J. Justice, S.A. Cummer, J.B. Pendry, A.F. Starr, and D.R. Smith, Metamaterial electromagnetic cloak at microwave frequencies, Science 314 (2006) 977–980.

[5] M. Kerker, Invisible bodies, J. Opt. Soc. Am. 65 (1975) 376–379.

[6] H. Chew and M. Kerker, Abnormally low electromagnetic scattering cross sections, J. Opt. Soc. Am. 66 (1976) 445–449.

[7] A. Sihvola, Properties of dielectric mixtures with layered spherical inclusions, Microwave Radiomet. Remote Sens. Appl. (1989) 115–123.

[8] P.-S. Kildal, A. A. Kishk, and A. Tengs, Reduction of forward scattering from cylindrical objects using hard surfaces, IEEE Trans. Antennas Propagat. 44 (1996) 1509–1520.

[9] A. Greenleaf, M. Lassas, G. Uhlmann, On nonuniqueness for Calderon's inverse problem, Math. Res. Lett. 10 (2003) 685–693.

[10] P. Alitalo, O. Luukkonen, L. Jylhä, J. Venermo, and S. A. Tretyakov, Transmission-line networks cloaking objects form electromagnetic fields, IEEE Trans. Antennas Propagat. 56 (2008) 416-424.

[11] P. Alitalo and S. Tretyakov, Cylindrical transmission-line cloak for microwave frequencies, in: Proceedings of the 2008 IEEE International Workshop on Antenna Technology (2008) 147-150.

[12] P. Alitalo, O. Luukkonen, J. Vehmas, and S. A. Tretyakov, Impedance-matched microwave lens, IEEE Antennas and Wireless Propagation Lett., in press (published online).

[13] S. Maslovski, S. A. Tretyakov, and P. Alitalo, Near-field enhancement and imaging in double planar polariton-resonant structures, Journal of Applied Physics 96 (2004) 1293-1300.

Appendix D

The following paper is under review for publication in the Proceedings of Metamaterials'2008, to be held 21-26 September 2008, in Pamplona, Spain.

Generalized field transformations using metamaterials

S. A. Tretyakov, I. S. Nefedov, P. Alitalo

Department of Radio Science and Engineering / SMARAD Center of Excellence, TKK Helsinki University of Technology, P.O. Box 3000, FI-02015 TKK, Finland, email: sergei.tretyakov@tkk.fi

Abstract

In this paper we generalize the concept of field-transforming metamaterials (introduced at the first edition of this Congress) and show that one can design bi-anisotropic metamaterials which "perform" the most general linear mapping of fields $\mathbf{E}_0(\mathbf{r})$, $\mathbf{H}_0(\mathbf{r})$ into a new set of fields $\mathbf{E}(\mathbf{r})$, $\mathbf{H}(\mathbf{r})$. We show what electromagnetic properties of the transforming medium are required if the transformed fields are arbitrary linear functions of the original fields, and analyse the basic properties of these media (reciprocity and passivity). The coefficients of these linear functions can be arbitrary functions of position and frequency, which opens a possibility to realize various unusual devices.

1. Introduction

It has been recently realized that metamaterials – artificial electromagnetic materials with engineered properties – can be designed to control electromagnetic fields in rather general ways. For example, it has been shown that transformation of spatial coordinates (accompanied by the corresponding transformation of electromagnetic fields) can be mimicked by introducing electromagnetic materials with specific electromagnetic properties into the domain where the coordinates have been transformed [1, 2]. Not only spatial coordinates can be transformed and the result simulated by some metamaterial, but also the time coordinate can be transformed with a similar interpretation. It has been known for a long time that the material relations of an isotropic magnetodielectric transform into certain bi-anisotropic relations if the medium is moving with a constant velocity (e.g., [3]). It was suggested that also this effect of time transformation can possibly be mimicked by a metamaterial [4, 5, 6].

Recently we have introduced the concept of field-transforming metamaterials [7]. In this concept we start directly from a desired transformation of electromagnetic fields and find the material properties that are necessary to realize this transformation. In this paper we extend this concept to arbitrary (bi-anisotropic) field transformations.

2. Field transformations with metamaterials

Let us assume that in a certain volume V of free space there exist electromagnetic fields $\mathbf{E}_0(\mathbf{r})$, $\mathbf{H}_0(\mathbf{r})$ created by sources located outside volume V (we work in the frequency domain, and these vectors are complex amplitudes of the fields). We fill volume V with a metamaterial in such a way that after the volume is filled, the original fields $\mathbf{E}_0$ and $\mathbf{H}_0$ are transformed to new fields $\mathbf{E}$ and $\mathbf{H}$ according to the following rule:

$$\begin{aligned} \mathbf{E}(\mathbf{r}) &= F(\mathbf{r},\omega)\mathbf{E_0}(\mathbf{r}) + \sqrt{\tfrac{\mu_0}{\varepsilon_0}}A(\mathbf{r},\omega)\mathbf{H_0}(\mathbf{r}) \\ \mathbf{H}(\mathbf{r}) &= G(\mathbf{r},\omega)\mathbf{H_0}(\mathbf{r}) + \sqrt{\tfrac{\varepsilon_0}{\mu_0}}C(\mathbf{r},\omega)\mathbf{E_0}(\mathbf{r}). \end{aligned} \tag{1}$$

Here, scalar functions $F(\mathbf{r},\omega)$, $G(\mathbf{r},\omega)$, $A(\mathbf{r},\omega)$ and $C(\mathbf{r},\omega)$ are arbitrary differentiable functions. Substituting (1) into the Maxwell equations and demanding that the "original" fields $\mathbf{E}_0$ and $\mathbf{H}_0$ satisfy the free-space equations, one finds that the "transformed" fields satisfy the Maxwell equations in a medium with the following constitutive relations between the induction vectors $\mathbf{B}$ and $\mathbf{D}$ and the fields $\mathbf{E}$ and $\mathbf{H}$:

$$\mathbf{B} = \sqrt{\frac{\mu_0}{\varepsilon_0}}\frac{j}{\omega}\frac{1}{FG-AC}(F\nabla A - A\nabla F)\times\mathbf{H} + \mu_0\frac{1}{FG-AC}\left(F^2+A^2\right)\mathbf{H}$$
$$+\frac{j}{\omega}\frac{1}{FG-AC}(G\nabla F - C\nabla A)\times\mathbf{E} - \sqrt{\varepsilon_0\mu_0}\frac{1}{FG-AC}\left(AG+CF\right)\mathbf{E}, \tag{2}$$

$$\mathbf{D} = \sqrt{\frac{\varepsilon_0}{\mu_0}}\frac{j}{\omega}\frac{1}{FG-AC}(C\nabla G - G\nabla C)\times\mathbf{E} + \varepsilon_0\frac{1}{FG-AC}\left(G^2+C^2\right)\mathbf{E}$$
$$+\frac{j}{\omega}\frac{1}{FG-AC}(A\nabla C - F\nabla G)\times\mathbf{H} - \sqrt{\varepsilon_0\mu_0}\frac{1}{FG-AC}\left(AG+CF\right)\mathbf{H}. \tag{3}$$

Using the notations of [4], we write the equations for $\mathbf{D}$ and $\mathbf{B}$ in the following form:

$$\begin{aligned}\mathbf{D} &= \overline{\overline{\varepsilon}}\cdot\mathbf{E} + \sqrt{\epsilon_0\mu_0}(\overline{\overline{\chi}} - j\overline{\overline{\kappa}})\cdot\mathbf{H},\\ \mathbf{B} &= \overline{\overline{\mu}}\cdot\mathbf{H} + \sqrt{\epsilon_0\mu_0}(\overline{\overline{\chi}} + j\overline{\overline{\kappa}})^T\cdot\mathbf{E}.\end{aligned} \tag{4}$$

From (2) and (3) we obtain the following expressions for the required material parameters $\overline{\overline{\varepsilon}}$, $\overline{\overline{\mu}}$, $\overline{\overline{\chi}}$ and $\overline{\overline{\kappa}}$ in terms of the transformation coefficients:

$$\overline{\overline{\varepsilon}} = \varepsilon_0\frac{1}{FG-AC}\left(G^2+C^2\right)\overline{\overline{I}} + \sqrt{\frac{\varepsilon_0}{\mu_0}}\frac{j}{\omega}\frac{1}{FG-AC}(C\nabla G - G\nabla C)\times\overline{\overline{I}}, \tag{5}$$

$$\overline{\overline{\mu}} = \mu_0\frac{1}{FG-AC}\left(F^2+A^2\right)\overline{\overline{I}} + \sqrt{\frac{\mu_0}{\varepsilon_0}}\frac{j}{\omega}\frac{1}{FG-AC}(F\nabla A - A\nabla F)\times\overline{\overline{I}}, \tag{6}$$

$$\overline{\overline{\chi}} = -\frac{1}{FG-AC}(AG+CF)\overline{\overline{I}} + \frac{1}{\sqrt{\epsilon_0\mu_0}}\frac{j}{2\omega}\frac{1}{FG-AC}\left[(A\nabla C - F\nabla G) - (G\nabla F - C\nabla A)\right]\times\overline{\overline{I}}, \tag{7}$$

$$\overline{\overline{\kappa}} = \frac{1}{\sqrt{\epsilon_0\mu_0}}\frac{1}{2\omega}\frac{1}{FG-AC}\left[-(A\nabla C - F\nabla G) - (G\nabla F - C\nabla A)\right]\times\overline{\overline{I}}. \tag{8}$$

Here $\overline{\overline{I}}$ is the unit dyadic.

Relations (2) and (3) describe a bi-anisotropic medium. Parameters $\overline{\overline{\varepsilon}}$ and $\overline{\overline{\mu}}$ are, apparently, effective permittivity and permeability. In the theory of bi-anisotropic media $\overline{\overline{\kappa}}$ is called the chirality dyadic, and $\overline{\overline{\chi}}$ is the nonreciprocity dyadic [4].

The effective permittivity and permeability contain both symmetric and antisymmetric parts, which indicates that in the most general case the required metamaterial is nonreciprocal (these dyadics are symmetric in reciprocal media). More specifically, the material cannot be reciprocal if $C\nabla G - G\nabla C \neq 0$ and $F\nabla A - A\nabla F \neq 0$.

Furthermore, in reciprocal media $\overline{\overline{\chi}} = 0$ (that is why $\overline{\overline{\chi}}$ is called the nonreciprocity dyadic). We see that except some very special cases (like position-independent transformation coefficients satisfying $AG = -CF$), the material is nonreciprocal due to its magnetoelectric coupling properties. The symmetric part of $\overline{\overline{\chi}}$ is called the Tellegen parameter [4]. This kind of magnetoelectric coupling exists in some natural crystals and in metamaterials which contain natural magnetic inclusions under external bias field (like small ferrite spheres) coupled to electrically polarizable objects (like metal strips) [8, 9]. The nonreciprocal part of $\overline{\overline{\chi}}$ describes the effects in moving media. In metamaterials (of course, at rest), such magnetoelectric coupling emulating moving media can be realized by coupling magnetized ferrite

spheres with specially shaped metal strips [6]. The chirality dyadic $\overline{\overline{\kappa}}$ is antisymmetric. This means that the medium is nonchiral (its structure is symmetric with respect to reflections in 3D space). This type of reciprocal magnetoelectric coupling can be realized by inclusions in the form of letter Ω arranged in pairs as "hats" [10].

According to the classification of linear materials developed in [4, 11], the most general field-transforming materials belong to the class of moving Tellegen omega media. In the most general case, some sources must be distributed inside the field-transforming metamaterial designed to realize particular field transformations, since calculation of $\nabla \cdot \mathbf{D}$ and $\nabla \cdot \mathbf{B}$ show that they may be nonzero in some situations.

3. Conclusion

We have introduced a general relation between the desired linear field transformations in a certain volume and the properties of metamaterials which "perform" the desired modification of fields. This approach to field transformations is not based on the transformation of spatial or time coordinates and directly links the desired field transformation with the required metamaterial properties.

Acknowledgements

This work has been partially funded by the Academy of Finland and TEKES through the Center-of-Excellence program and by the European Space Agency (ESA-ESTEC) under contract 21261/07/NL/CB (Ariadna program). P. Alitalo acknowledges financial support by GETA, Tekniikan Edistämissäätiö, and the Nokia Foundation.

References

[1] J.B. Pendry, D. Schurig, D.R. Smith, Controlling electromagnetic fields, *Science,* vol. 312, pp. 1780-1782, 2006.

[2] U. Leonhardt, Optical conformal mapping, *Science*, vol. 312, pp. 1777-1780, 2006.

[3] L.D. Landau and E.M. Lifshits, *Electrodynamics of Continuous Media*, 2^{nd} edition, Oxford, England: Pergamon Press, 1984.

[4] A.N. Serdyukov, I.V. Semchenko, S.A. Tretyakov, A. Sihvola, *Electromagnetics of bi-anisotropic materials: Theory and applications,* Amsterdam: Gordon and Breach Science Publishers, 2001.

[5] U. Leonhardt and T. Philbin, General relativity in electrical engineering, *New J. of Physics* vol. 8, p. 247, 2006.

[6] S.A. Tretyakov, Physical interpretation of the transparent absorbing boundary for the truncation of the computational domain, *Microwave and Guided Wave Letters,* vol. 8, no. 10, pp. 321-323, 1998.

[7] S.A. Tretyakov and I.S. Nefedov, Field-transforming metamaterials, *Proceedings of Metamaterials'2007*, pp. 474-477, Rome, Italy, 22-24 October 2007.

[8] S.V. Zagriadski, S.A. Tretyakov, Electrodynamic theory of magnetoelectric particles on the base of strip-line-coupled magnetostatic wave resonators, *Electromagnetics,* vol. 22, no. 2, pp. 85-95, 2002.

[9] S.A. Tretyakov, S.I. Maslovski, I.S. Nefedov, A.J. Viitanen, P.A. Belov, A. Sanmartin, Artificial Tellegen particle, *Electromagnetics,* vol. 23, no. 8, pp. 665-680, 2003.

[10] S.A. Tretyakov, A.A. Sochava, Proposed composite material for non-reflecting shields and antenna radomes, *Electronics Letters,* vol. 29, no. 12, pp. 1048-1049, 1993.

[11] S.A. Tretyakov, A.H. Sihvola, A.A. Sochava, C.R. Simovski, Magnetoelectric interactions in bi-anisotropic media, *Journal of Electromagnetic Waves and Applications,* vol. 12, no. 4, pp. 481-497, 1998.

Appendix E

The following paper is under review for publication in *New Journal of Physics*.

Generalized field-transforming metamaterials

Sergei A Tretyakov, Igor S Nefedov, and Pekka Alitalo

Department of Radio Science and Engineering/SMARAD Center of Excellence, Helsinki University of Technology, P.O. Box 3000, FI-02015 TKK, Finland

E-mail: sergei.tretyakov@tkk.fi

Abstract.

In this paper we introduce a generalized concept of field-transforming metamaterials, which perform field transformations defined as linear relations between the original and transformed fields. These artificial media change the fields in a prescribed fashion in the volume occupied by the medium. We show what electromagnetic properties of transforming medium are required. The coefficients of these linear functions can be arbitrary scalar functions of position and frequency, which makes the approach quite general and opens a possibility to realize various unusual devices.

1. Introduction

It has been recently realized that metamaterials – artificial electromagnetic materials with engineered properties – can be designed to control electromagnetic fields in rather general ways. The concept of "transformation optics", which is based on finding artificial materials that create the desired configuration of electromagnetic fields, has been developed by several research teams, see e.g., [1, 2, 3]

In the known approaches one starts from a certain transformation of spatial coordinates and possibly also time, which corresponds to a desired transformation of electromagnetic fields. It has been shown that transformation of spatial coordinates (accompanied by the corresponding transformation of electromagnetic fields) can be mimicked by introducing electromagnetic materials with specific electromagnetic properties into the domain where the coordinates have been transformed [1, 2, 4]. As an example of such "coordinate-transforming" device an "invisibility cloak" has been suggested [1, 4]. In addition to perfect invisibility devices, similar approaches were applied to perfect lenses, description of the Aharonov-Bohm effect and artificial black holes. It has been known for a long time that the material relations of an isotropic magnetodielectric transform into certain bi-anisotropic relations if the medium is moving with a constant velocity (e.g., [5]). It was suggested that also this effect of time transformation can possibly be mimicked by a metamaterial [2, 6, 7].

We have recently introduced an alternative paradigm of transformation optics, where the required material properties are defined directly from the desired transformation of electromagnetic fields. This concept of field-transforming metamaterials was proposed in [8], where it was shown what metamaterial properties are required in order to perform the field transformation of the form $\mathbf{E}_0 \rightarrow \mathbf{E} = F(\mathbf{r}, \omega)\mathbf{E}_0$, $\mathbf{H}_0 \rightarrow \mathbf{H} = G(\mathbf{r}, \omega)\mathbf{H}_0$, where F and G are arbitrary differentiable functions of position and frequency. In this concept we start directly from a desired transformation of electromagnetic fields and do not involve any space nor time transforms. A special case of similar transformations was proposed earlier as a numerical technique for termination of computational domain by modulating fields with a function decaying to zero at the termination [9]. The physical interpretation of this numerical technique in terms of a slab of a material with the moving-medium material relations was presented in [6], and the pulse propagation in a slab of this medium backed by a boundary was studied in [10].

In this paper we generalize the concept of field-transforming metamaterials introducing methods to perform general bi-anisotropic field transformations, where the desired fields depend, in the general linear fashion, on both electric and magnetic fields of the original field distribution. Due to generality of the approach, the concept can be applied to a great variety of field transformations, not limited to cloaking devices.

2. Field transformations with metamaterials

Let us assume that in a certain volume V of free space there exist electromagnetic fields $\mathbf{E}_0(\mathbf{r})$, $\mathbf{H}_0(\mathbf{r})$ created by sources located outside volume V (we work in the frequency domain, and these vectors are complex amplitudes of the fields). The main idea is to fill volume V with a material in such a way that after the volume is filled, the original fields $\mathbf{E}_0$ and $\mathbf{H}_0$ would be transformed to other fields, according to the design goals. Here we consider metamaterials performing the general linear field transformation defined as

$$\mathbf{E}(\mathbf{r}) = F(\mathbf{r},\omega)\mathbf{E_0}(\mathbf{r}) + \sqrt{\frac{\mu_0}{\varepsilon_0}}A(\mathbf{r},\omega)\mathbf{H_0}(\mathbf{r}) \tag{1}$$

$$\mathbf{H}(\mathbf{r}) = G(\mathbf{r},\omega)\mathbf{H_0}(\mathbf{r}) + \sqrt{\frac{\varepsilon_0}{\mu_0}}C(\mathbf{r},\omega)\mathbf{E_0}(\mathbf{r}). \tag{2}$$

Here, scalar functions $F(\mathbf{r},\omega)$, $G(\mathbf{r},\omega)$ $A(\mathbf{r},\omega)$ and $C(\mathbf{r},\omega)$ are arbitrary differentiable functions. In this paper we consider only the case of scalar coefficients in the above relations, although the method can be extended to the most general linear relations between original and transformed fields by replacing scalar coefficients by arbitrary dyadics.

2.1. Required constitutive parameters

Substituting (1),(2) into the Maxwell equations and demanding that the original fields $\mathbf{E}_0$ and $\mathbf{H}_0$ satisfy the free-space Maxwell equations, one finds that the transformed fields $\mathbf{E}$ and $\mathbf{H}$ satisfy Maxwell equations $\nabla\times\mathbf{E} = -j\omega\mathbf{B}$, $\nabla\times\mathbf{H} = j\omega\mathbf{D}$ in a medium with the following material relations:

$$\mathbf{B} = \sqrt{\frac{\mu_0}{\varepsilon_0}}\frac{j}{\omega}\frac{1}{FG-AC}(F\nabla A - A\nabla F)\times\mathbf{H} + \mu_0\frac{1}{FG-AC}\left(F^2+A^2\right)\mathbf{H}$$
$$+\frac{j}{\omega}\frac{1}{FG-AC}(G\nabla F - C\nabla A)\times\mathbf{E} - \sqrt{\varepsilon_0\mu_0}\frac{1}{FG-AC}\left(AG+CF\right)\mathbf{E}, \tag{3}$$

$$\mathbf{D} = \sqrt{\frac{\varepsilon_0}{\mu_0}}\frac{j}{\omega}\frac{1}{FG-AC}(C\nabla G - G\nabla C)\times\mathbf{E} + \varepsilon_0\frac{1}{FG-AC}\left(G^2+C^2\right)\mathbf{E}$$
$$+\frac{j}{\omega}\frac{1}{FG-AC}(A\nabla C - F\nabla G)\times\mathbf{H} - \sqrt{\varepsilon_0\mu_0}\frac{1}{FG-AC}\left(AG+CF\right)\mathbf{H}. \tag{4}$$

Relations (3) and (4) describe a bi-anisotropic medium, whose constitutive relations can be conveniently written as [7]

$$\mathbf{B} = \overline{\overline{\mu}}\cdot\mathbf{H} + \sqrt{\epsilon_0\mu_0}(\overline{\overline{\chi}} + j\overline{\overline{\kappa}})^T\cdot\mathbf{E}, \tag{5}$$

$$\mathbf{D} = \overline{\overline{\varepsilon}}\cdot\mathbf{E} + \sqrt{\epsilon_0\mu_0}(\overline{\overline{\chi}} - j\overline{\overline{\kappa}})\cdot\mathbf{H}. \tag{6}$$

Comparing with (3) and (4) we can identify the required material parameters of the field-transforming medium:
The permittivity dyadic

$$\overline{\overline{\varepsilon}} = \varepsilon_0 \frac{1}{FG - AC} \left(G^2 + C^2\right) \overline{\overline{I}} + \sqrt{\frac{\varepsilon_0}{\mu_0}} \frac{j}{\omega} \frac{1}{FG - AC} (C\nabla G - G\nabla C) \times \overline{\overline{I}}, \quad (7)$$

the permeability dyadic

$$\overline{\overline{\mu}} = \mu_0 \frac{1}{FG - AC} \left(F^2 + A^2\right) \overline{\overline{I}} + \sqrt{\frac{\mu_0}{\varepsilon_0}} \frac{j}{\omega} \frac{1}{FG - AC} (F\nabla A - A\nabla F) \times \overline{\overline{I}}, \quad (8)$$

the nonreciprocity dyadic $\overline{\overline{\chi}}$

$$\overline{\overline{\chi}} = -\frac{1}{FG - AC}(AG + CF)\overline{\overline{I}} +$$

$$+\frac{1}{\sqrt{\epsilon_0 \mu_0}} \frac{j}{2\omega} \frac{1}{FG - AC} \left[(A\nabla C - F\nabla G) - (G\nabla F - C\nabla A)\right] \times \overline{\overline{I}}, \quad (9)$$

and the reciprocal magneto-electric coupling dyadic (also called chirality dyadic) $\overline{\overline{\kappa}}$

$$\overline{\overline{\kappa}} = \frac{1}{\sqrt{\epsilon_0 \mu_0}} \frac{1}{2\omega} \frac{1}{FG - AC} \left[-(A\nabla C - F\nabla G) - (G\nabla F - C\nabla A)\right] \times \overline{\overline{I}}. \quad (10)$$

In the above equations $\overline{\overline{I}}$ is the unit dyadic.

3. Classification of generalized field-transforming metamaterials

In this Section we classify the various cases of different materials that may need to be obtained depending on the required transformation (1), (2).

3.1. Reciprocity and nonreciprocity

Considering the required permittivity and permeability we see that in the general case they both contain symmetric and anti-symmetric parts, so the material is nonreciprocal. The nonreciprocal parts of permittivity and permeability vanish, if coefficients A and C in (1) and (2) equal zero, meaning that the desired field transformation does not involve magnetoelectric coupling, as in [8]. Note that in this case the medium can be still nonreciprocal due to its magnetoelectric properties, see below. The other important case when the permittivity and permeability are symmetric (actually scalar in the present case) is when the coefficients F and G vanish. These transformations define new electric field as a function of the original magnetic field and vice versa. Furthermore, we notice that if $A = C = 0$ and, in addition, $G = F$, the wave impedance of the medium does not change. This is expected, because this is the case when the electric and magnetic fields are transformed in the same way.

Next, let us consider what types of magnetoelectric coupling in field-transforming metamaterials are required for various transformations of fields. Here we will use the general classification of bi-anisotropic media according to [7, 11]. This classification is

based on splitting the coupling dyadics $\overline{\overline{\chi}}$ and $\overline{\overline{\kappa}}$ into three components, e.g. for $\overline{\overline{\kappa}}$ we write

$$\overline{\overline{\kappa}} = \kappa\overline{\overline{I}} + \overline{\overline{N}} + \overline{\overline{J}}, \tag{11}$$

where $\overline{\overline{N}}$ and $\overline{\overline{J}}$ denote the symmetric and antisymmetric parts, respectively. The scalar coefficient κ equals to the trace of $\overline{\overline{\kappa}}$, and it is the chirality parameter. In our case it is identically zero, meaning that field-transforming metamaterials (with scalar transformation coefficients) are nonchiral (their microstructure is mirror-symmetric). Also, the symmetric part $\overline{\overline{N}}$ is identically zero, and only the antisymmetric part

$$\overline{\overline{\kappa}} = \frac{1}{\sqrt{\epsilon_0\mu_0}}\frac{1}{2\omega}\frac{1}{FG-AC}\left[-(A\nabla C - F\nabla G) - (G\nabla F - C\nabla A)\right] \times \overline{\overline{I}} \tag{12}$$

remains.

Table 1. Classification of reciprocal bi-anisotropic media.

Coupling parameters	Class
$\kappa \neq 0$, $\overline{\overline{N}} = 0$, $\overline{\overline{J}} = 0$	Isotropic chiral medium
$\kappa \neq 0$, $\overline{\overline{N}} \neq 0$, $\overline{\overline{J}} = 0$	Anisotropic chiral medium
$\kappa = 0$, $\overline{\overline{N}} \neq 0$, $\overline{\overline{J}} = 0$	Pseudochiral medium
$\kappa = 0$, $\overline{\overline{N}} = 0$, $\overline{\overline{J}} \neq 0$	Omega medium
$\kappa \neq 0$, $\overline{\overline{N}} = 0$, $\overline{\overline{J}} \neq 0$	Chiral omega medium
$\kappa = 0$, $\overline{\overline{N}} \neq 0$, $\overline{\overline{J}} \neq 0$	Pseudochiral omega medium
$\kappa \neq 0$, $\overline{\overline{N}} \neq 0$, $\overline{\overline{J}} \neq 0$	General reciprocal bi-anisotropic medium

Classification of reciprocal bi-anisotropic media is given by Table 1 [7]. Field-transforming metamaterials possess reciprocal magneto-electric coupling as in omega media. The required effects can be realized by introducing inclusions in form of pairs of the letter Ω, arranging them in pairs forming "hats" [11, 12].

Similarly, we split the nonreciprocity dyadic $\overline{\overline{\chi}}$ as

$$\overline{\overline{\chi}} = \chi\overline{\overline{I}} + \overline{\overline{Q}} + \overline{\overline{S}}, \tag{13}$$

where $\overline{\overline{Q}}$ and $\overline{\overline{S}}$ denote the symmetric and antisymmetric parts, respectively, and χ is the trace of dyadic $\overline{\overline{\chi}}$. From (9) we can identify the parts of $\overline{\overline{\chi}}$ as

$$\chi = -\frac{1}{FG-AC}(AG + CF), \tag{14}$$

$$\overline{\overline{Q}} = 0, \tag{15}$$

$$\overline{\overline{S}} = \frac{1}{\sqrt{\epsilon_0\mu_0}}\frac{j}{2\omega}\frac{1}{FG-AC}\left[(A\nabla C - F\nabla G) - (G\nabla F - C\nabla A)\right] \times \overline{\overline{I}}. \tag{16}$$

In contrast to the reciprocal magneto-electric coupling, in this case the trace of the dyadic $\overline{\overline{\chi}}$ is generally non-zero. Looking at Table 2 [7], we see that the transformation

Table 2. Classification of nonreciprocal bi-anisotropic media.

Coupling parameters	Class
$\chi \neq 0$, $\overline{\overline{Q}} = 0$, $\overline{\overline{S}} = 0$	Tellegen medium
$\chi \neq 0$, $\overline{\overline{Q}} \neq 0$, $\overline{\overline{S}} = 0$	Anisotropic Tellegen medium
$\chi = 0$, $\overline{\overline{Q}} \neq 0$, $\overline{\overline{S}} = 0$	pseudoTellegen medium
$\chi = 0$, $\overline{\overline{Q}} = 0$, $\overline{\overline{S}} \neq 0$	Moving medium
$\chi \neq 0$, $\overline{\overline{Q}} = 0$, $\overline{\overline{S}} \neq 0$	Moving Tellegen medium
$\chi = 0$, $\overline{\overline{Q}} \neq 0$, $\overline{\overline{S}} \neq 0$	Moving pseudoTellegen medium
$\chi \neq 0$, $\overline{\overline{Q}} \neq 0$, $\overline{\overline{S}} \neq 0$	Nonreciprocal (nonchiral) medium

medium can be either a Tellegen medium, a moving medium, or a moving Tellegen medium.

If all the transformation coefficients do not depend on the spatial coordinates, the field-transforming metamaterial is the Tellegen medium [7, 11], except the special case when $AG = -CF$. Tellegen media can be synthesized as composites containing magnetized ferrite inclusions coupled with small metal strips or wires [13] or as mechanically bound particles having permanent electric and magnetic moments [14, 15].

3.2. Losses and gain

A bi-anisotropic medium is lossless if the permittivity and permeability dyadics are hermittian:

$$\overline{\overline{\varepsilon}} = \overline{\overline{\varepsilon}}^{\dagger}, \qquad \overline{\overline{\mu}} = \overline{\overline{\mu}}^{\dagger} \tag{17}$$

In addition, the magneto-electric dyadics for lossless media satisfy

$$\overline{\overline{\chi}} + j\overline{\overline{\kappa}} = (\overline{\overline{\chi}} - j\overline{\overline{\kappa}})^{*} \tag{18}$$

where $*$ denotes complex conjugate [7].

Analysing formulas (7)–(10) for the required material parameters we see that if the transformation coefficients are complex numbers, in general the required material can be a lossy or gain-medium. For real-valued coefficients F, G, A, and C the permittivity, permeability, and reciprocal magnetoelectric coupling coefficient correspond to lossless media. However, the antisymmetric part of the nonreciprocity dyadic (describing effects of "moving" media) may correspond to lossy or gain media, depending on how the transformation coefficients depend on the position.

3.3. Presence or absence of sources

In the derivation of the material relations in field-transforming metamaterials (3), (4) we have assumed that in the medium there are no source currents, that is, the field equations are $\nabla \times \mathbf{E} = -j\omega\mathbf{B}$, $\nabla \times \mathbf{H} = j\omega\mathbf{D}$. In addition, conditions

$$\nabla \cdot \mathbf{D} = 0, \qquad \nabla \cdot \mathbf{B} = 0 \tag{19}$$

should be also satisfied in source-free media. For the general case we have no proof that conditions (19) always hold. However, we have checked that they are satisfied in many important special cases, which include, for example, position-independent transformation coefficients and exponential dependence of the coefficients on the position vector.

4. Particular cases

Let us next consider some particular cases of field-transforming metamaterials to reveal the physical meaning of such transformations of fields.

4.1. Backward-wave medium

Consider the case of the field transformation $\mathbf{E}_0 \rightarrow \sqrt{\frac{\mu_0}{\varepsilon_0}}\,\mathbf{H}$, $\mathbf{H}_0 \rightarrow \sqrt{\frac{\varepsilon_0}{\mu_0}}\,\mathbf{E}$, which corresponds to $F = G = 0$ and $A = C = 1$ in (1),(2). Transforming electric field into magnetic field and *vice versa*, we reverse the propagation direction of plane waves in the transformation volume, so we expect that this would correspond to a backward-wave material filling the volume. And indeed we see that the material relations (3) and (4) reduce to

$$\mathbf{B} = -\mu_0 \mathbf{H}, \tag{20}$$

$$\mathbf{D} = -\varepsilon_0 \mathbf{E}, \tag{21}$$

which are the material relations of the Veselago medium [16].

4.2. Field rotation

Consider the case of the field transformation $\mathbf{E}_0 \rightarrow \sqrt{\frac{\mu_0}{\varepsilon_0}}\,\mathbf{H}$, $\mathbf{H}_0 \rightarrow -\sqrt{\frac{\varepsilon_0}{\mu_0}}\,\mathbf{E}$, which corresponds to $F = G = 0$ and $A = -1$, $C = 1$ in (1),(2). This kind of transformation relates to changing the polarization of the field: fields of a plane wave are rotated by -90 degrees around the propagation axis. The material relations (3) and (4) reduce to

$$\mathbf{B} = \mu_0 \mathbf{H}, \tag{22}$$

$$\mathbf{D} = \varepsilon_0 \mathbf{E}, \tag{23}$$

which are the material relations of free space. The reason why we do not see the change of polarization here is simply due to the fact that we wanted to consider F, G, A and C as *scalars*. The media (original or transformed) do not "feel" the polarization of the fields, so the rotation does not have any influence on the material relations. For instance, unpolarized light is obviously invariant under this transformation. We want to remind the reader that by considering the transformation coefficients F, G, A, C as dyadics, one can obtain more general transformations, which tailor also the field polarization in the general way.

4.3. Isotropic Tellegen medium

Consider next a more general case when all the transformation coefficients do not depend on the position vector inside the transformation domain. In this case, gradients of these functions vanish, and we see that the material relations are that of an isotropic Tellegen material:

$$\mathbf{B} = \mu_0 \frac{1}{FG - AC} \left(F^2 + A^2\right) \mathbf{H} - \sqrt{\varepsilon_0 \mu_0}\, \frac{AG + CF}{FG - AC}\, \mathbf{E}, \tag{24}$$

$$\mathbf{D} = \varepsilon_0 \frac{1}{FG - AC} \left(G^2 + C^2\right) \mathbf{E} - \sqrt{\varepsilon_0 \mu_0}\, \frac{AG + CF}{FG - AC}\, \mathbf{H}. \tag{25}$$

The medium is reciprocal only if $\chi = -\frac{AG+CF}{FG-AC} = 0$. We can note that if the transformation coefficients vary within the transformation volume, this generally requires simulation of a moving medium with the transformation metamaterial.

4.4. Tellegen nihility

Let us consider again the case where all the coefficients are position-independent, that is,

$$\nabla F = \nabla G = \nabla A = \nabla C = 0 \tag{26}$$

and also demand that the permittivity and permeability of the transforming medium become zero. This takes place when either

$$A = jF, \qquad C = jG \tag{27}$$

or

$$A = -jF, \qquad C = -jG \tag{28}$$

The material relations of the medium become

$$\begin{aligned} \mathbf{B} &= -j\sqrt{\varepsilon_0 \mu_0}\, \mathbf{E} \\ \mathbf{D} &= -j\sqrt{\varepsilon_0 \mu_0}\, \mathbf{H} \end{aligned} \tag{29}$$

for the case (27) or

$$\begin{aligned} \mathbf{B} &= j\sqrt{\varepsilon_0 \mu_0}\, \mathbf{E} \\ \mathbf{D} &= j\sqrt{\varepsilon_0 \mu_0}\, \mathbf{H} \end{aligned} \tag{30}$$

for the case (28).

These constitutive relations look similar to that of chiral nihility [17], but in this case the only non-zero material parameter is the Tellegen parameter. The Maxwell equations corresponding to relations (30) take the form

$$\nabla \times \mathbf{H} = -k_0 \mathbf{H}, \quad \nabla \times \mathbf{E} = k_0 \mathbf{E}, \tag{31}$$

where $k_0 = \omega\sqrt{\varepsilon_0\mu_0}$ is the free-space wavenumber. Thus, solutions of Eq. (31) are eigenfunctions of operator rot=$\nabla \times \overline{\overline{I}}$. If $\partial/\partial x = \partial/\partial y = 0$ then for the waves propagating in z-direction

$$\begin{array}{ll} E_x = -e_0 \exp(-jk_0 z) & H_x = e_0\eta^{-1} \exp(-jk_0 z) \\ E_y = je_0 \exp(-jk_0 z) & H_y = je_0\eta^{-1} \exp(-jk_0 z) \\ E_z = 0 & H_x = 0 \end{array} \tag{32}$$

where η is the wave impedance. Substituting expressions (27) or (28) for A and C into the original definitions (1),(2), we obtain the following formula for the wave impedance:

$$\eta = \frac{F}{G}\eta_0 \tag{33}$$

where η_0 is the wave impedance of vacuum.

As in the case of chiral nihility [17] and the Beltrami fields in chiral media [14, 18], the fields (32) correspond to circularly-polarized waves. However, in contrast to those two cases, where the phase shift between electric and magnetic fields equals exactly to $\pi/2$, in the considered case it depends on relation between F and G according to (33). If $F = G$, the electric and magnetic fields oscillate in phase.

4.5. Position-independent transformation coefficients

An interesting general conclusion can be drawn with regard to field transformations with all the coefficients being position-independent. In this case the wavenumber in the field-transforming metamaterial is the same as in the original medium (free space in our case). This can be shown by using the equation for the wavenumber k in a Tellegen medium [14]

$$k = k_0\sqrt{\varepsilon_r\mu_r - \chi^2}, \tag{34}$$

where ε_r and μ_r are the relative permittivity and permeability. Since

$$\varepsilon_r\mu_r - \chi^2 = \frac{(G^2 + C^2)(F^2 + A^2)}{(FG - AC)^2} - \frac{(AG + CF)^2}{(FG - AC)^2} = 1, \tag{35}$$

(34) simplifies to

$$k = k_0. \tag{36}$$

This means that for transformations of this class only the wave impedance of the transforming medium needs to be changed, but not the wavenumber. One can notice that this property indeed holds in all of the above special cases where the coefficients are position-independent.

4.6. Moving omega medium

Next we consider another class of field-transforming media assuming $A(\mathbf{r}, \omega) = C(\mathbf{r}, \omega) = 0$. Transformations of this type correspond to moving omega materials with the constitutive relations of the form:

$$\mathbf{D} = \varepsilon_0\tfrac{G}{F}\mathbf{E} - \tfrac{j}{\omega G}\nabla G \times \mathbf{H}, \quad \mathbf{B} = \mu_0\tfrac{F}{G}\mathbf{H} + \tfrac{j}{\omega F}\nabla F \times \mathbf{E}. \tag{37}$$

Both the nonreciprocity dyadic $\overline{\overline{\chi}}$ and the reciprocal magnetoelectric coupling dyadic $\overline{\overline{\kappa}}$ are antisymmetric:

$$\overline{\overline{\chi}} = -\frac{j}{2k_0}\left(\frac{\nabla F}{F} + \frac{\nabla G}{G}\right) \times \overline{\overline{I}}, \qquad \overline{\overline{\kappa}} = -\frac{1}{2k_0}\left(\frac{\nabla F}{F} - \frac{\nabla G}{G}\right) \times \overline{\overline{I}}, \tag{38}$$

where the first quantity describes moving-media effects and the second one corresponds to omega-medium properties. If the two transformation coefficients are equal ($F = G$), the omega coupling vanishes.

The Maxwell equation for the transformed fields read:

$$\begin{aligned} \nabla \times \mathbf{E}(\mathbf{r}) &= -j\omega\mu_0 \tfrac{F(\mathbf{r})}{G(\mathbf{r})}\mathbf{H}(\mathbf{r}) + \tfrac{1}{F(\mathbf{r})}\nabla F(\mathbf{r}) \times \mathbf{E}(\mathbf{r}), \\ \nabla \times \mathbf{H}(\mathbf{r}) &= j\omega\epsilon_0 \tfrac{G(\mathbf{r})}{F(\mathbf{r})}\mathbf{E}(\mathbf{r}) + \tfrac{1}{G(\mathbf{r})}\nabla G(\mathbf{r}) \times \mathbf{H}(\mathbf{r}). \end{aligned} \tag{39}$$

4.7. Artificial moving medium

Let us consider a more special case when the transformation preserves the wave impedance of the medium [$F(\mathbf{r}) = G(\mathbf{r})$] [8]. Material relations (37) take the form of material relations of slowly moving media (velocity $v \ll c$, where c is the speed of light in vacuum), see, e.g., [19]:

$$\begin{aligned} \mathbf{D} &= \tfrac{1}{\sqrt{1-v^2/c^2}}\left(\epsilon_0\mathbf{E} + \tfrac{1}{c^2}\mathbf{v} \times \mathbf{H}\right) \approx \epsilon_0\mathbf{E} + \tfrac{1}{c^2}\mathbf{v} \times \mathbf{H} \\ \mathbf{B} &= \tfrac{1}{\sqrt{1-v^2/c^2}}\left(\mu_0\mathbf{H} - \tfrac{1}{c^2}\mathbf{v} \times \mathbf{E}\right) \approx \mu_0\mathbf{H} - \tfrac{1}{c^2}\mathbf{v} \times \mathbf{E} \end{aligned} \tag{40}$$

In the last relation we have neglected the second-order terms v^2/c^2. The "velocity" of the transforming medium can be identified by comparing with (37) as

$$\mathbf{v} = -j\frac{c^2}{\omega}\frac{\nabla F}{F} \tag{41}$$

To get more insight, let us analyze the one-dimensional case considering transformation functions depending only on one coordinate z and assuming that $F(z) = G(z)$ is an exponential function of z. Two cases should be distinguished:

- $\nabla F/F$ is *imaginary*, e.g., $F(z) = e^{-j\alpha z}$ with a real parameter α. In this case the effective "velocity" is **real**. This metamaterial simulates moving media. Note that the required material relations have the form of the relations for slowly moving media even if the equivalent velocity is not small.
- $F(z)$ is a purely *real* function, e.g., $F(z) = e^{-\alpha z}$, where α is real. In this case the effective "velocity" of the medium is **imaginary**. Note that the material relations of a medium traveling faster than light formally have an imaginary vector coefficient in the second term of (40). However, one cannot say that this metamaterial simulates media moving faster than light, because in that case also the effective permittivity and permeability would be imaginary quantities.

Let us examine the source-free conditions $\nabla \cdot \mathbf{D} = 0$ and $\nabla \cdot \mathbf{B} = 0$ for this special case of $F = G = e^{-\alpha z}$. Actually, $\frac{\nabla F(\mathbf{r})}{F(\mathbf{r})} = \frac{\nabla G(\mathbf{r})}{G(\mathbf{r})} = -\alpha\,\mathbf{z}_0$. Then it follows from (37)

$$\nabla \cdot \mathbf{D} = \nabla \cdot [F(\mathbf{r})\epsilon_0\mathbf{E}_0(\mathbf{r})] + \frac{j}{\omega}\nabla \cdot [\alpha\mathbf{z}_0 \times F(\mathbf{r})\mathbf{H}_0] \tag{42}$$

Simple calculation using the free-space Maxwell equations relating $\mathbf{E}_0$ and $\mathbf{H}_0$ shows that $\nabla \cdot \mathbf{D} = 0$. Condition $\nabla \cdot \mathbf{B} = 0$ can be checked similarly.

Let us check the passivity condition for this medium. The period-average of the time derivative of the field energy is expressed as [7]:

$$\left\langle \frac{dW}{dt} \right\rangle_t = \frac{j\omega}{4} \mathrm{f}^* \cdot (\mathrm{M} - \mathrm{M}^\dagger) \cdot \mathrm{f} \tag{43}$$

where

$$\mathrm{f} = \begin{pmatrix} \mathbf{E} \\ \mathbf{H} \end{pmatrix}, \quad \mathrm{M} = \begin{pmatrix} \epsilon_0 \overline{\overline{I}} & \sqrt{\epsilon_0 \mu_0}\, \overline{\overline{\chi}}^\dagger \\ \sqrt{\epsilon_0 \mu_0}\, \overline{\overline{\chi}} & \mu_0 \overline{\overline{I}} \end{pmatrix}. \tag{44}$$

For real transformation coefficients we take as an example $F(z) = e^{-\alpha z}$, where $\alpha > 0$. For a plane wave propagating along z, calculation leads to

$$\left\langle \frac{dW}{dt} \right\rangle_t = \frac{\alpha}{\eta} e^{-2\alpha z} > 0 \tag{45}$$

This implies that the medium possesses losses. However, for a plane wave traveling in the opposite direction (along $-z$), the sign in the above expression is reversed, corresponding to a gain medium. This is expected because in the last case the field amplitude grows along the propagation direction. In the case of imaginary α this value is equal to zero and the medium is lossless.

5. Transmission through a slab of a field-transforming medium

Let us consider an infinite slab of a field-transforming metamaterial in vacuum, which is excited by a normally incident plane wave. Here we continue studying the case of moving-medium transformations, that is, $F = G$ and $A = C = 0$. Let the thickness of the slab be d, and the field-transforming properties be defined by a function of one variable z — the coordinate in the direction normal to the interfaces: $F(z) = G(z)$. The general solution for the eigenwaves in the slab is, obviously,

$$E(z) = F(z)(ae^{-jk_0 z} + be^{jk_0 z}) \tag{46}$$

where E is the electric field amplitude, and a and b are constants, because this is how the free-space solution is transformed in this metamaterial slab. If $F = G$, the wave impedance in the transforming medium does not change.

Writing the boundary conditions on two interfaces, reflection and transmission coefficients can be found in the usual way. As a result, we have found that the reflection coefficient does not depend on function $F(z)$ at all, and it is given by the standard formula for a reflection coefficient from an isotropic slab at normal incidence. In particular, if the permittivity and permeability of the slab equal to that of free space, the reflection coefficient $R = 0$. The transmission coefficient in this matched case reads

$$T = \frac{F(d)}{F(0)}\, e^{-jk_0 d} \tag{47}$$

where $F(d)$ and $F(0)$ are the values of the transformation function at the two sides of the slab.

The non-reciprocal nature of field-transforming metamaterials is clearly visible here. If function $F(z)$ is real and it decays with z, then fields of waves traveling in the positive direction of z decay, while fields of waves traveling in the opposite directions grow. Obviously, such performance cannot be realized by passive media (see the calculation of the absorbed power in Section 4.7). If $F(d) = F(0) = 1$, the slab is "invisible", although inside the slab the field distribution can be pretty arbitrary, as dictated by the given function $F(z)$.

6. Conclusions

Two different approaches to design of metamaterials which transform fields in a desired way are known. The first one has been proposed and developed in [1, 2], and it is based on coordinate transformations. The second one has been introduced in [8] and developed here, and it transforms the fields directly, according to a desired prescription. This technique can be potentially applied to a very wide variety of engineering problems, where a certain field transformation is required. One of the most important property of the field transformation approach is that a medium with prescribed parameters turns out to be nonreciprocal with except of some special cases. Most often, a metamaterial simulating moving media is required. Potential physical realizations of metamaterials with the properties required for general linear field transformations (such as artificial moving media) are discussed in [6, 7, 13, 15, 20].

Acknowledgements

This work has been partially funded by the Academy of Finland and TEKES through the Center-of-Excellence program and partially by the European Space Agency (ESA–ESTEC) contract no. 21261/07/NL/CB (Ariadna program). The authors wish to thank prof. Constantin Simovski for helpful discussions. P. Alitalo acknowledges financial support by the Finnish Graduate School in Electronics, Telecommunications, and Automation (GETA), the Emil Aaltonen Foundation, and the Nokia Foundation.

References

[1] Pendry J B, Shurig D and Smith D R 2006 *Science* 312 1780
[2] Leonhardt U and Philbin T 2006 *New J. Phys.* 8 247
[3] Cai W, Chettiar U K, Kildishev A V and Shalaev V M 2007 *Nature Photonics* 1 224
[4] Leonhardt U 2006 *Science* 312 1777
[5] Landau L D and Lifshits E M 1984 *Electrodynamics of Continuous Media, 2nd edition* (Oxford: Pergamon Press)
[6] Tretyakov S A 1998 *Microwave and Guided Wave Letters* 8 321

[7] Serdyukov A N, Semchenko I V, Tretyakov S A and Sihvola A 2001 *Electromagnetics of bi-anisotropic materials: Theory and applications* (Amsterdam: Gordon and Breach Science Publishers)
[8] Tretyakov S A and Nefedov I S 2007 *Proc. Metamaterials'2007* 474
[9] Peng J and Balanis C A 1997 *IEEE Microwave and Guided Wave Letters* 7 347
[10] Maslovski S I and Tretyakov S A 1999 *Microwave and Optical Technology Letters* 23 59
[11] Tretyakov S A, Sihvola A H, Sochava A A and Simovski C R 1998 *J. Electromagnetic Waves and Applications* 12 481
[12] Tretyakov S A and Sochava A A 1993 *Electronics Letters* 29 1048
[13] Tretyakov S A, Maslovski S I, Nefedov I S, Viitanen A J, Belov P A and Sanmartin A *Electromagnetics* 23 665
[14] Lindell I V, Sihvola A H, Tretyakov S A and Viitanen A J 1994 *Electromagnetic Waves in Chiral and Bi-Isotropic Media* (London: Artech House)
[15] Ghosh A, Sheridon N K and Fischer P, *Janus particles with coupled electric and magnetic moments make a disordered magneto-electric medium* published online: http://arxiv.org/abs/0708.1126v1
[16] Veselago V G, 1068 *Soviet Physics Uspekhi* 10 509 (Originally in Russian in *Uspekhi Fizicheskikh Nauk,* vol. 92, no. 3, pp. 517-526, July 1967)
[17] Tretyakov S, Nefedov I, Sihvola A, Maslovski S and Simovski C 2003 *Journal of Electromagnetic Waves and Applications* 17 595
[18] Lakhtakia A 1994 *Beltrami fields in Chiral Media* (World Scientific)
[19] Kong J A 2005 *Electromagnetic Wave Theory* (Cambridge, MA: EMW Publishing)
[20] Zagriadski S V, Tretyakov S A 2002 *Electromagnetics* 22 85

Appendix F

The following paper is under review for publication in the Proceedings of Metamaterials'2008, to be held 21-26 September 2008, in Pamplona, Spain.

Triple-spacetime Metamaterials

L. Bergamin

European Space Agency, The Advanced Concepts Team
Keplerlaan 1, 2201AZ Noordwijk, The Netherlands
Fax: + +31–71 565 8018; email: Luzi.Bergamin@esa.int

Abstract

In this paper an extension of the coordinate transformation approach to artificial media as introduced by Pendry and Leonhardt is presented. It is based upon the fact that a separate transformation of the two pairs $(\vec{E},\vec{B})$ and $(\vec{D},\vec{H})$ is a symmetry of Maxwell's equations, but changes the constitutive relation. This allows a geometric interpretation of non-reciprocal and indefinite media.

1. Introduction

The concept of Metamaterials mimicking coordinate transformations [1, 2, 3] has been very successful to design and understand novel types of media, such as invisibility cloaks [1, 2], perfect lenses, artificial black holes [3] or magnification devices [4]. Nevertheless, the class of constitutive relations available in this way is rather limited as the medium must be reciprocal and have equal permittivity and permeability, a complementary approach not making use of symmetries and geometric interpretations has been proposed in [5]. In this paper we provide a generalization of [3], which in terms of accessible media is less general than [5], but allows an immediate geometric interpretation and is based on symmetry transformations.

2. Triple-spacetime Metamaterials

When written in terms an arbitrary (not necessarily flat) metric $g_{\mu\nu}$ the constitutive relations of electromagnetism resemble those of a reciprocal medium [6]. Therefore, if empty space can look as a medium, a medium could also look as empty space. This is indeed possible [3]: one starts from laboratory space x^μ with metric $g_{\mu\nu}$ and applies a (eventually singular) symmetry transformation (diffeomorphism), which locally is expressed by a coordinate transformation $x^\mu \to \bar{x}^\mu$. The new space with metric $\bar{g}_{\mu\nu}$ describes the behavior of the electromagnetic fields, but the equations are re-interpreted in terms of the original coordinates x^μ. This leads to the constitutive relations [3]

$$\tilde{D}^i = \pm\frac{\bar{g}^{ij}}{\sqrt{-\bar{g}_{00}}}\frac{\sqrt{\bar{\gamma}}}{\sqrt{\gamma}}\tilde{E}_j - \frac{\bar{g}_{0j}}{\bar{g}_{00}}\epsilon^{jil}\tilde{H}_l\,, \qquad \tilde{B}^i = \pm\frac{\bar{g}^{ij}}{\sqrt{-\bar{g}_{00}}}\frac{\sqrt{\bar{\gamma}}}{\sqrt{\gamma}}\tilde{H}_j + \frac{\bar{g}_{0j}}{\bar{g}_{00}}\epsilon^{jil}\tilde{E}_l\,, \tag{1}$$

where the sign ambiguity refers to the fact that the transformation can change the orientation. One can extend this approach by realizing that the equations of motion may exhibit invariant transformations that are not symmetries of the action. Indeed, Maxwell's equations divide into two sets of equations,

$$\nabla_i B^i = 0\,, \qquad \nabla_0 B^i + \epsilon^{ijk}\partial_j E_k = 0\,, \qquad \text{and} \qquad \nabla_i D^i = \rho\,, \qquad \epsilon^{ijk}\partial_j H_k - \nabla_0 D^i = j^i\,, \tag{2}$$

which have mutually excluding field content and do not depend on the media properties. Therefore, two different diffeomorphisms applied to the two sets leave Maxwell's equations invariant, i.e. any source-free solution thereof is mapped upon another source-free solution. Still, the action as well as the constitutive relation are not invariant and thus the two situations are physically inequivalent. Nonetheless,

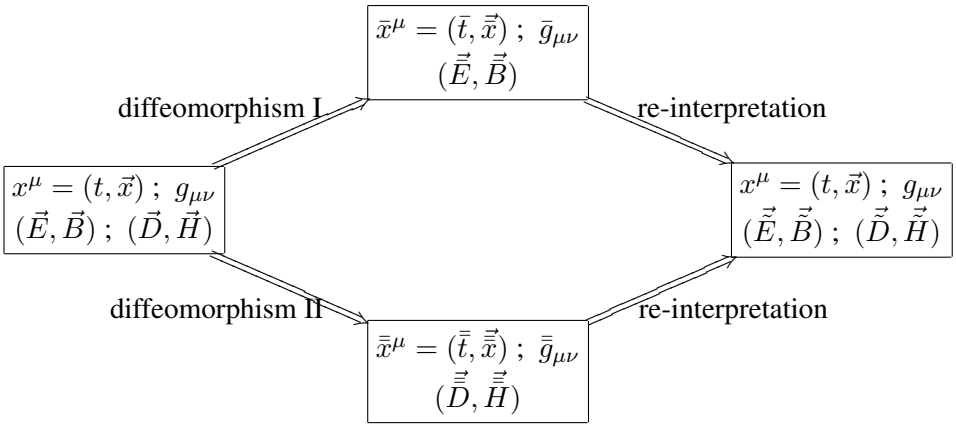

Fig. 1: Illustration and notation of the generalized "triple spacetime Metamaterials". Notice that the diffeomorphism I only acts on the fields $\vec{E}$ and $\vec{B}$, while diffeomorphism II acts on $\vec{D}$ and $\vec{H}$.

this deformation allows an immediate geometric interpretation, as it simply states that we can deform independently from each others the spaces for $(\vec{E}, \vec{B})$ and $(\vec{D}, \vec{H})$ (cf. Fig. 1.)

To arrive at the constitutive relations we proceed analogously to Ref. [3]: all equations are rewritten in terms of the laboratory metric $g_{\mu\nu}$, whereby the field strength tensor $\bar{F}_{\mu\nu}$, the excitation tensor $\bar{\mathcal{H}}^{\mu\nu}$ and the four-current $\bar{J}^\mu$ must be rescaled as

$$\tilde{F}_{\mu\nu} = \pm \bar{F}_{\mu\nu}\ , \qquad \tilde{\mathcal{H}}^{\mu\nu} = \frac{\sqrt{-\bar{\bar{g}}}}{\sqrt{-g}} \bar{\bar{\mathcal{H}}}^{\mu\nu}\ , \qquad \tilde{J}^\mu = \frac{\sqrt{-\bar{\bar{g}}}}{\sqrt{-g}} \bar{\bar{J}}^\mu\ . \tag{3}$$

From this, the relativistically covariant formulation of the constitutive relation follows immediately. After rewriting everything in terms of space vectors one finds

$$\tilde{D}^i = -\bar{s} \frac{\sqrt{-\bar{\bar{g}}}}{\sqrt{\gamma} g_{\bar{0}\bar{\bar{0}}}} g^{\bar{\bar{i}}\bar{j}} \tilde{E}_j - \bar{s}\bar{\bar{s}} \frac{\sqrt{-\bar{g}}\sqrt{-\bar{\bar{g}}}}{\gamma g_{\bar{0}\bar{\bar{0}}}} g^{\bar{\bar{i}}\bar{k}} g^{\bar{0}\bar{l}} \epsilon_{klm} g^{\bar{m}\bar{\bar{j}}} \tilde{H}_j\ , \tag{4}$$

$$\tilde{B}^i = -\bar{\bar{s}} \frac{\sqrt{-\bar{\bar{g}}}}{\sqrt{\gamma} g_{\bar{0}\bar{\bar{0}}}} g^{\bar{\bar{i}}\bar{j}} \tilde{H}_j + \bar{s}\bar{\bar{s}} \frac{\sqrt{-\bar{g}}\sqrt{-\bar{\bar{g}}}}{\gamma g_{\bar{0}\bar{\bar{0}}}} g^{\bar{i}\bar{\bar{k}}} \epsilon_{klm} g^{\bar{\bar{l}}\bar{0}} g^{\bar{m}\bar{j}} \tilde{E}_j\ , \tag{5}$$

where $\bar{s}$ and $\bar{\bar{s}}$ are the respective signs from possible changes of orientation in the mappings $x^\mu \to \bar{x}^\mu$ and $x^\mu \to \bar{\bar{x}}^\mu$ and the symbol $g^{\bar{\mu}\bar{\bar{\nu}}}$ is defined as

$$g^{\bar{\bar{\mu}}\bar{\bar{\nu}}} = \frac{\partial \bar{\bar{x}}^\mu}{\partial x^\rho} \frac{\partial \bar{x}^\nu}{\partial x^\sigma} g^{\rho\sigma} = \bar{\bar{g}}^{\mu\rho} \frac{\partial \bar{x}^\nu}{\partial \bar{\bar{x}}^\rho} = \frac{\partial \bar{\bar{x}}^\mu}{\partial \bar{x}^\rho} \bar{g}^{\rho\nu}\ . \tag{6}$$

The result (4) and (5) reduces to the relations (1) if $g_{\bar{\mu}\bar{\bar{\nu}}}$ is a symmetric matrix of signature $(3, 1)$. This does not imply $\bar{x}^\mu = \bar{\bar{x}}^\mu$ but rather that there exists yet a different space which describes the same media properties in terms of a single transformation. Our generalization exhibits the following features:

- As $g^{\bar{\bar{i}}\bar{j}} = (g^{\bar{j}\bar{\bar{i}}})^T$ it follows that permittivity and permeability are related as $\bar{\bar{s}}\sqrt{-\bar{\bar{g}}}\mu^{ij} = \bar{s}\sqrt{-\bar{g}}\epsilon^{ji}$. It should not come as a surprise that permittivity and permeability cannot be independent as by virtue of the definition of the relativistically covariant tensors $F_{\mu\nu}$ and $\mathcal{H}_{\mu\nu}$ no invariant transformation can act independently on $\vec{E}$ and $\vec{B}$ or $\vec{D}$ and $\vec{H}$, resp.

- Permittivity and permeability need no longer be symmetric. Therefore it is possible to describe non-reciprocal materials. This happens if the mapping between the two electromagnetic spaces, $\partial \bar{x}^\mu / \partial \bar{\bar{x}}^\nu$, is not symmetric in μ and ν, e.g. for a material with mapping $\bar{x} = x - z$, $\bar{\bar{x}} = x + z$.

- The generalized transformations yield many more possibilities considering the signs of the eigenvalues of permittivity and permeability. Within the method of Ref. [3], μ and ϵ are determined by the spatial metric of the deformed space, which by definition must have three positive eigenvalues. Thus in any medium of this type the eigenvalues of ϵ and μ are all of the same sign.

  Within the generalized setup of "triple space Metamaterials", however, the signs of the eigenvalues in ϵ can be chosen freely as no restrictions of this type exist for the transformation matrices. Such indefinite media [7, 8] emerge if certain space directions are inverted differently in the two mappings, e.g. $\bar{x} = -x$, $\bar{\bar{x}} = x$. Furthermore the relative sign between the eigenvalues of ϵ and those of μ can be chosen as is seen from (4) and (5). This allows media exhibiting evanescent waves as a consequence of different time directions, $\bar{t} = -t$ but $\bar{\bar{t}} = t$. We note that all eight classes of materials discussed in Ref. [7] allow a geometric interpretation within the setup of "triple spacetime Metamaterials."

- More complicated than permittivity and permeability are the bi-anisotropic couplings. From

$$\xi^{ij} = -\bar{s}\bar{\bar{s}}\frac{\sqrt{-\bar{g}}\sqrt{-\bar{\bar{g}}}}{\gamma g_{\bar{0}\bar{\bar{0}}}} g^{\bar{\bar{i}}\bar{k}} g^{\bar{\bar{0}}\bar{l}} \epsilon_{klm} g^{\bar{m}\bar{\bar{j}}} \,, \qquad \kappa^{ij} = \bar{s}\bar{\bar{s}}\frac{\sqrt{-\bar{g}}\sqrt{-\bar{\bar{g}}}}{\gamma g_{\bar{0}\bar{\bar{0}}}} g^{\bar{i}\bar{\bar{k}}} \epsilon_{klm} g^{\bar{\bar{l}}\bar{0}} g^{\bar{\bar{m}}\bar{j}} \,, \tag{7}$$

  it follows similarly to Eq. (1) that all electric-magnetic couplings vanish if $x^0 = \bar{x}^0 = \bar{\bar{x}}^0$. Indeed, in this case the expressions $g^{\bar{\bar{0}}\bar{l}} = \bar{g}^{\mu l}\partial\bar{\bar{x}}^0/\partial\bar{x}^\mu$ and $g^{\bar{0}\bar{\bar{l}}} = \bar{\bar{g}}^{\mu l}\partial\bar{x}^0/\partial\bar{\bar{x}}^\mu$ vanish. Thus again we find that electric-magnetic couplings are the result of non-trivial transformations of time.

4. Conclusion

We have introduced in this paper a generalization of the concept of coordinate transformations to design artificial materials. Similar to the standard coordinate transformations this technique offers a geometric interpretation, but in contrast to the former it allows to design a wider class of media, including non-reciprocal media, indefinite media and materials exhibiting evanescent waves. We mention that that the most general class of media from invariant transformations of the equations of motion is slightly more general than the class presented here: indeed a continuous version of electric-magnetic duality leaves Eqs. (2) invariant, however a geometric interpretation thereof is less immediate. Besides practical applications also theoretical questions remain open, such as impedance matching with the vacuum and the behavior of the Poynting vector under the suggested transformations.

References

[1] J. Pendry, D. Schurig, and D. Smith, Controlling electromagnetic fields, *Science* vol. 312, p.1780, 2006.

[2] U. Leonhardt, Optical conformal mapping, *Science* vol. 312, p.1777, 2006.

[3] U. Leonhardt and T. G. Philbin, General relativity in electrical engineering, *New Journal of Physics* vol. 8, p. 247, 2006.

[4] D. Schurig, J. Pendry, and D. Smith, Transformation-designed optical elements, *Opt. Express* vol. 15, p. 14772, 2007.

[5] S.A. Tretyakov and I.S. Nefedov, Field-transforming metamaterials, Proceedings of *Metamaterials'2007,* pp. 474-477, Rome, Italy, 22-24 October 2007.

[6] L.D. Landau and E.M. Lifshits, *The classical theory of fields,* 4th edition, Oxford, England: Butterworth-Heinemann, 2006.

[7] D. Smith and D. Schurig, Electromagnetic wave propagation in media with indefinite permeability and permittivity tensors, *Phys. Rev. Lett.* vol. 90, p. 077405, 2003.

[8] D. Smith, P. Kolilnko, and D. Schurig, Negative refraction in indefinite media, *J. Opt. Soc. Am. B* vol. 21, p.1032, 2004.

Appendix G

The following paper is under review for publication in the Physical Review A.

Generalized transformation optics from triple spacetime metamaterials

Luzi Bergamin*
European Space Agency, The Advanced Concepts Team (DG-PI),
Keplerlaan 1, 2201 AZ Noordijk, The Netherlands
(Dated: July 25, 2008)

In this paper various extensions of the design strategy of transformation media are proposed. We show that it is possible to assign different transformed spaces to the field strength tensor (electric field and magnetic induction) and to the excitation tensor (displacement field and magnetic field), resp. In this way, several limitations of standard transformation media can be overcome. In particular it is possible to provide a geometric interpretation of non-reciprocal as well as indefinite materials. We show that these transformations can be complemented by a continuous version of electric-magnetic duality and comment on the relation to the complementary approach of field-transforming metamaterials.

I. INTRODUCTION

In the field of metamaterials, artificial electromagnetic materials, the use of spacetime transformations as a design tool for new materials has been proved very successful recently [1–3]. As basic idea of this concept a metamaterial mimics a transformed, but empty space. The light rays follow the trajectories according to Fermat's principle in this transformed (electromagnetic) space instead of laboratory space. This allows to design in an efficient way materials with various characteristics such as invisibility cloaks [1, 2, 4], perfect lenses [3], magnification devices [5], an optical analogue of the Aharonov-Bohm effect or even artificial black holes [3]. Still the media relations accessible in this way are rather limited, in particular non-reciprocal or indefinite media (materials exhibiting strong anisotropy) are not covered. But this type of materials also have been linked to some of the mentioned concepts, in particular perfect lenses [6, 7] and hyperlenses [8]. This raises the question whether there exists an extension of the concept of transformation media such as to cover those materials as well and to provide a geometric interpretation thereof.

In this paper we propose an extension of this type. As in Refs. [1–3] our concept is based on diffeomorphisms locally represented as coordinate transformations. Therefore many of our result allow a geometric interpretation similar to the one of Refs. [3, 9] as opposed to another recently suggested route to overcome the restrictions of diffeomorphism transforming media [10, 11]. The starting point of our considerations are Maxwell's equations in possibly curved, but vacuous space [23]:

$$\nabla_i B^i = 0 \ , \qquad \nabla_0 B^i + \epsilon^{ijk}\partial_j E_k = 0 \ , \tag{1}$$

$$\nabla_i \mathcal{D}^i = \rho \ , \qquad \epsilon^{ijk}\partial_j \mathcal{H}_k - \nabla_0 \mathcal{D}^i = j^i \ . \tag{2}$$

Here, ∇_i is the covariant derivative in three dimensions

$$\nabla_i A^i = (\partial_i + \Gamma^i_{ij})A^j = \frac{1}{\sqrt{\gamma}}\partial_i(\sqrt{\gamma}A^i) \ , \tag{3}$$

with the space metric γ_{ij} and its determinant γ.

For many manipulations it will be advantageous to use relativistically covariant quantities. Therefore, Eqs. (1) and (2) are rewritten in terms of the field strength tensor $F_{\mu\nu}$, the excitation tensor $H^{\mu\nu}$ and a four current J^μ (cf. Appendix):

$$\epsilon^{\mu\nu\rho\sigma}\partial_\nu F_{\rho\sigma} = 0 \ , \quad D_\nu H^{\mu\nu} = -J^\mu \ , \quad D_\mu J^\mu = 0 \ . \tag{4}$$

The four dimensional covariant derivative D_μ is defined analogously to (3), whereby the space metric is replaced by the spacetime metric $g_{\mu\nu}$ and its volume element $\sqrt{-g}$.

We wish to analyze these equations of motion from the point of view of transformation media. All transformation materials have in common that they follow as a transformation from a (not necessarily source-free) vacuum solution of the equations of motion, which maps this solution onto a solution of the equations of motion of the transformation material [24]. The crucial ingredient in the definition of transformation media then is the class of transformations to be considered. As space of all transformations we restrict to all *linear* transformations in four-dimensional spacetime. Consequently all media exhibit linear constitutive relations, which may be written within the covariant formulation as [12]

$$H^{\mu\nu} = \frac{1}{2}\chi^{\mu\nu\rho\sigma}F_{\rho\sigma} \ . \tag{5}$$

In vacuum one obtains [25]

$$\chi^{\mu\nu\rho\sigma} = \frac{1}{2}\left(g^{\mu\rho}g^{\nu\sigma} - g^{\mu\sigma}g^{\nu\rho}\right) \ , \tag{6}$$

such that the standard result $\vec{E} = \vec{\mathcal{D}}$ and $\vec{B} = \vec{\mathcal{H}}$ emerges.

These transformations and the ensuing media properties (5) have the advantage to be relativistically invariant and thus very easy to handle. However, they do not include any frequency dependence and remain strictly real, which perhaps is the most severe restriction that follows from the coordinate transformation approach. As long as the linear transformations are seen as transformations of spacetime (rather than of the fields) this restriction is not surprising, though. Indeed, from energy conservation it follows that a process of absorption by the medium is

*Electronic address: Luzi.Bergamin@esa.int

not possible to model as a local transformation of spacetime (notice that the spacetime itself is not dynamical and thus cannot contribute to the energy).

II. DIFFEOMORPHISM TRANSFORMING METAMATERIALS

Obviously, the concept of transformation materials as sketched above is related to symmetry transformations, as those are by definition linear transformations that map a solution of the equations of motion onto another one. Therefore it is worth to work out this relation a little bit more in detail.

A symmetry is a transformation which leaves the source-free [26] action of the theory, here

$$\mathcal{S} = \int d^4x \sqrt{-g} F_{\mu\nu} H^{\mu\nu} \ , \tag{7}$$

invariant, whereby surface terms are dropped. It straightforwardly follows that a symmetry transformation applied on a solution of the equations of motion still solves the latter. In the above action a general, not necessarily flat spacetime is considered. The symmetries of this action are well known: these are the $U(1)$ gauge symmetry of electromagnetism and the symmetries of spacetime (diffeomorphisms). The gauge symmetry cannot help to design materials as the media relations are formulated exclusively in terms of gauge invariant quantities. However, diffeomorphisms change the media relations, as is pointed out e.g. in Ref. [13] and as it has been applied to metamaterials in Ref. [3]. Thus one way to define transformation media is:

Definition 1. *A transformation material follows from a symmetry transformation applied to a vacuum solution of Maxwell's equations. This vacuum solution need not be source free.*

The space of all possible transformation materials of this kind has been derived in Ref. [3], here we shortly want to summarize the result of that paper. The starting point is the observation that a curved space in Maxwell's equations looks like a medium. Indeed, in empty but possibly curved space the constitutive relation among the electromagnetic fields is found by exploiting

$$F_{0i} = (g_{00} g_{ij} - g_{0j} g_{i0}) H^{0j} + g_{0k} g_{il} H^{kl} \ , \tag{8}$$

$$H^{ij} = 2 g^{i0} g^{jk} F_{0k} + g^{ik} g^{jl} F_{kl} \ , \tag{9}$$

which in terms of the space vectors reads

$$\mathcal{D}^i = \frac{g^{ij}}{\sqrt{-g_{00}}} E_j - \frac{g_{0j}}{g_{00}} \epsilon^{jil} \mathcal{H}_l \ , \tag{10}$$

$$B^i = \frac{g^{ij}}{\sqrt{-g_{00}}} \mathcal{H}_j + \frac{g_{0j}}{g_{00}} \epsilon^{jil} E_l \ . \tag{11}$$

Thus empty space can appear like a medium with permeability and permittivity $\epsilon^{ij} = \mu^{ij} = g^{ij}/\sqrt{-g_{00}}$ and with bi-anisotropic couplings $\xi^{ij} = -\kappa^{ij} = \epsilon^{lij} g_{0l}/g_{00}$.

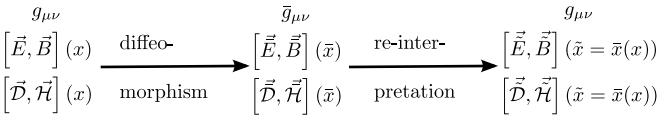

FIG. 1: Diffeomorphism transforming metamaterials according to Ref. [3].

Now, as basic idea of Ref. [3], if empty space can appear like a medium, a medium should also be able to appear as empty space. One starts with electrodynamics in vacuo, we call these fields $F_{\mu\nu}$ and $H^{\mu\nu}$ with flat metric $g_{\mu\nu}$. Now we apply a diffeomorphism, locally represented as a coordinate transformation $x^\mu \to \bar{x}^\mu(x)$. As the equations of motion by definition are invariant under diffeomorphisms, all relations remain the same with the fields F, H and the metric $g_{\mu\nu}$ replaced by the new barred quantities. As a last step one re-interprets in the dynamical equations (1) and (2) the coordinates $\bar{x}^\mu$ as the original ones x^μ, while keeping $\bar{g}_{\mu\nu}$ in the constitutive relation. To make this possible some fields must be rescaled in order to transform barred covariant derivatives (containing $\bar{g}$) into unbarred (containing g.) The situation of diffeomorphism transforming metamaterials is illustrated in Figure 1, which also summarizes our notation. As a more technical remark it should be noted that this manipulation is possible as we consider just Maxwell's theory on a curved background rather than Einstein-Maxwell theory (general relativity coupled to electrodynamics.) In the former case the metric is an external parameter and thus this manipulation is possible as long as none of the involved quantities depends explicitly on the metric.

To keep the whole discussion fully covariant the fields are transformed at the level of the field strength and excitation tensor (rather than at the level of space vectors as done in Ref. [3]). To transform the covariant derivatives $\bar{D}_\mu$ into the original D_μ we have to apply the rescalings

$$\tilde{H}^{\mu\nu} = \frac{\sqrt{-\bar{g}}}{\sqrt{-g}} \bar{H}^{\mu\nu} \qquad \tilde{J}^\mu = \frac{\sqrt{-\bar{g}}}{\sqrt{-g}} \bar{J}^\mu \ . \tag{12}$$

In addition the transformation $x^\mu \to \bar{x}^\mu(x)$ may not preserve the orientation of the manifold, which technically means that the Levi-Civita tensor changes sign [3]. This is corrected by introducing the sign ambiguity

$$\tilde{F}_{\mu\nu} = \pm \bar{F}_{\mu\nu} \tag{13}$$

with the plus sign for orientation preserving, the minus for non-preserving transformations. These new fields again live in the original space with metric $g_{\mu\nu}$, but now the space is filled with a medium with

$$\tilde{\chi}^{\mu\nu\rho\sigma} = \pm \frac{1}{2} \frac{\sqrt{-\bar{g}}}{\sqrt{-g}} \left(\bar{g}^{\mu\rho} \bar{g}^{\nu\sigma} - \bar{g}^{\mu\sigma} \bar{g}^{\nu\rho} \right) \ , \tag{14}$$

or, in terms of space vectors,

$$\tilde{\mathcal{D}}^i = s\frac{\bar{g}^{ij}}{\sqrt{-\bar{g}_{00}}}\frac{\sqrt{\bar{\gamma}}}{\sqrt{\gamma}}\tilde{E}_j - \frac{\bar{g}_{0j}}{\bar{g}_{00}}\epsilon^{jil}\tilde{\mathcal{H}}_l \ , \tag{15}$$

$$\tilde{B}^i = s\frac{\bar{g}^{ij}}{\sqrt{-\bar{g}_{00}}}\frac{\sqrt{\bar{\gamma}}}{\sqrt{\gamma}}\tilde{\mathcal{H}}_j + \frac{\bar{g}_{0j}}{\bar{g}_{00}}\epsilon^{jil}\tilde{E}_l \ , \tag{16}$$

with $s = \pm 1$ being the sign in (13) and (14). As can be seen the media properties are restricted to reciprocal materials ($\epsilon = \epsilon^T$, $\mu = \mu^T$, $\kappa = \chi^T$), which, in addition, obey $\epsilon = \mu$. This result has been obtained in Ref. [3] in a slightly different way and encompasses the transformations in Refs. [1, 14]. We do not want to go into further details of this approach but refer to the review [9], where its geometric optics interpretation is discussed in detail. Indeed, light travels in transformation media of this type along null geodesics of the electromagnetic space $\bar{x}^\mu$, which allows (with some restrictions to be discussed in Section IV) a simple and intuitive interpretation of the transformation.

III. TRIPLE SPACETIME METAMATERIALS

Despite the variety of applications of diffeomorphism transforming metamaterials some results suggest to search for extensions. Indeed, there exist e.g. designs of super- and hyperlenses that make use of indefinite materials (strong anisotropy) [6–8]. Though both concepts should be perfectly understandable in terms of transformation media, the specific material relations used in these works do not fall under the class of diffeomorphism transforming metamaterials.

To understand a possible route to generalize the concept of diffeomorphism transforming media we have to consider again their basis, namely symmetry transformation. The concept of symmetries is used to identify different solutions of the equations of motion that effectively describe the same physics. By means of the reinterpretation in the last step of Figure 1, such symmetry transformations can be used as a simple tool to derive within a restricted class of constitutive relations new media properties in a geometrically intuitive and completely algebraic way.

Nonetheless, within the concept of metamaterials it is not important that the transformed solution in principle describes the same physics as the original one. Still, one may want to keep the possibility of mapping source free solutions onto other source free solutions in a straightforward way, as only in this way we have an effective control over passive media and do not risk to introduce exotic sources such as magnetic monopoles. Furthermore a geometric interpretation of the transformations is kept, which is advantageous in many applications. To weaken the conditions on transformation materials while keeping the advantages of symmetry transformations we thus propose the following definition:

Definition 2. *Consider the set of all transformations T which map a source free solution of the equations of motion* (1) *and* (2) *onto another source free solution. A transformation material is a material obtained by applying a transformation T onto a (not necessarily source free) vacuum solution.*

There are two types of extensions contained in this definition compared to the previous section:

1. There exist transformations that leave the equations of motion invariant, but change the action by a constant and thus are not symmetry transformations. A transformation of this type is the so-called electric-magnetic duality. Its effect will shortly be discussed in Section III A.

2. We do allow for transformations which leave all Maxwell's equations (1) and (2) invariant, but change the media relations (5). This indeed generalizes the concept in an important way.

To see the origin of the second extension it is important to realize that the equations of motion of electrodynamics separate into two different sets (Eqs. (1) and (2), resp.) with mutually exclusive field content. This characteristic is not just an effect of our notation, but as has been shown e.g. in Refs. [15, 16], the equations of motion of electrodynamics can be derived from first principles without using explicitly the constitutive relation $H = H(F)$. As the two sets of equations are separately invariant under diffeomorphisms it should be possible to assign *different* transformed spaces to $H = (\vec{\mathcal{D}}, \vec{\mathcal{H}})$ and $F = (\vec{E}, \vec{B})$. In other words, it must be possible to distort the spaces (or the coordinates) of the field strength tensor and the excitation tensor separately, whereby the resulting transformation material per constructionem fulfills all conditions of the Definition 2. The ensuing constitutive relation as well as the solutions of the equations of motion still follow (almost) as simple as in the case of Ref. [3].

To prove the potential of this method we have to extend the notation compared to the previous section: as before laboratory space has metric $g_{\mu\nu}$, its fields in vacuo are $H = (\vec{\mathcal{D}}, \vec{\mathcal{H}})$ and $F = (\vec{E}, \vec{B})$; the fields of the transformation material (living in the space with metric $g_{\mu\nu}$) are again labeled with a tilde. The transformed space of the field strength tensor has metric $\bar{g}_{\mu\nu}$ and fields $\bar{F} = (\vec{\bar{E}}, \vec{\bar{B}})$, the one of the excitation tensor $\bar{\bar{g}}_{\mu\nu}$ and $\bar{\bar{H}} = (\vec{\bar{\mathcal{D}}}, \vec{\bar{\mathcal{H}}})$. This new transformation is illustrated in Figure 2. Applying the two transformations

$$\bar{x}^\mu = \bar{x}^\mu(x) \ , \qquad \bar{\bar{x}}^\mu = \bar{\bar{x}}^\mu(x) \tag{17}$$

to the constitutive relation (5) with χ being the vacuum relation (6) yields

$$\bar{\bar{H}}^{\mu\nu} = \frac{1}{2}\frac{\partial\bar{\bar{x}}^\mu}{\partial x^\lambda}\frac{\partial\bar{\bar{x}}^\nu}{\partial x^\tau}\left(g^{\lambda\alpha}g^{\tau\beta} - g^{\lambda\beta}g^{\tau\alpha}\right)\frac{\partial\bar{x}^\rho}{\partial x^\alpha}\frac{\partial\bar{x}^\sigma}{\partial x^\beta}\bar{F}_{\rho\sigma} \ . \tag{18}$$

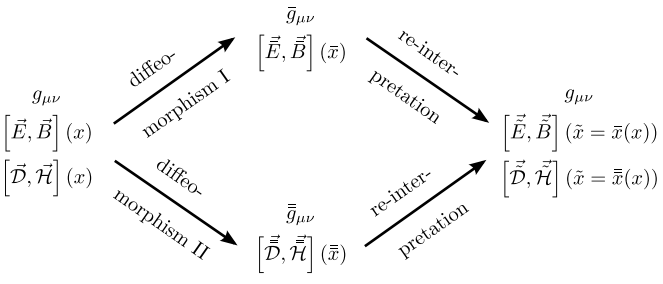

FIG. 2: Illustration and notation of the generalized "triple spacetime metamaterials". Notice that the diffeomorphism I only acts on the fields $\vec{E}$ and $\vec{B}$, while diffeomorphism II acts on $\vec{\mathcal{D}}$ and $\vec{\mathcal{H}}$.

Introducing the notation

$$g^{\bar{\bar{\mu}}\bar{\nu}} = \frac{\partial\bar{\bar{x}}^{\mu}}{\partial x^{\rho}}\frac{\partial\bar{x}^{\nu}}{\partial x^{\sigma}}g^{\rho\sigma} = \bar{g}^{\mu\rho}\frac{\partial\bar{x}^{\nu}}{\partial\bar{\bar{x}}^{\rho}} = \frac{\partial\bar{\bar{x}}^{\mu}}{\partial\bar{x}^{\rho}}\bar{g}^{\rho\nu} \tag{19}$$

the relation may be written as

$$\bar{\bar{H}}^{\mu\nu} = \frac{1}{2}\left(g^{\bar{\bar{\mu}}\bar{\rho}}g^{\bar{\bar{\nu}}\bar{\sigma}} - g^{\bar{\bar{\mu}}\bar{\sigma}}g^{\bar{\bar{\nu}}\bar{\rho}}\right)\bar{F}_{\rho\sigma} \ . \tag{20}$$

It should be noted that $g^{\bar{\bar{\mu}}\bar{\nu}}$ in Eq. (19) is no longer a metric, in particular it need not be symmetric in its indices and it need not have signature $(3,1)$.

To derive the new constitutive relations in the original (laboratory) space we proceed analogously to the previous section. All fields have to be rescaled in order to obey the equations of motion in the original space with metric $g_{\mu\nu}$, which implies

$$\tilde{F}_{\mu\nu} = \pm\bar{F}_{\mu\nu} \ , \quad \tilde{H}^{\mu\nu} = \frac{\sqrt{-\bar{\bar{g}}}}{\sqrt{-g}}\bar{\bar{H}}^{\mu\nu} \ , \quad \tilde{J}^{\mu} = \frac{\sqrt{-\bar{\bar{g}}}}{\sqrt{-g}}\bar{\bar{J}}^{\mu} \ . \tag{21}$$

Thus the constitutive relation becomes

$$\tilde{H}^{\mu\nu} = \tilde{\chi}^{\mu\nu\rho\sigma}\tilde{F}_{\rho\sigma} = \pm\frac{1}{2}\frac{\sqrt{-\bar{\bar{g}}}}{\sqrt{-g}}\left(g^{\bar{\bar{\mu}}\bar{\rho}}g^{\bar{\bar{\nu}}\bar{\sigma}} - g^{\bar{\bar{\mu}}\bar{\sigma}}g^{\bar{\bar{\nu}}\bar{\rho}}\right)\tilde{F}_{\rho\sigma} \ , \tag{22}$$

where the sign refers to the possible change of orientation in the transformation $x^{\mu} \to \bar{\bar{x}}^{\mu}$. For the equivalent relation in terms of space vectors the notation

$$\epsilon_{\mu\nu\rho\sigma} = \bar{s}\frac{\sqrt{-g}}{\sqrt{-\bar{g}}}\bar{\epsilon}_{\mu\nu\rho\sigma} = \bar{\bar{s}}\frac{\sqrt{-g}}{\sqrt{-\bar{\bar{g}}}}\bar{\bar{\epsilon}}_{\mu\nu\rho\sigma} \tag{23}$$

is used, where $\bar{s}$ and $\bar{\bar{s}}$ are the respective signs due to the change of orientation in the transformations to laboratory space. Now it easily follows from (A.16)–(A.19) that

$$\mathfrak{A}^{ij} = -\bar{\bar{s}}\frac{\sqrt{-\bar{\bar{g}}}}{\sqrt{\gamma}}(g^{\bar{\bar{0}}\bar{\bar{0}}}g^{\bar{\bar{i}}\bar{\bar{j}}} - g^{\bar{\bar{0}}\bar{\bar{j}}}g^{\bar{\bar{i}}\bar{\bar{0}}}) \ , \tag{24}$$

$$\mathfrak{B}_{ij} = -\bar{\bar{s}}\frac{\sqrt{\gamma}}{\sqrt{-\bar{\bar{g}}}}(g_{\bar{\bar{0}}\bar{\bar{0}}}g_{\bar{\bar{i}}\bar{\bar{j}}} - g_{\bar{\bar{0}}\bar{\bar{j}}}g_{\bar{\bar{i}}\bar{\bar{0}}}) \ , \tag{25}$$

$$\mathfrak{C}_i{}^j = -\frac{\bar{\bar{s}}}{2}\frac{\sqrt{-\bar{\bar{g}}}}{\sqrt{\gamma}}\epsilon_{ikl}(g^{\bar{\bar{k}}\bar{\bar{0}}}g^{\bar{\bar{l}}\bar{\bar{j}}} - g^{\bar{\bar{k}}\bar{\bar{j}}}g^{\bar{\bar{l}}\bar{\bar{0}}}) \ , \tag{26}$$

$$\mathfrak{D}^i{}_j = \frac{\bar{\bar{s}}}{2}\frac{\sqrt{-\bar{\bar{g}}}}{\sqrt{\gamma}}\epsilon_{jkl}(g^{\bar{\bar{0}}\bar{\bar{k}}}g^{\bar{\bar{i}}\bar{\bar{l}}} - g^{\bar{\bar{0}}\bar{\bar{l}}}g^{\bar{\bar{i}}\bar{\bar{k}}}) \ , \tag{27}$$

which are the defining tensors of the Boys-Post relation. After some algebra the Tellegen relation

$$\tilde{\mathcal{D}}^i = -\bar{s}\frac{\sqrt{-\bar{\bar{g}}}}{\sqrt{\gamma}g_{\bar{0}\bar{0}}}g^{\bar{\bar{i}}\bar{\bar{j}}}\tilde{E}_j - \bar{s}\bar{\bar{s}}\frac{\sqrt{-\bar{g}}\sqrt{-\bar{\bar{g}}}}{\gamma g_{\bar{0}\bar{0}}}g^{\bar{\bar{i}}\bar{k}}g^{\bar{\bar{0}}\bar{l}}\epsilon_{klm}g^{\bar{m}\bar{\bar{j}}}\tilde{\mathcal{H}}_j \ , \tag{28}$$

$$\tilde{B}^i = -\bar{\bar{s}}\frac{\sqrt{-\bar{g}}}{\sqrt{\gamma}g_{\bar{0}\bar{0}}}g^{\bar{i}\bar{\bar{j}}}\tilde{\mathcal{H}}_j + \bar{s}\bar{\bar{s}}\frac{\sqrt{-\bar{g}}\sqrt{-\bar{\bar{g}}}}{\gamma g_{\bar{0}\bar{0}}}g^{\bar{i}\bar{\bar{k}}}\epsilon_{klm}g^{\bar{\bar{l}}\bar{0}}g^{\bar{m}\bar{\bar{j}}}\tilde{E}_j \tag{29}$$

is found, which in the limit of $\bar{\bar{g}}_{\mu\nu} = \bar{g}_{\mu\nu}$ is equivalent to Eqs. (15) and (16). An important comment is in order: due to the different transformations applied to $H^{\mu\nu}$ and $F_{\mu\nu}$, resp., the constitutive relation (22), or (28) and (29), relates fields from *different* spacetime points in the original space, e.g. $\tilde{E}_i\left(\tilde{x}=\bar{x}(x)\right)$ refers the field $E_i(x)$ at a different point x^{μ} in the original space than $\tilde{\mathcal{D}}^i\left(\tilde{x}=\bar{\bar{x}}(x)\right)$ does.

Let us comment on the more technical parts of this result. In Section II we saw that transformation materials derived from symmetry transformations are restricted to reciprocal materials with $\epsilon = \mu$. These restrictions can be overcome partially with the above result:

- As $g^{\bar{\bar{i}}\bar{\bar{j}}} = (g^{\bar{j}\bar{\bar{i}}})^T$ it follows that permittivity and permeability are related as

$$\bar{\bar{s}}\sqrt{-\bar{\bar{g}}}\mu^{ij} = \bar{s}\sqrt{-\bar{g}}\epsilon^{ji} \ . \tag{30}$$

  It should not come as a surprise that permittivity and permeability cannot be independent, as by virtue of the definition of the relativistically covariant tensors $F_{\mu\nu}$ and $H_{\mu\nu}$ such transformations cannot act independently on $\vec{E}$ and $\vec{B}$ or $\vec{\mathcal{D}}$ and $\vec{\mathcal{H}}$, resp. A possible route to relax this restriction is discussed in Section V.

- Permittivity and permeability need no longer be symmetric. Therefore it is possible to describe non-reciprocal materials, or, in the language of Eq. (A.22), the skewon part need not vanish. This happens if the mapping between the two electromagnetic spaces, $\partial\bar{x}^{\mu}/\partial\bar{\bar{x}}^{\nu}$, is not symmetric in μ and ν, e.g. for a material with mapping $\bar{x} = x - z$, $\bar{\bar{x}} = x + z$.

- The generalized transformations yield many more possibilities considering the signs of the eigenvalues of permittivity and permeability. Within the method of Ref. [3], μ and ϵ are essentially determined by the spatial metric of the electromagnetic space (cf. Eqs. (15) and (16) and recall the relation $g^{ij} = \gamma^{ij}$.) However, a spatial metric by definition must have three positive eigenvalues, a characteristic that cannot be changed by any diffeomorphism. Thus it follows that in any medium of this type the eigenvalues of ϵ and μ are all of the same sign.

  – Within the generalized setup of "triple spacetime metamaterials", however, the signs of the eigenvalues in ϵ can be chosen freely, as the metric is multiplied by a transformation matrix,

  $$g^{\bar{\bar{i}}\bar{\bar{j}}} = \bar{\bar{g}}^{i\mu}\frac{\partial \bar{x}^j}{\partial \bar{\bar{x}}^\mu} \ , \tag{31}$$

  and no restrictions on the signs of the eigenvalues of the transformation matrix exist. In this way indefinite materials [6, 7] can be designed as a result of different space inversions in the two different mappings. As an example the mapping $\bar{z} = -z$, $\bar{\bar{z}} = z$ (with all other directions mapped trivially) yields $\epsilon^{ij} = \mathrm{diag}(-1,-1,1)$, $\mu^{ij} = \mathrm{diag}(1,1,-1)$.

  – Furthermore the relative sign between the eigenvalues of ϵ and those of μ can be chosen as a consequence of the factor $\bar{\bar{s}}$ in Eq. (30). This change in the relative sign may be interpreted as a partial reversal of time as can be seen in the following list (space maps trivially here and all media are assumed to be homogeneous):

	$\bar{t}$	$\bar{\bar{t}}$	ϵ	μ
I	t	t	1	1
II	t	$-t$	-1	1
III	$-t$	t	1	-1
IV	$-t$	$-t$	-1	-1

  We note that all eight classes of materials discussed in Ref. [6] allow a geometric interpretation within the setup of "triple spacetime metamaterials."

- More complicated than permittivity and permeability are the bi-anisotropic couplings. With the standard assumption of $g^{0i} = 0$ in laboratory space it follows from

$$\xi^{ij} = -\bar{s}\bar{\bar{s}}\frac{\sqrt{-\bar{g}}\sqrt{-\bar{\bar{g}}}}{\gamma g_{\bar{0}\bar{\bar{0}}}} g^{\bar{i}\bar{k}} g^{\bar{\bar{0}}\bar{l}} \epsilon_{klm} g^{\bar{m}\bar{\bar{j}}} \ , \tag{32}$$

$$\kappa^{ij} = \bar{s}\bar{\bar{s}}\frac{\sqrt{-\bar{g}}\sqrt{-\bar{\bar{g}}}}{\gamma g_{\bar{0}\bar{\bar{0}}}} g^{\bar{i}\bar{\bar{k}}} \epsilon_{klm} g^{\bar{\bar{l}}\bar{0}} g^{\bar{\bar{m}}\bar{j}} \ , \tag{33}$$

  similarly to Eq. (15) that all electric-magnetic couplings vanish if the transformation does not mix space and time. In this case the crucial components $g^{\bar{0}\bar{\bar{l}}}$ and $g^{\bar{\bar{0}}\bar{l}}$ may be written as

$$g^{\bar{0}\bar{\bar{l}}} = \frac{\partial \bar{x}^0}{\partial x^0} g^{00} \frac{\partial \bar{\bar{x}}^l}{\partial x^0} + \frac{\partial \bar{x}^0}{\partial x^i} g^{ij} \frac{\partial \bar{\bar{x}}^l}{\partial x^j} \ , \tag{34}$$

$$g^{\bar{\bar{0}}\bar{l}} = \frac{\partial \bar{\bar{x}}^0}{\partial x^0} g^{00} \frac{\partial \bar{x}^l}{\partial x^0} + \frac{\partial \bar{\bar{x}}^0}{\partial x^i} g^{ij} \frac{\partial \bar{x}^l}{\partial x^j} \ . \tag{35}$$

  Most importantly it is found from these expressions that one of the two bi-anisotropic couplings may vanish while the other one is non-vanishing, which is impossible within the context of diffeomorphism transforming media. Moreover, in the latter case the bi-anisotropic couplings must be symmetric matrices, which need no longer be the case in the present context.

- Finally, the result (28) and (29) reduces to the relations (15), (16) if $g_{\bar{\mu}\bar{\bar{\nu}}}$ is a symmetric matrix of signature $(3,1)$. This does not necessarily imply $\bar{x}^\mu = \bar{\bar{x}}^\mu$ but rather that there exists yet a different space which describes the same media properties in terms of the transformations of Section (II).

A. Electric-magnetic duality and rotation

Finally we should ask, whether Eqs. (28), (29) indeed describe the most general media fulfilling Definition 2. Taken separately, the two sets of equations in (1) and (2) do not exhibit more symmetries than diffeomorphisms. However, there exists the possibility of transformations that mix $F_{\mu\nu}$ and $H^{\mu\nu}$. Indeed a transformation of this type is known as electric-magnetic duality, which has important implications in modern theoretical high-energy physics [17]. It represents the fact that under the exchange

$$F_{\mu\nu} \leftrightarrow *H_{\mu\nu} \tag{36}$$

or in terms of space vectors

$$B^i \to -\mathcal{D}^i \ , \qquad \mathcal{H}_i \to -E_i \ , \tag{37}$$

$$E_i \to \mathcal{H}_i \ , \qquad \mathcal{D}^i \to B^i \ , \tag{38}$$

the source-free equations of motion do not change (the action changes by an overall sign.) Of course, this duality transformation is problematic when applied to a solution with sources, as it transforms electric charges and currents into magnetic charges and currents and vice versa. In the remainder of this section we thus restrict to source-free solutions or should allow the possibility of artificial magnetic monopoles. Then it can be checked straightforwardly that electric-magnetic duality applied to the result (20), or (28) and (29), does not yield media relations not yet covered by diffeomorphisms alone.

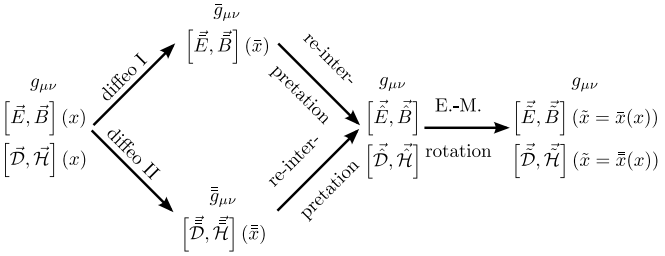

FIG. 3: Illustration and notation of the generalized "triple spacetime metamaterials" complemented by electric-magnetic rotation. The electric-magnetic rotation must act after the transformation of spacetime as these two steps do not commute.

However, as far as the equations of motion (1) and (2) are concerned, electric-magnetic duality can be promoted to a continuous $U(1)$ symmetry with transformation [27]

$$\tilde{B}^i = \cos\alpha B^i - \sin\alpha \mathcal{D}^i \ , \quad \tilde{\mathcal{D}}^i = \cos\alpha \mathcal{D}^i + \sin\alpha B^i \ , \tag{39}$$

$$\tilde{E}_i = \cos\alpha E_i + \sin\alpha \mathcal{H}_i \ , \quad \tilde{\mathcal{H}}_i = \cos\alpha \mathcal{H}_i - \sin\alpha E_i \ . \tag{40}$$

These transformations comply with Definition 2 and thus their action onto a medium with general constitutive relation (A.12) should be studied. The result

$$\begin{aligned}\tilde{\mathcal{D}}^i = &\left(\cos^2\alpha\epsilon + \sin^2\alpha\mu + \sin\alpha\cos\alpha(\kappa+\xi)\right)^{ij}\tilde{E}_j \\ &+ \left(\cos^2\alpha\kappa - \sin^2\alpha\xi + \sin\alpha\cos\alpha(\mu-\epsilon)\right)^{ij}\tilde{\mathcal{H}}_j \ ,\end{aligned} \tag{41}$$

$$\begin{aligned}\tilde{B}^i = &\left(\cos^2\alpha\mu + \sin^2\alpha\epsilon - \sin\alpha\cos\alpha(\kappa+\xi)\right)^{ij}\tilde{\mathcal{H}}_j \\ &+ \left(\cos^2\alpha\xi - \sin^2\alpha\kappa + \sin\alpha\cos\alpha(\mu-\epsilon)\right)^{ij}\tilde{E}_j\end{aligned} \tag{42}$$

shows that the transformation acts trivially if $\epsilon = \mu$ and $\xi = -\kappa$, in particular in vacuo and consequently for all diffeomorphism transforming media (15). However, they yield new media relations when acting on a solution of the type (28) and (29). Therefore these new relations are part of the materials covered by Definition 2. They are derived here for completeness, though their geometric interpretation is not immediate. The coordinate lines $\bar{x}^\mu(x)$ and $\bar{\bar{x}}^\mu(x)$ could be understood as the electromagnetic spaces of the linear combinations $(\vec{\tilde{E}},\vec{\tilde{B}})$ and $(\vec{\tilde{\mathcal{D}}},\vec{\tilde{\mathcal{H}}})$ as given in (39) and (40), resp. Still, one should be careful with this interpretation: as the transformation of spacetime does not commute with the electric-magnetic rotation one cannot modify the situation in Figure 3 in such a way that the two electromagnetic spaces, $\bar{x}^\mu$ and $\bar{\bar{x}}^\mu$, are identified with certain linear combinations of $(\vec{E},\vec{B})$ and $(\vec{\mathcal{D}},\vec{\mathcal{H}})$, resp.; rather the electric-magnetic rotation acts upon the fields after the transformation of spacetime.

IV. ENERGY, MOMENTUM AND WAVE VECTOR

So far we studied solutions of Maxwell's equations which—up to rescalings—are equivalent to certain vacuum solutions. Still we did not ask up to which point these transformation materials really are "media that look as empty space." To do so it is not sufficient to consider the transformation of the fields and sources, but equally well we should look at the conservation laws, summarized in the conservation of the stress-energy-momentum tensor (SEM tensor.) While in the generic situation of electrodynamics in media, the definition of the "SEM tensor of electrodynamics" is not unique [18, 19], we do not have to deal with these subtleties in the present situation as our (idealized) media are lossless and dispersion free and thus allow for a definition of a complete action (cf. Eq. (7)) without any reference to "matter." Therefrom we immediately derive the covariant SEM tensor

$$T^{\mu\nu} = -\frac{1}{4\pi}\left(F_{\rho\sigma}g^{\sigma\{\mu}H^{\nu\}\rho} + \frac{1}{4}g^{\mu\nu}F_{\rho\sigma}H^{\rho\sigma}\right) \ , \tag{43}$$

$$D_\mu T^{\mu\nu} = 0 \ . \tag{44}$$

The advantage of this tensor over the canonical SEM tensor is the simple behavior under diffeomorphisms: being a real tensor field, $T_{\mu\nu}$ transforms exactly in the same way as the metric.

Let us now look at the materials as described in Section II. Thanks to its transformation properties the SEM tensor in the electromagnetic space follows immediately as

$$\bar{T}^{\mu\nu} = -\frac{1}{4\pi}\left(\bar{F}_{\rho\sigma}\bar{g}^{\sigma\{\mu}\bar{H}^{\nu\}\rho} + \frac{1}{4}\bar{g}^{\mu\nu}\bar{F}_{\rho\sigma}\bar{H}^{\rho\sigma}\right) \ . \tag{45}$$

But how about $\tilde{T}_{\mu\nu}$? Of course one could define an "induced SEM tensor" from the electromagnetic space as (cf. Eqs. (12) and (13))

$$\tilde{T}_I^{\mu\nu} = \mp\frac{\sqrt{-g}}{\sqrt{-\bar{g}}}\frac{1}{4\pi}\left(\tilde{F}_{\rho\sigma}\bar{g}^{\sigma\{\mu}\tilde{H}^{\nu\}\rho} + \frac{1}{4}\bar{g}^{\mu\nu}\tilde{F}_{\rho\sigma}\tilde{H}^{\rho\sigma}\right) \ , \tag{46}$$

but obviously this tensor is not conserved in laboratory space, $D_\mu T_I^{\mu\nu} \neq 0$, since it depends explicitly on the metric $\bar{g}_{\mu\nu}$. In other words, the crucial trick to re-interpret in the dynamical equations the coordinates in electromagnetic space, $\bar{x}^\mu$, as those in laboratory space, x^μ, works in the equations of motion (1) and (2), but does not work for the SEM tensor and its conservation.

Of course, the correct SEM tensor in laboratory space immediately follows from (43) as

$$\tilde{T}^{\mu\nu} = -\frac{1}{4\pi}\left(\tilde{F}_{\rho\sigma}g^{\sigma\{\mu}\tilde{H}^{\nu\}\rho} + \frac{1}{4}g^{\mu\nu}\tilde{F}_{\rho\sigma}\tilde{H}^{\rho\sigma}\right) \ . \tag{47}$$

Clearly, requiring equivalence of the two tensors would not even allow for conformal transformations. But even

when looking at integrated quantities (total energy and momentum flux in the material),

$$P^\mu = \int d^3x \sqrt{\gamma}\, T^{0\mu} \ , \tag{48}$$

the induced tensor does not yield the correct quantity in laboratory space. Of course, the situation is even more complicated for triple spacetime metamaterials: since the transformation of the explicit metrics appearing in Eq. (43) is not defined, an "induced SEM tensor" cannot even be defined.

Instead of the correct, directly evaluated SEM tensor (47) a slightly different tensor is considered in the following. To see its advantage we make the standard assumption that our laboratory space metric has $g_{00} = -1$ (x^0 is our laboratory time) and $g_{0i} = 0$ (the measure of distances is time independent.) Then it is straightforward that the quantity

$$M^{\mu\nu} = -g^{\mu\rho} F_{\rho\sigma} H^{\sigma\nu} \tag{49}$$

contains the Poynting vector and the direction of the wave vector,

$$S^i = M^{0i} = \epsilon^{ijk} E_j \mathcal{H}_k \ , \tag{50}$$

$$n^i = M^{i0} = \gamma^{ij} \epsilon_{jkl} \mathcal{D}^k B^l \parallel k^i \ . \tag{51}$$

We recall that the original fields obey the constitutive relations of vacuous space and thus trivially $M^{0i} = M^{i0}$. From the transformation rules (21) the transformed tensor is found as

$$\begin{aligned} \tilde{M}^{\mu\nu} &= -\bar{s} \frac{\sqrt{-\bar{\bar{g}}}}{\sqrt{-g}} g^{\mu\rho} \bar{F}_{\rho\sigma} \bar{\bar{H}}^{\sigma\nu} \\ &= -\bar{s} \frac{\sqrt{-\bar{\bar{g}}}}{\sqrt{-g}} g^{\mu\rho} \frac{\partial x^\lambda}{\partial \bar{x}^\rho} F_{\lambda\tau} \frac{\partial x^\tau}{\partial \bar{x}^\sigma} \frac{\partial \bar{\bar{x}}^\sigma}{\partial x^\alpha} H^{\alpha\beta} \frac{\partial \bar{\bar{x}}^\nu}{\partial x^\beta} \ . \end{aligned} \tag{52}$$

The transformation law of $M^{\mu\nu}$ encodes in a geometric language how energy flux and phase velocity behave in a medium. For simplicity let us now concentrate on media without bi-anisotropic couplings, in other words we allow for general spatial transformations as well as stretchings and reversal of time, but keep $\bar{g}_{0i} = \bar{\bar{g}}_{0i} = 0$. Then we find for the transformed space vectors (cf. Eqs. (A.8)–(A.11)):

$$\tilde{S}^i = \tilde{M}^{0i} = -\bar{s}\bar{\bar{s}} \frac{\sqrt{-\bar{\bar{g}}_{00}}}{g_{00}} \frac{\partial x^0}{\partial \bar{x}^0} \epsilon^{ijk} \frac{\partial x^m}{\partial \bar{x}^j} E_m \frac{\partial x^n}{\partial \bar{\bar{x}}^k} \mathcal{H}_n \tag{53}$$

$$\tilde{n}^i = \tilde{M}^{i0} = \frac{\sqrt{-\bar{\bar{g}}}\sqrt{\bar{\gamma}}}{\sqrt{\gamma}} \frac{\partial \bar{\bar{x}}^0}{\partial x^0} \gamma^{ij} \epsilon_{jkl} \frac{\partial \bar{\bar{x}}^k}{\partial x^m} \mathcal{D}^m \frac{\partial \bar{x}^l}{\partial x^n} B^n \tag{54}$$

The transformation of the Poynting vector may be abbreviated as

$$\tilde{S}^i = T^{ijk} E_j \mathcal{H}_k \ , \tag{55}$$

and it is then easily seen that n_i transforms as

$$\tilde{n}_i = \bar{s}\bar{\bar{s}} \frac{\sqrt{\bar{\bar{\gamma}}\bar{\gamma}}}{2\gamma} g_{00} \frac{\partial \bar{\bar{x}}^0}{\partial x^0} \frac{\partial \bar{x}^0}{\partial x^0} U_{ikj} D^j B^k \ , \tag{56}$$

where U_{ijk} is the inverse of T^{ijk} in the sense of

$$U_{ijk} T^{ljk} = \delta_i^l \ . \tag{57}$$

While these formulae might look cumbersome, their geometric interpretation actually is quite straightforward. In the case of diffeomorphism transforming materials, $\bar{g}_{\mu\nu} = \bar{\bar{g}}_{\mu\nu}$, Eq. (53) states that S^i behaves under purely spatial transformations as a covector [1], while n_i from Eq. (54) behaves as a vector:

$$\tilde{S}^i = \bar{s} \frac{\sqrt{-\bar{\bar{g}}}}{\sqrt{-g_{00}}\sqrt{-g}} \frac{\partial x^0}{\partial \bar{x}^0} \frac{\partial \bar{x}^i}{\partial x^j} S^j \ , \tag{58}$$

$$\tilde{n}_i = \bar{s} \sqrt{-\bar{\bar{g}}} \frac{\partial \bar{x}^0}{\partial x^0} \frac{\partial x^j}{\partial \bar{x}^i} n_j \ . \tag{59}$$

Of course, the relative orientation of S^i and n^i is preserved under the diffeomorphisms, but this is no longer true for $\tilde{S}^i$ and $\tilde{n}^i$, since indices are raised/lowered by the space metric γ_{ij} in laboratory space as opposed to $\bar{\gamma}_{ij}$ in electromagnetic space.

For triple spacetime metamaterials no linear transformation $\tilde{S}^i = T^i{}_j S^j$ exists. This makes the interpretation a little bit more complicated, but at the same time is the source of the numerous additional possibilities within this generalized setup. In general, the value of the element T^{ijk} defines the component of the Poynting vector in direction x^i as generated by electric and magnetic fields that point in the original space in the directions x^j and x^k, resp. In this way it is easy to engineer the direction of the Poynting vector in the medium for a given polarization of the incoming wave in vacuum. Similar conclusions apply for the transformation matrix U_{ijk}, with the notable restriction that $\tilde{n}^i$ can be parallel or anti-parallel to k^i. Whether $(\tilde{\mathcal{D}}^i, B^j, k^l)$ form a right- or left-handed triple can be deduced from

$$\epsilon_{ijk} \tilde{\mathcal{D}}^j \tilde{B}^k = \frac{\tilde{k}_i}{\tilde{\omega}} \tilde{E}_j \epsilon^{jk} \tilde{E}_k = -\bar{s} \frac{\sqrt{-\bar{\bar{g}}}}{\sqrt{\gamma} g_{\bar{0}\bar{0}}} \frac{\tilde{k}_i}{\tilde{\omega}} \tilde{E}_j \gamma^{\bar{\bar{j}}\bar{k}} \tilde{E}_k \ . \tag{60}$$

A. Wave vector and dispersion relations

While the above relations correctly reproduce the direction of the Poynting and the wave vector, they cannot distinguish between propagating and evanescent modes. Consider as an example the following transformation:

$$\bar{x}^0 = x^0 \ , \quad \bar{x}^i = x^i \ , \quad \bar{\bar{x}}^0 = -x^0 \ , \quad \bar{\bar{x}}^i = x^i \ . \tag{61}$$

From Eqs. (15) and (16) it is found that this is a homogeneous material with $\epsilon = -1$ and $\mu = 1$. As fields in vacuo, $\vec{E} = \vec{\mathcal{D}}$ and $\vec{B} = \vec{\mathcal{H}}$, we consider a monochromatic wave

$$\vec{E} = \vec{e} e^{i(\vec{k}\vec{x} - \omega t)} + \text{c.c.} \ , \qquad \vec{k} \cdot \vec{e} = 0 \ , \tag{62}$$

$$\vec{B} = \vec{b} e^{i(\vec{k}\vec{x} - \omega t)} + \text{c.c.} \ , \qquad \vec{b} = \frac{1}{\omega} \vec{k} \times \vec{e} \ . \tag{63}$$

After the transformation the fields $\vec{\tilde{E}}$, $\vec{\tilde{B}}$ and $\vec{\tilde{\mathcal{D}}}$, $\vec{\tilde{\mathcal{H}}}$ refer to the original fields at different time instances:

$$\vec{\tilde{E}}\,(\tilde{x}^\mu = \bar{x}^\mu(x)) = \vec{E}(\vec{x},t)\ , \tag{64}$$

$$\vec{\tilde{B}}\,(\tilde{x}^\mu = \bar{x}^\mu(x)) = \vec{B}(\vec{x},t)\ , \tag{65}$$

$$\vec{\tilde{\mathcal{D}}}\,(\tilde{x}^\mu = \bar{\tilde{x}}^\mu(x)) = -\vec{\mathcal{D}}(\vec{x},-t)\ , \tag{66}$$

$$\vec{\tilde{\mathcal{H}}}\,(\tilde{x}^\mu = \bar{\tilde{x}}^\mu(x)) = \vec{\mathcal{H}}(\vec{x},-t)\ . \tag{67}$$

Of course, Maxwell's equations are satisfied by the new fields by construction. Still, the partial exchange of positive and negative angular frequencies has important implications in the dispersion relation as any propagating wave in vacuo becomes evanescent in the medium and vice versa.

Though this behavior may not appear immediate when transforming the monochromatic wave (62) and (63) with (64)–(67), it can be made explicit from geometric quantities as well. Indeed, from the relativistic wave equation [12]

$$D_\nu \chi^{\mu\nu\rho\sigma} D_\rho A_\sigma = -J^\nu \tag{68}$$

it follows straightforwardly that "triple-space metamaterials" in the absence of charges and currents and in the limit of approximate homogeneity obey the dispersion relation

$$g^{\bar{\mu}\bar{\nu}} k_\mu k_\nu = 0\ , \qquad k_\mu = (\omega, \vec{k})\ . \tag{69}$$

In our example the partial reversal of time yields $g^{\bar{0}\bar{0}} = 1$ and thus $\omega^2 + \vec{k}^2 = 0$.

V. NON-INVARIANT TRANSFORMATIONS

Within the approaches to transformation media discussed so far invariant transformations of the equations of motions were used exclusively. This means that the transformations "do not introduce charges or currents", in other words the transformation medium based on a source free vacuum solution will be source free as well. What happens if this restriction is abandoned? Still insisting on a constitutive relation of the form (5) this suggests the definition:

Definition 3. *A transformation medium is defined by an arbitrary linear transformation applied to a (not necessarily source free) vacuum solution of Maxwell's equations. The linear transformation constitutes the media properties as well as charges and currents of the transformation medium.*

Though not in its most general form, this approach was proposed in [10, 11]. Starting from the vacuum relation (6) the most general linear relation can be achieved by the field transformations [28]

$$\bar{H}^{\mu\nu} = \Omega^{\mu\nu}{}_{\rho\sigma} H^{\rho\sigma}\ , \qquad F_{\mu\nu} = \Psi_{\mu\nu}{}^{\rho\sigma} \bar{F}_{\rho\sigma}\ , \tag{70}$$

with the transformed $\bar{\chi}$,

$$\bar{\chi}^{\mu\nu\rho\sigma} = (\Omega\chi\Psi)^{\mu\nu\rho\sigma}\ . \tag{71}$$

The original fields $F_{\mu\nu}$ and $H^{\mu\nu}$ by assumption are solutions to the equations of motion. If we allow besides the standard electric four-current J^μ also a magnetic four-current J^μ_M, any transformation of the type (70) can be mapped on a solution of the new equations ($\hat{\Psi}_{\mu\nu}{}^{\rho\sigma}$ is the inverse matrix $\hat{\Psi}_{\mu\nu}{}^{\lambda\tau}\Psi_{\lambda\tau}{}^{\rho\sigma} = (\delta^\rho_\mu\delta^\sigma_\nu - \delta^\sigma_\mu\delta^\rho_\nu)/2$)

$$D_\mu \bar{H}^{\mu\nu} = \bar{J}^\nu = D_\mu(\Omega^{\mu\nu}{}_{\rho\sigma} H^{\rho\sigma})\ , \tag{72}$$

$$\epsilon^{\mu\nu\rho\sigma}\partial_\nu \bar{F}_{\rho\sigma} = \bar{J}^\mu_M = \epsilon^{\mu\nu\rho\sigma}\partial_\nu(\hat{\Psi}_{\rho\sigma}{}^{\tau\lambda} F_{\tau\lambda})\ , \tag{73}$$

provided appropriate currents are introduced. These transformations in general are not symmetry transformations and accordingly a source free solution is no longer mapped on another source free solution. The transformations (70) and the ensuing equations of motion (72) and (73) are the relativistic form of the transformations proposed in Refs. [10, 11].

We recover the invariant transformations of Section (III) by introducing the restrictions

$$\Omega^{\mu\nu}{}_{\rho\sigma} = S^\mu{}_\rho S^\nu{}_\sigma\ , \qquad \Psi_{\mu\nu}{}^{\rho\sigma} = T_\mu{}^\rho T_\nu{}^\sigma\ . \tag{74}$$

Let us first count the degrees of freedom in the transformations. $\chi^{\mu\nu\rho\sigma}$ is a rank four tensor, anti-symmetric in (μ,ν) and (ρ,σ) and thus has 36 independent components (20 components of the principle part, 15 of the skewon part and one axion coupling). The same applies to the transformation matrices Ω and Ψ. Restricting to diffeomorphisms according to Eq. (74) reduces this number to 6 parameters for each, Ω and Ψ, the electric-magnetic rotation of Section III A adds another parameter in form of a rotation angle. Here, another important difference between a transformation material according to Definition 2 and 3 emerges. In both cases the transformation yielding certain media properties is not unique. In the former case, however, different transformations are physically equivalent as they are connected by symmetry transformations (isometries of the laboratory metric $g_{\mu\nu}$). In the more general case of Eq. (70) the different transformations need not be physically equivalent. As is immediate from Eq. (70) a certain medium exhibiting sources due to non-invariant transformations can be designed using electric charges and currents, magnetic charges and currents or both, which clearly characterizes physically different situations with the same media properties χ.

Does there exist the possibility of a geometric interpretation of Eq. (70)? If this shall be possible space must be transformed differently for different components of $F^{\mu\nu}$ and $H_{\mu\nu}$. In fact, the most general linear transformation can be interpreted as a separate transformation of spacetime for each component of the two tensors. Let us provide a simplified example, where independent spatial transformations are applied to $\vec{E}$, $\vec{B}$, $\vec{\mathcal{D}}$ and $\vec{\mathcal{H}}$. Laboratory space is denoted by x^i, the electromagnetic spaces

by x^i_E, x^i_B, x^i_D and x^i_H, resp. Under time-independent spatial transformations all four fields transform as (co-)vectors and thus Eqs. (A.8)–(A.11) suggest the interpretations

$$\tilde{E}_i = s_E \frac{\partial x^j}{\partial x^i_E} E_j \ , \qquad \tilde{B}^i = \frac{\sqrt{\gamma_B}}{\sqrt{\gamma}} \frac{\partial x^i_B}{\partial x^j} B^j \ , \tag{75}$$

$$\tilde{\mathcal{D}}^i = \frac{\sqrt{\gamma_D}}{\sqrt{\gamma}} \frac{\partial x^i_D}{\partial x^j} \mathcal{D}^j \ , \qquad \tilde{\mathcal{H}}_i = s_H \frac{\partial x^j}{\partial x^i_H} \mathcal{H}_j \ , \tag{76}$$

yielding for permittivity and permeability

$$\epsilon^{ij} = s_E \frac{\sqrt{\gamma_D}}{\sqrt{\gamma}} \frac{\partial x^i_D}{\partial x^k} \gamma^{kl} \frac{\partial x^j_E}{\partial x^l} \ , \tag{77}$$

$$\mu^{ij} = s_H \frac{\sqrt{\gamma_B}}{\sqrt{\gamma}} \frac{\partial x^i_B}{\partial x^k} \gamma^{kl} \frac{\partial x^j_H}{\partial x^l} \ . \tag{78}$$

As is seen from (1) and (2) Gauss' law for $\tilde{B}^i$ and $\tilde{\mathcal{D}}^i$ remain unchanged, while Faraday's and Ampère's law are changed according to

$$\frac{\sqrt{\gamma_E}}{\sqrt{\gamma_B}} \frac{\partial x^i_E}{\partial x^j_B} \nabla_0 \tilde{B}^j + \epsilon^{ijk} \partial_j \tilde{E}_k = 0 \ , \tag{79}$$

$$\epsilon^{ijk} \partial_j \tilde{\mathcal{H}}_k - \frac{\sqrt{\gamma_H}}{\sqrt{\gamma_D}} \frac{\partial x^i_H}{\partial x^j_D} \nabla_0 \tilde{\mathcal{D}}^j = 0 \ , \tag{80}$$

making the electric and magnetic currents

$$j^i = - \left(\delta^i_j - \frac{\sqrt{\gamma_H}}{\sqrt{\gamma_D}} \frac{\partial x^i_H}{\partial x^j_D} \right) \nabla_0 \tilde{\mathcal{D}}^j \ , \tag{81}$$

$$j^i_M = \left(\delta^i_j - \frac{\sqrt{\gamma_E}}{\sqrt{\gamma_B}} \frac{\partial x^i_E}{\partial x^j_B} \right) \nabla_0 \tilde{B}^j \tag{82}$$

necessary. For completeness it should be mentioned that the transformations (75) and (76) allow a straightforward interpretation since each of the four Maxwell's equations still can be transformed as a whole. Taking even more general transformations, e.g. transforming each component of the electric and magnetic fields separately, does no longer allow this manipulation in a simple way and thus will make the derivation of the necessary media parameters more complicated.

VI. CONCLUSIONS

In this paper we have introduced a generalization of the concept of diffeomorphism transforming media, the basis of transformation optics [1–3]. As basic idea we have found that spacetime can be transformed differently for the field strength tensor (containing $\vec{E}$ and $\vec{B}$) and the excitation tensor (encompassing $\vec{\mathcal{D}}$ and $\vec{\mathcal{H}}$). This extension allows to design non-reciprocal media, in particular permittivity and permeability need not longer be symmetric. Furthermore this approach permits a geometric interpretation of indefinite media [6, 7].

Diffeomorphism transforming media are motivated by the wish to produce a medium that looks as a transformed but empty space. The basis of this interpretation is Fermat's principle applied to these media [9]: indeed it is found that in a transformation medium the light rays travel along trajectories as if the medium was a transformed, empty space. Still, the transformation medium in general is quite different from transformed empty space, if the conservation laws from the stress-energy-momentum tensor are considered. This aspect is even more important within the extension proposed here, as there exist two different transformed (electromagnetic) spaces and light rays don't follow the geodesics of any of them. We have shown that one can make a virtue out of necessity: the geometric approach does not just provide a tool to design the path of light in a medium, but equally well it may be used to design the behavior of (parts of) the stress-energy-momentum tensor, e.g. the direction of the Poynting vector, and/or the behavior of the wave vector. Here the proposed generalization offers many more possibilities compared to the known diffeomorphism transforming media. In particular we have derived the geometric relations that describe the transformation of the Poynting vector, of the direction of the wave vector as well as the dispersion relation.

Finally we have commented on a different route to generalize the notion of transformation media [10, 11]. These field-transforming media are not based on invariant transformations of the equations of motion and consequently source free solutions of the original configuration are not mapped onto source free solutions of the new medium. We have shown that also this approach may be covered by a generalized concept of coordinate transformations. Still, there remains a fundamental difference between the approach of Refs. [10, 11] and the one discussed here: While in the former case the transformations are ultra-local (the transformed fields at the point x^μ are defined in terms of the original fields at this point), in the latter they are essentially non-local, as the transformed fields at $\tilde{x}^\mu$ are related to the original fields at some $x^\mu \neq \tilde{x}^\mu$. The preferable approach depends on the specific problem at hand, also a combination of the two is conceivable.

Acknowledgments

The author wishes to thank J. Llorens Montolio for helpful discussions. This work profited a lot from fruitful discussion with C. Simovski, S.A. Tretyakov, I.S. Nevedov, P. Alitalo, M. Qiu and M. Yan during a cooperation of the Advanced Concepts Team of the European Space Agency with the Helsinki University of Technology and the Royal Institute of Technology (KTH). The cooperation was funded under the Ariadna program of ESA.

APPENDIX: COVARIANT FORMULATION

In this Appendix we present our notations and conventions regarding the covariant formulation of Maxwell's equations on a possibly curved manifold. For a detailed introduction to the topic we refer to the relevant literature, e.g. [12, 13]. Throughout the whole paper natural units with $\epsilon_0 = \mu_0 = c = 1$ are used.

Greek indices $\mu, \nu, \rho, \ldots$ are spacetime indices and run from 0 to 3, Latin indices $i, j, k, \ldots$ space indices with values from 1 to 3. For the metric we use the "mostly plus" convention, so the standard flat metric is $g_{\mu\nu} = \mathrm{diag}(-1, 1, 1, 1)$. If we interpret $x^0 = t$ with (laboratory) time the space metric can be obtained as [13]

$$\gamma^{ij} = g^{ij} \ , \qquad \gamma_{ij} = g_{lk} - \frac{g_{0i}g_{0j}}{g_{00}} \ , \qquad \gamma^{ij}\gamma_{jk} = \delta^i_k \ . \tag{A.1}$$

This implies as relation between the determinant of the spacetime metric, g, and the one of the space metric, γ,

$$-g = -g_{00}\gamma \tag{A.2}$$

The four dimensional Levi-Civita tensor is defined as

$$\epsilon_{\mu\nu\rho\sigma} = \sqrt{-g}[\mu\nu\rho\sigma] \ , \quad \epsilon^{\mu\nu\rho\sigma} = -\frac{1}{\sqrt{-g}}[\mu\nu\rho\sigma] \ , \tag{A.3}$$

with $[0123] = 1$. Therefore the reduction of the four dimensional to the three dimensional tensor reads

$$\epsilon_{0ijk} = \sqrt{-g_{00}}\epsilon_{ijk} \ , \qquad \epsilon^{0ijk} = -\frac{1}{\sqrt{-g_{00}}}\epsilon^{ijk} \ . \tag{A.4}$$

The field strength tensor $F_{\mu\nu}$ encompasses the electric field and the magnetic induction, the excitation tensor $H^{\mu\nu}$ the displacement vector and the magnetic field with the identification:

$$E_i = F_{0i} \ , \qquad B^i = -\frac{1}{2}\epsilon^{ijk}F_{jk} \ , \tag{A.5}$$

$$\mathcal{D}^i = -\sqrt{-g_{00}}H^{0i} \ , \quad \mathcal{H}_i = -\frac{\sqrt{-g_{00}}}{2}\epsilon_{ijk}H^{jk} \ . \tag{A.6}$$

Finally, electric charge and current are combined into a four-current $J^\mu = (\rho/\sqrt{-g_{00}}, j^i/\sqrt{-g_{00}})$. $F_{\mu\nu}$ and $H^{\mu\nu}$ are tensors, thus under the transformations of Section III they behave as

$$\bar{F}_{\mu\nu} = \frac{\partial x^\rho}{\partial \bar{x}^\mu}F_{\rho\sigma}\frac{\partial x^\sigma}{\partial \bar{x}^\nu} \ , \quad \bar{\bar{H}}^{\mu\nu} = \frac{\partial \bar{\bar{x}}^\mu}{\partial x^\rho}H^{\rho\sigma}\frac{\partial \bar{\bar{x}}^\nu}{\partial x^\sigma} \ . \tag{A.7}$$

This implies for the transformed space vectors in laboratory space

$$\tilde{E}_i = \bar{s}\bigg(\left(\frac{\partial x^0}{\partial \bar{x}^0}\frac{\partial x^j}{\partial \bar{x}^i} - \frac{\partial x^0}{\partial \bar{x}^i}\frac{\partial x^j}{\partial \bar{x}^0}\right)E_j - \frac{\partial x^j}{\partial \bar{x}^0}\frac{\partial x^k}{\partial \bar{x}^i}\epsilon_{jkl}B^l\bigg) \ , \tag{A.8}$$

$$\tilde{B}^i = \frac{\sqrt{\bar{\gamma}}}{\sqrt{\gamma}}\frac{\partial \bar{x}^i}{\partial x^n}B^n - \bar{s}\epsilon^{ijk}\frac{\partial x^0}{\partial \bar{x}^j}\frac{\partial x^l}{\partial \bar{x}^k}E_l \ , \tag{A.9}$$

$$\tilde{\mathcal{D}}^i = \frac{\sqrt{-\bar{\bar{g}}}}{\sqrt{-g}}\bigg(\left(\frac{\partial \bar{\bar{x}}^0}{\partial x^0}\frac{\partial \bar{\bar{x}}^i}{\partial x^j} - \frac{\partial \bar{\bar{x}}^0}{\partial x^j}\frac{\partial \bar{\bar{x}}^i}{\partial x^0}\right)\mathcal{D}^j + \frac{\partial \bar{\bar{x}}^0}{\partial x^j}\frac{\partial \bar{\bar{x}}^i}{\partial x^k}\epsilon^{jkl}\mathcal{H}_l\bigg) \ , \tag{A.10}$$

$$\tilde{\mathcal{H}}_i = \bar{\bar{s}}\frac{\sqrt{-\bar{\bar{g}}_{00}}}{\sqrt{-g_{00}}}\frac{\partial x^j}{\partial \bar{\bar{x}}^i}\mathcal{H}_j + \frac{\sqrt{-\bar{\bar{g}}}}{\sqrt{-g}}\epsilon_{ijk}\frac{\partial \bar{\bar{x}}^j}{\partial x^0}\frac{\partial \bar{\bar{x}}^k}{\partial x^l}\mathcal{D}^l \ . \tag{A.11}$$

We characterize the general linear, lossless media usually by means of the Tellegen relations

$$\mathcal{D}^i = \epsilon^{ij}E_j + \kappa^{ij}\mathcal{H}_j \ , \quad B^i = \mu^{ij}\mathcal{H}_j + \xi^{ij}E_j \ . \tag{A.12}$$

In terms of field strength and excitation tensor the media relations become the Boys-Post relation

$$H^{\mu\nu} = \frac{1}{2}\chi^{\mu\nu\rho\sigma}F_{\rho\sigma} \ , \tag{A.13}$$

where χ must be invertible with inverse

$$\hat{\chi}_{\mu\nu\lambda\tau}\chi^{\lambda\tau\rho\sigma} = (\delta^\rho_\mu\delta^\sigma_\nu - \delta^\sigma_\mu\delta^\rho_\nu) \ . \tag{A.14}$$

By virtue of Eqs. (A.5) and (A.6) Eq. (A.13) may be written as

$$\begin{pmatrix}\mathcal{H}_i \\ \mathcal{D}^i\end{pmatrix} = \begin{pmatrix}\mathfrak{C}_i{}^j & \mathfrak{B}_{ij} \\ \mathfrak{A}^{ij} & \mathfrak{D}^i{}_j\end{pmatrix}\begin{pmatrix}E_j \\ B^j\end{pmatrix} \ , \tag{A.15}$$

with

$$\mathfrak{A}^{ij} = -\sqrt{-g_{00}}\chi^{0i0j} \ , \tag{A.16}$$

$$\mathfrak{B}_{ij} = \frac{1}{8}\sqrt{-g_{00}}\epsilon_{ikl}\epsilon_{jmn}\chi^{klmn} \ , \tag{A.17}$$

$$\mathfrak{C}_i{}^j = -\frac{1}{2}\sqrt{-g_{00}}\epsilon_{ikl}\chi^{kl0j} \ , \tag{A.18}$$

$$\mathfrak{D}^i{}_j = \frac{1}{2}\sqrt{-g_{00}}\epsilon_{jkl}\chi^{0ikl} \ . \tag{A.19}$$

The Tellegen and Boys-Post formulations are related by

$$\epsilon^{ij} = \left(\mathfrak{A} - \mathfrak{D}\mathfrak{B}^{-1}\mathfrak{C}\right)^{ij} \qquad \kappa^{ij} = \left(\mathfrak{D}\mathfrak{B}^{-1}\right)^{ij} \tag{A.20}$$

$$\mu^{ij} = (\mathfrak{B}^{-1})^{ij} \qquad \xi^{ij} = -\left(\mathfrak{B}^{-1}\mathfrak{C}\right)^{ij} \tag{A.21}$$

Finally, we mention that the rank 4 tensor $\chi^{\mu\nu\rho\sigma}$ may be decomposed as [15, 16]

$$\chi^{\mu\nu\rho\sigma} = {}^{(1)}\chi^{\mu\nu\rho\sigma} + \epsilon^{\mu\nu\lambda[\rho}S_\lambda{}^{\sigma]} - \epsilon^{\rho\sigma\lambda[\mu}S_\lambda{}^{\nu]} + \alpha\epsilon^{\mu\nu\rho\sigma} \ , \tag{A.22}$$

where the principal part ${}^{(1)}\chi^{\mu\nu\rho\sigma}$ has no part completely anti-symmetric in its indices and is symmetric under the

exchange $(\mu,\nu) \leftrightarrow (\rho,\sigma)$. The principle part has been discussed extensively in [12]. $S_\mu{}^\nu$ was introduced in Refs. [15, 16] as skewon part (related to chiral properties of the material [16, 20]), while α represents the well-known axion coupling [21].

[1] J. Pendry, D. Schurig, and D. Smith, Science **312**, 1780 (2006).

[2] U. Leonhardt, Science **312**, 1777 (2006).

[3] U. Leonhardt and T. G. Philbin, New J. Ph. **8**, 247 (2006).

[4] D. Schurig, J. Mock, B. Justice, S. Cummer, J. Pendry, A. Starr, and D. Smith, Science **314**, 977 (2006).

[5] D. Schurig, J. Pendry, and D. Smith, Opt. Express **15**, 14772 (2007).

[6] D. Smith and D. Schurig, Phys. Rev. Lett. **90**, 077405 (2003).

[7] D. Smith, P. Kolilnko, and D. Schurig, J. Opt. Soc. Am. B **21**, 1032 (2004), URL `http://josab.osa.org/abstract.cfm?URI=josab-21-5-1032`.

[8] Z. Jacob, L. Alekseyev, and E. Narimanov, Opt. Express **14**, 8247 (2006).

[9] U. Leonhardt and T. Philbin (2008), to appear in Progress in Optics, arXiv:0805.4778 [physics.optics].

[10] S. Tretyakov and I. Nefedov, in *Metamaterials' 2007* (Rome, 2007).

[11] S. Tretyakov, I. Nefedov, and P. Alitalo (2008), to appear in New Journal of Physics, arXiv:0806.0489 [physics.optics].

[12] E. Post, *Formal structure of electromagnetics: general covariance and electromagnetics* (Dover Publications, 1997).

[13] L. Landau and E. Lifshitz, *The classical theory of fields*, vol. 2 of *Course of theoretical physics* (Butterworth-Heinemann, Oxford, 2006), 4th ed.

[14] A. Ward and J. Pendry, J. Mod. Opt. **43**, 773 (1996).

[15] F. Hehl and Y. Obukhov, *Foundations of classical electrodynamics: charge, flux and metric*, vol. 33 of *Prog. Math. Phys.* (Birkhäuser, Boston, MA, 2003).

[16] F. W. Hehl and Y. N. Obukhov, Lect. Notes Phys. **702**, 163 (2006), gr-qc/0508024.

[17] C. Montonen and D. I. Olive, Phys. Lett. **B72**, 117 (1977).

[18] W. Israel and J. Stewart, in *General relativity and gravitation*, edited by A. Held (Plenum, 1980), vol. 2, p. 491.

[19] T. Dereli, J. Gratus, and R. Tucker, Phys. Lett. A **361**, 190 (2007).

[20] I. Lindell, A. Sihvola, S. Tretyakov, and A. Viitanen, *Electromagnetic waves in chiral and bi-isotropic media* (Artech House, Boston, MA, 1994).

[21] F. Wilczek, Phys. Rev. Lett. **58**, 1799 (1987).

[22] A. Greenleaf, Y. Kurylev, M. Lassas, and G. Uhlmann, Comm. Math. Phys. **275**, 749 (2007).

[23] Here and in the following we use Einstein's summation convention, in which a summation over all repeated indices is assumed: $A^iB_i = \sum_i A^iB_i$. For Latin indices this sum runs over the values 1,2,3 (spatial indices), while for Greek indices it runs from 0–4 with $x^0 = t$ being time.

[24] Strictly speaking this applies to transformations which are regular everywhere, only. Several singular transformations have been proposed in the literature in the context of metamaterials, e.g. the invisibility cloak [1, 2, 4]. In this case a careful study of the global solution is indispensable, as has been done for the case of the cloak in Ref. [22].

[25] Throughout the paper natural units with $\epsilon_0 = \mu_0 = c = 1$ are used. Notice that the corresponding relation in Ref. [3] differs from the one used here. According to our conventions $F^{\mu\nu} = H^{\mu\nu}$ in vacuum, while there $\sqrt{-g}F^{\mu\nu} = H^{\mu\nu}$.

[26] Sources are external parameters and thus should be set to zero for a symmetry transformation. Even together with sources the symmetry can be restored, if an appropriate transformation rule of the sources is defined.

[27] Notice that under the continuous transformation the action behaves as $\mathcal{S} \to (\cos^2\alpha - \sin^2\alpha)\mathcal{S}$ and thus for $\alpha = \pi/4$ transforms to zero. Therefore at the level of the action only the discrete duality transformation can be considered.

[28] Alternatively, one could start from a relation of the form

$$\bar{H}^{\mu\nu} = A^{\mu\nu}{}_{\rho\sigma}H^{\rho\sigma} + B^{\mu\nu\rho\sigma}F_{\rho\sigma}$$

but the form (70) appears more transparent to us.